ELSEVIER

Physics Reports 306 (1998) 1–108

PHYSICS REPORTS

Nonlinear dynamics of the Frenkel–Kontorova model

Oleg M. Braun[a], Yuri S. Kivshar[b,*]

[a] *Institute of Physics, The National Academy of Sciences of the Ukraine, 46 Science Avenue, 252022 Kiev, Ukraine*
[b] *Optical Sciences Centre, Research School of Physical Sciences and Engineering, The Australian National University, ACT 0200 Canberra, Australia*

Received March 1998; editor: D.K. Campbell

Contents

Abstract

An overview of the dynamics of one of the fundamental models of low-dimensional nonlinear physics, *the Frenkel–Kontorova* (*FK*) *model*, is presented. In its simplest form, the FK model describes the motion of a chain of interacting particles ("atoms") subjected to an external on-site periodic potential. Physically important generalizations of the FK model are discussed including nonsinusoidal on-site potentials and anharmonic (e.g., nonconvex, Kac–Baker,

* Corresponding author. E-mail: ysk124@rsphy1.anu.edu.au.

PII: S0370-1573(98)00029-5

NONLINEAR DYNAMICS OF THE FRENKEL–KONTOROVA MODEL

Oleg M. BRAUN[a], **Yuri S. KIVSHAR**[b]

[a]*Institute of Physics, The National Academy of Sciences of the Ukraine, 46 Science Avenue, 252022 Kiev, Ukraine*

[b]*Optical Sciences Center, Research School of Physical Sciences and Engineering, The Australian National University, ACT 0200 Canberra, Australia*

ELSEVIER

AMSTERDAM – LAUSANNE – NEW YORK – OXFORD – SHANNON – TOKYO

power-law) interactions between the particles. The results are summarized for the one-dimensional dynamics of *kinks* – topological excitations, including the kink diffusion and effects of disorder, and also for nonlinear localized modes, *discrete breathers*. A special attention is paid to the numerous applications of the FK model in the problems of low-dimensional solid state physics.

PACS: 63.20.Pw; 46.10. + z

Keywords: Non-linear dynamics; Kinks; Frenkel–Kontorova model; Discrete breathers; Nonlinear impurity modes; Peierls–Nabarro potential; sine-Gordon equation; Kink diffusion; Disorder

1. Introduction

Theoretical physics deals with physical models. Universal models which can be applied to describe a variety of effects of different physical origin are rare and, therefore, they are of key importance. Such models attract special attention and they can be employed to present the basic physical concepts in the simplest way. A simple model which describes a chain of classical particles (atoms) harmonically coupled with their nearest neighbors and subjected to a periodic on-site (substrate) potential has become in recent years one of the fundamental and universal models of low-dimensional nonlinear physics. In spite of the fact that a link with the classical model is not often stated explicitly in many applications, many kinds of nonlinear problems involving the dynamics of discrete nonlinear chains are in fact based on the classical formulation introduced in the papers by Ya. Frenkel and T. Kontorova (see Frenkel and Kontorova, 1938, 1939; Kontorova and Frenkel, 1938a, b) who suggested to use this kind of a nonlinear chain to describe, in the simplest way, the structure and dynamics of a crystal lattice in the vicinity of the dislocation core. As a matter of fact, this is one of the first examples in the solid state physics when the dynamics of an extended two-dimensional defect in a bulk is modeled by a simple one-dimensional chain.

Simplicity of the Frenkel–Kontorova (FK) model, due to the assumptions of the harmonic interatomic force and sinusoidal on-site (substrate) potential, as well as its surprising capability to describe a broad spectrum of nonlinear, physically important phenomena, such as propagation of charge–density waves, the dynamics of absorbed layers of atoms on crystal surfaces, commensurable–incommensurable phase transitions, domain walls in magnetically ordered structures, etc., have attracted a great deal of attention from physicists working in solid state physics and nonlinear physics.

One of the important features which can explain *why* the FK model has attracted much attention in different branches of solid state physics is the fact that in the continuum-limit approximation the model reduces to the exactly integrable sine-Gordon (SG) equation which possesses nice properties and allows exact solutions describing different types of nonlinear waves and their interaction. In particular, the SG equation gives us an example of a fundamental nonlinear model for which we know almost everything about the dynamics of *nonlinear excitations*. As is known, the SG system describes simultaneously three different types of elementary excitations, namely *phonons*, *kinks* (topological solitons), and *breathers* (dynamical solitons), whose dynamics determines the general behaviour of the system as a whole. And, although the FK model is inherently *discrete* and not exactly integrable, one may get deep physical insights and significantly simplify the understanding of its nonlinear dynamics using the language of the SG quasi-particles as weakly interacting nonlinear excitations. Discreteness of the FK model manifests itself in such a phenomenon as the effective periodic potential, known as the Peierls–Nabarro relief, affecting the quasiparticle motion.

The most familiar application of the FK model can be found in *the theory of dislocations in metals* (Frenkel and Kontorova, 1938, 1939; Kontorova and Frenkel, 1938a,b; Frank and van der Merwe, 1949a,b; Seeger and Kochendörfer, 1951; Seeger et al., 1953; Atkinson and Cabrera, 1965; Flytzanis et al., 1977). In such applications, the FK model has a simple physical origin. Indeed, let us consider an additional semi-infinite plane of atoms inserted into a perfect crystal lattice. Then the layer of atoms perpendicular to the inserted plane divides the crystal into two different parts and plays a role of an interface layer. The atoms belonging to the interface layer can be treated as

a one-dimensional chain subjected to an external potential produced by surrounding atoms of the lattice. The interaction with these other atoms can be modelled by an effective periodic potential. *This idea gives birth to the FK model.* Similar models arise in the description of the dynamics of plane defects such as *twin boundaries* (e.g., Suezawa and Sumino, 1976; Sugiyama, 1979) and *domain walls in ferroelectrics* (e.g., Döring, 1948; Becker, 1951; Cowley et al., 1976; Bruce, 1981), and *ferro-* or *antiferromagnetics* (e.g., Enz, 1964; Mikeska, 1978; Bishop and Lewis, 1979; Kovalev, 1994). Importantly, the effective periodic potential can be justified via a self-consistent microscopic model where only interparticle interaction is taken into account (Christiansen et al., 1998).

The FK model can be also derived for *the problem of crowdion in a metal* (see Paneth, 1950; Frenkel, 1972; see also more recent studies by Landau et al., 1993; Kovalev et al., 1993) when one extra atom is inserted into a closely packed row of atoms in a metal with an ideal crystal lattice. In many such cases the crystalline potential is organized in the way that the atoms can move only along the row direction, and the inserted atom (together with the neighboring atoms) forms a one-dimensional configuration which can be treated as a kink of the FK model.

More deeper background of the applications of the FK model can be found in the cases when the atoms belonging to the chain and the atoms creating the external (substrate) potential have a different physical origin. For example, in the so-called *superionic conductors* (see, e.g., Bishop, 1978; and also the review papers by Boyce and Huberman, 1979; Dieterich et al., 1980) an anisotropic crystalline structure forms quasi-one-dimensional channels along which ions may easily move, so that this kind of models may be also reduced to the analysis of a one-dimensional chain subjected to an effective on-site potential.

Another similar example corresponds to *a sub-monolayer film of atoms adsorbed on a crystal surface* (see, e.g., Lyuksyutov et al., 1988). In this case, adsorbed atoms (adatoms) play a role of the atoms of the chain while the surface atoms produce an effective substrate potential. This type of model can also be used to describe processes of crystal growth (e.g., Franzosi et al., 1988).

Besides, the same model is employed to describe the clean surface, if one treats the surface atoms as the atoms from the effective FK chain, while the atoms of the first underlying layer are assumed to produce an effective substrate potential. In particular, the FK model can be used to describe *the surface reconstruction phenomena* (Harten et al., 1985; Mansfield and Needs, 1990) and the structure of the vicinal semiconductor surfaces (Yang et al., 1991).

We would like to mention also applications of the FK model to the theory of *the proton conductivity of hydrogen-bonded chains.* The main idea of a general physical model describing a chain with hydrogen bonds is based on the fact that protons move in double wells due to hydrogen bonds with a heavy-ion lattice (oxygen lattice) which is deformable (e.g., Antonchenko et al., 1983; Zolotaryuk, 1986). The local distortions of the oxygen lattice can lower the activation barrier for the protons and thus promote their motion. In order to describe this phenomenon, one- or two-component nonlinear models should include the proton sublattice which supports topological solitons (kinks) while the oxygen sublattice can be modelled as the other sublattice or as an effective external potential to the proton motion. Several models of this kind have been proposed (Antonchenko et al., 1983; Zolotaryuk et al., 1984; Zolotaryuk, 1986; Peyrard et al., 1987; Hochstrasser et al., 1988; Pnevmatikos, 1988) and they give a simple and effective description of the proton mobility in hydrogen-bonded chains. Similar models may also play an important role in interpreting certain biological processes like *the DNA dynamics and denaturation* (see Yomosa,

1983; Homma and Takeno, 1984; Peyrard and Bishop, 1989; Dauxois et al., 1993; Gonzalez and Martín-Landrove, 1994; and also review papers by Zhou and Zhang, 1991; Gaeta et al., 1994).

Last but not least, we mention more recent applications of the FK model in *the theory of Josephson junctions*, where a discrete chain of effective particles appears when one considers the flux flow in discrete parallel arrays of weak links between superconductors (see, e.g., Hontsu and Ishii, 1988; Pagano et al., 1989; Ustinov et al., 1993, 1994; van der Zant et al., 1995; Watanabe et al., 1996).

The present review paper has a purpose to describe, from a rather general point of view, different kinds of physical problems and various results involving the analysis of *the nonlinear dynamics* of the FK model and its generalizations. We do not restrict ourselves by specific applications but try to present a panoramic view on general features of the dynamics of the FK model and summarize the basic physical concepts and results based on this model. Section 2 makes a brief introduction into the conventional ("classical") FK model also referring to its continuum version described by the exactly integrable SG equation. In Sections 3 and 4 we present some important generalizations of the FK model which take into account more general types of the on-site substrate potential (Section 3) as well as anharmonic interaction between particles in the chain (Section 4). Section 5 gives a brief overview of the kink diffusion dynamics in the FK chain. Nonlinear spatially localized oscillating states (also called "intrinsic localized modes" or "discrete breathers") are briefly discussed in Section 6, where we show that these nonlinear modes may be understood as a natural generalization of the breather modes but existing in the lattices with strong discreteness effects. Effects of disorder on the dynamics of kinks, and also on the structure and stability of nonlinear impurity modes are discussed in Section 7. Section 8 concludes the paper with more examples of the problems of different physical context where the basic concepts can be demonstrated with the help of the FK model. Some more recent topics of research and important future directions are also mentioned.

2. Classical model

2.1. Basic properties

A simple model describing a chain of particles (atoms) interacting with the nearest neighbors and subjected to a periodic on-site (substrate) potential was firstly analytically treated, to the best of our knowledge, by Dehlinger (1929) (for a brief history of early work on imperfections in crystals, see Seeger, 1980a) and then introduced, as a dynamical discrete model, by Frenkel and Kontorova (Frenkel and Kontorova, 1938, 1939; Kontorova and Frenkel, 1938a,b). The model is presented schematically in Fig. 1, and it is characterized by the Hamiltonian,

$$\mathscr{H} = K + U \,, \tag{2.1}$$

where K is the kinetic energy,

$$K = \frac{m_a}{2} \sum_n \left(\frac{\mathrm{d}x_n}{\mathrm{d}t} \right)^2 \,, \tag{2.2}$$

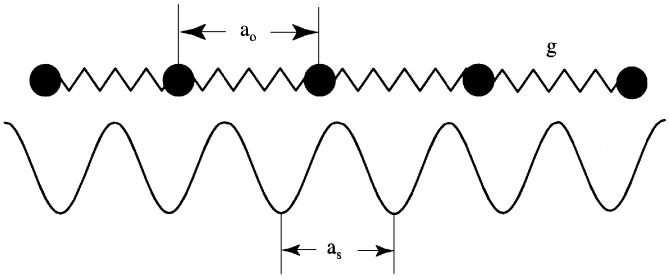

Fig. 1. Schematic presentation of a chain of particles (atoms), interacting via harmonic springs with the elastic constant g and subjected to an external sinusoidal potential with the period a_s.

m_a is the particle mass and x_n is the coordinate of the nth particle in the chain. The potential energy U consists of two parts,

$$U = U_{\text{sub}} + U_{\text{int}} , \tag{2.3}$$

where the first term characterizes an interaction of the chain with an external on-site periodic potential taken in the simplest form,

$$U_{\text{sub}} = \frac{\varepsilon_s}{2} \sum_n \left[1 - \cos\left(\frac{2\pi x_n}{a_s} \right) \right] , \tag{2.4}$$

with the amplitude ε_s and the period a_s, while the second term in Eq. (2.3) takes into account the harmonic interaction of the nearest neighbors in the chain,

$$U_{\text{int}} = \frac{g}{2} \sum_n (x_{n+1} - x_n - a_0)^2 , \tag{2.5}$$

where g is the elastic constant and a_0 is the equilibrium distance of the interatomic potential. The model introduced by Eqs. (2.2), (2.3), (2.4) and (2.5) can be justified under the following assumptions:

(i) The atomic motion is restricted by one direction only;

(ii) In the general expression for the substrate potential energy,

$$U_{\text{sub}} = \sum_n V_{\text{sub}}(x_n) , \tag{2.6}$$

the function $V_{\text{sub}}(x)$ is expanded into the Fourier series, and only the first harmonic is kept;

(iii) The interparticle interaction energy takes into account only interactions between nearest neighbors, i.e.

$$U_{\text{int}} = \sum_n V_{\text{int}}(x_{n+1} - x_n) , \tag{2.7}$$

and, expanding $V_{\text{int}}(x)$ into the Taylor series, only the harmonic interaction is considered, so that

$$g = V''_{\text{int}}(a_0) . \tag{2.8}$$

In the dimensionless variables,

$$x_n \to (2\pi/a_s)x_n \ , \tag{2.9}$$

$$t \to (2\pi/a_s)\sqrt{\varepsilon_s/2m_a}\ t \ , \tag{2.10}$$

the Hamiltonian (2.1)–(2.5) takes the form

$$H = \frac{\mathscr{H}}{(\varepsilon_s/2)} = \sum_n \left\{ \frac{1}{2}\left(\frac{\mathrm{d}x_n}{\mathrm{d}t}\right)^2 + (1-\cos x_n) + \frac{1}{2}g(x_{n+1}-x_n-a_0)^2 \right\}, \tag{2.11}$$

where $a_0 \to a_0(2\pi/a_s)$, and the dimensionless coupling constant changes to be

$$g \to g\frac{(a_s/2\pi)^2}{(\varepsilon_s/2)} \ . \tag{2.12}$$

In such a renormalized form, the Hamiltonian (2.11) describes a harmonic chain of atoms of unit masses, subjected to the external sinusoidal potential with the period $a_s = 2\pi$ and amplitude $\varepsilon_s = 2$. To calculate all the values in the corresponding dimensions, one should multiply the spatial variables by $(a_s/2\pi)$, the frequencies by $(2\pi/a_s)\sqrt{\varepsilon_s/2m_a}$, the masses, by m_a, and the energies, by $(\varepsilon_s/2)$.

From the Hamiltonian (2.11) it follows the equation of motion,

$$\frac{\mathrm{d}^2x_n}{\mathrm{d}t^2} + \sin x_n - g(x_{n+1}+x_{n-1}-2x_n) = 0 \ , \tag{2.13}$$

and we notice that this equation does not include the parameter a_0, the equilibrium lattice spacing without the periodic potential. In the present survey we will consider the case of an infinite chain with $a_0 = a_s$ when the ground state of the chain (i.e., a stationary state corresponding to the minimum of the potential energy) is a commensurate structure of atoms. This means that each minimum of the substrate potential is occupied by one atom, so that the "coverage" parameter θ, defined as a ratio of the number of atoms to the number of minima of the substrate potential, is equal to 1. Therefore, it is convenient to introduce the variables u_n defined through the relation,

$$x_n = na_s + u_n \ . \tag{2.14}$$

Here we discuss only the case of an infinite chain with "fixed ends". Such a case can be treated also as a finite chain of N atoms with periodic boundary conditions,

$$x_{N+1} = x_1 + Na_s \mp \sigma p a_s \ , \tag{2.15}$$

where p is integer, equal to the number of kinks with the topological charge σ ($\sigma = \pm 1$) which are inserted into the chain, then considering the limit $N \to \infty$.

When the atomic displacements u_n are small, i.e. $|u_n| \ll a_s$, the linearized form of the motion equation,

$$\frac{\mathrm{d}^2u_n}{\mathrm{d}t^2} + u_n - g(u_{n+1}+u_{n-1}-2u_n) = 0 \ , \tag{2.16}$$

describes linear excitations, or phonons,

$$u_n(t) \propto \exp\{\mathrm{i}\omega_{\mathrm{ph}}(\kappa)t - \mathrm{i}\kappa n\} \ ,$$

which are characterized by the dispersion relation,

$$\omega_{\rm ph}^2(\kappa) = \omega_{\rm min}^2 + 2g(1 - \cos\kappa) , \tag{2.17}$$

where κ is the dimensionless wavenumber ($|\kappa| \le \pi$). Thus, the frequency spectrum of the FK chain is characterized by a finite band with the gap

$$\omega_{\rm min} \equiv \omega_{\rm ph}(0) = 1 , \tag{2.18}$$

and the cut-off frequency,

$$\omega_{\rm max} \equiv \omega_{\rm ph}(\pi) = \sqrt{\omega_{\rm min}^2 + 4g} . \tag{2.19}$$

When atomic displacements are not small, the linear approximation is not valid anymore, and the primary nonlinear motion equation (2.13) has very rich dynamics supporting new types of localized excitations. To show this, let us consider first the continuum limit approximation to the FK model. A standard procedure to derive equations in the continuum limit starting from a discrete lattice was proposed by Rosenau (1986), and such an approach can be applied to the chains with arbitrary interparticle and substrate potentials. Indeed, from the Hamiltonian (2.2)–(2.5) it follows that the motion equation can be rewritten in the form,

$$\frac{{\rm d}^2 u_n}{{\rm d}t^2} = F_{\rm int}(a_s + u_n - u_{n-1}) - F_{\rm int}(a_s + u_{n+1} - u_n) + F_{\rm sub}(u_n) , \tag{2.20}$$

where

$$F_{\rm int}(u) = -\frac{\partial}{\partial u} V_{\rm int}(u) \quad \text{and} \quad F_{\rm sub}(u) = -\frac{\partial}{\partial u} V_{\rm sub}(u).$$

Eq. (2.20) may be reduced to the equation

$$a_s \frac{{\rm d}^2 v_n}{{\rm d}t^2} = -\left[F_{\rm int}(a_s + a_s v_{n+1}) + F_{\rm int}(a_s + a_s v_{n-1}) - 2F_{\rm int}(a_s + a_s v_n)\right] + \left[F_{\rm sub}(u_n) - F_{\rm int}(u_{n-1})\right] , \tag{2.21}$$

for the so-called nth bond lengths,

$$v_n = (u_n - u_{n-1})/a_s . \tag{2.22}$$

Now, expanding v_{n+1} around v_n, introducing the new variables x and $v(x)$ by changing $n \to x = na_s$ and

$$v_n \to \left|\frac{\partial u}{\partial x}\right|_{x = na_s} , \tag{2.23}$$

we obtain (Rosenau, 1986)

$$u_{tt} + a_s L_A\{F_{\rm int}[a_s(1 + u_x)]\}_x - F_{\rm sub}(u) = 0 , \tag{2.24}$$

where the indices "t" and "x" stand for partial derivatives in respect to the corresponding variables, and

$$L_A = 1 + \frac{1}{12} a_s^2 \frac{\partial^2}{\partial x^2} + \cdots .$$

Then, acting by L_A^{-1} on Eq. (2.24), we obtain the continuum theory equation up to the order $\mathcal{O}(a_s^4)$,

$$u_{tt} - \frac{1}{12} a_s^2 u_{xxtt} - F_{\rm sub}(u) + a_s \frac{\partial}{\partial x}\left\{ F_{\rm int}[a_s(1+u_x)] - \frac{1}{12} a_s \frac{\partial}{\partial x} F_{\rm sub}(u) \right\} = 0 \ . \tag{2.25}$$

The method described above takes into account all the terms of the lowest order which are due to the lattice discreteness, and, in particular, for the FK model considered here this method leads to the perturbed SG equation,

$$u_{tt} + \sin u - \mathrm{d}^2 u_{xx} = \varepsilon f(u) \ , \tag{2.26}$$

where $d = a_s\sqrt{g}$ and the function

$$\varepsilon f(u) = \tfrac{1}{12} a_s^2 [u_{xxtt} + u_x^2 \sin u - u_{xx} \cos u] \tag{2.27}$$

describes, in the first order, the effects produced by the chain discreteness.

2.2. The sine-Gordon equation

If we neglect the discreteness effects in the standard FK model, the equation of motion reduces to the sine-Gordon (SG) equation,

$$u_{tt} - \mathrm{d}^2 u_{xx} + \sin u = 0 \ , \tag{2.28}$$

where

$$d = a_s\sqrt{g} \quad \text{and} \quad g = V''_{\rm int}(a_s) \ . \tag{2.29}$$

Changing the spatial scale by introducing $x \to x/d$, one can transform Eq. (2.28) to its canonical form,

$$u_{tt} - u_{xx} + \sin u = 0 \ . \tag{2.30}$$

As a matter of fact, Eq. (2.30) was the first partial differential equation whose multi-soliton properties were recognized. Indeed, in its transformed form Eq. (2.30) was originally considered by Enneper (1870) in the differential geometry of surfaces of a constant negative Gaussian curvature. The study of Eq. (2.30) in the context of the differential geometry revealed very interesting properties, including the possibility to generate from one known solution of Eq. (2.30) a new unknown solution by means of the Bäcklund transformation (Bäcklund, 1882).

In physics, Eq. (2.30) found its first applications in dislocation models (see Seeger, 1948; see also Seeger, 1980a for historical details), and kink–antikink and breathers of the SG equation have been first introduced by A. Seeger and co-workers more than 40 years ago (Kochendorfer and Seeger, 1950; Seeger and Kochendörfer, 1951; Seeger et al., 1953; see also Seeger, 1980b; Döttling et al., 1990). The original German names for the kinks and breathers were "translatorische and

oszillatorische Eigenbewegungen", and from a historical point of view it is interesting to note that this preceded the discovery of the solitonic properties of the Korteweg–de Vries equation (Zabusky and Kruskal, 1965; Gardner et al., 1967) by more than a decade. Independently, Perring and Skyrme (1962) introduced the SG equation as a simple one-dimensional model of the scalar field theory modelling a classical particle. Almost simultaneously, the SG equation appeared in the theory of weak superconductivity to be the main nonlinear equation describing the so-called long Josephson junctions (see, e.g., Josephson, 1965), where the kink solution describes a quantum of magnetic field, *a fluxon*. The two next important steps of the history of the SG equation were the emphasis of its pedagogical power by use of the very simple chain of coupled pendulums (the mechanical analog of the FK chain) made by Scott (1969), and the solution of the related inverse scattering transform problem obtained by Ablowitz et al. (1973).

Later, the SG equation (2.30) was proved to be completely integrable with the canonical variables introduced through the auxiliary scattering data, and its properties have been described in many survey papers and books (see, e.g., Zakharov et al., 1980). Here we only mention the main properties of Eq. (2.30) and its solutions, which are necessary for us to discuss properties of solutions of a discrete FK model.

As is well known, elementary excitations of the SG system are *phonons*, *kinks*, and *breathers*.

Phonons, or continuous waves in the linear limit take the standard form, $u(x,t) \propto \exp(\mathrm{i}\omega t - \mathrm{i}kx)$, and they are characterized by the dispersion relation, the dependence of the wave frequency on its wave number, $\omega_{\mathrm{ph}}^2(k) = 1 + k^2$, which is a long-wave expansion of Eq. (2.17).

Kinks, or topological solitons, appear due to a degeneracy of the system ground state. Indeed, a kink can be understood as the solution connecting two nearest identical minima of the periodic on-site potential,

$$u_{\mathrm{k}}(x,t) = 4\tan^{-1}\exp[-\sigma\gamma(v)(x - vt)]. \tag{2.31}$$

Here $\sigma = \pm 1$ stands for the so-called topological charge, and we call the solution (2.31) *kink*, for the case $\sigma = +1$, and *antikink*, for $\sigma = -1$. The kink's velocity v is measured in units of the sound velocity c, and it determines the kink's width, $\gamma(v) = 1/\sqrt{1 - v^2}$, the latter result follows from the relativistic invariance of the SG model and it may be treated as a Lorentz contraction of the kink width. Here we are interested in "nonrelativistic" kink motion when $v^2 \ll c^2$, so that the factor γ is approximately 1.

The kink's energy, expressed in the dimensionless units, is

$$E_{\mathrm{k}}(v) = mc^2\gamma(v) \approx mc^2 + \tfrac{1}{2}mv^2\,, \tag{2.32}$$

allows to introduce the rest mass of the kink, which in dimensionless units may be written as

$$m = 2/(\pi^2\sqrt{g})\,, \tag{2.33}$$

and the kink's rest energy, as

$$\varepsilon_{\mathrm{k}} = mc^2 = 8\sqrt{g}\,. \tag{2.34}$$

The energy of the repulsion between two neighboring static kinks is shown to be equal to (see, e.g., Hsu, 1980)

$$v_{\mathrm{int}}(R) \approx \varepsilon_{\mathrm{k}}\sinh^{-2}(R/2d)\,,$$

while the kink and antikink attract each other with the interaction potential,

$$v_{\rm int}(R) \approx -\varepsilon_{\rm k} \cosh^{-2}(R/2d).$$

Thus, the energy of the interaction between two static kinks with topological charges σ_1 and σ_2 separated by the distance R ($R \gg d$) may be approximately presented as

$$v_{\rm int}(R) \approx 32\sigma_1\sigma_2\sqrt{g}\exp(-R/d)\,. \tag{2.35}$$

A breather, or a dynamical soliton, has the form

$$u_{\rm br}(x,t) = 4\tan^{-1}\left\{\left(\frac{\sqrt{1-\Omega^2}}{\Omega}\right)\frac{\sin(\Omega t)}{\cosh(x\sqrt{1-\Omega^2})}\right\}. \tag{2.36}$$

Eq. (2.36) describes a nonlinear oscillating state with the internal frequency Ω lying within the gap of the linear spectrum, $0 < \Omega < \omega_{\rm min}$, with the amplitude, $u_{\rm max} = 4\tan^{-1}(\sqrt{1-\Omega^2}/\Omega)$, oscillation being localized on the spatial scale,

$$b = d/\sqrt{1-\Omega^2}\,. \tag{2.37}$$

The breather energy is

$$\varepsilon_{\rm br} = 2\varepsilon_{\rm k}\sqrt{1-\Omega^2}\,, \tag{2.38}$$

so that $0 < \varepsilon_{\rm br} < 2\varepsilon_{\rm k}$. In the limit of low frequencies, $\Omega \ll 1$, the breather can be qualitatively treated as a coupled kink–antikink pair.

In the framework of the model described by the SG equation, kinks and breathers move freely along the chain without loss of their energy for dissipation (the solution for a moving breather can be easily obtained from Eq. (2.36) applying the Lorentz transformation). The SG equation is exactly integrable, i.e. it allows elastic interactions between all the excitations, and the only effect of such collisions is a phase shift (see, e.g., Zakharov et al., 1980, for more details). That is why kinks and breathers can be treated as *nonlinear quasi-particles* of the SG model, and such an approach is still valid for nearly integrable modifications of the SG equation, when the model includes small perturbations like those which appear when deriving the SG equation from the primary FK model in the quasi-continuum approximation, assuming the effects of the model discreteness small. In fact, being perturbed by small (conservative or nonconservative) perturbations, kinks behave like *deformable* quasi-particles, i.e. they may also change their shapes. Besides that, some new features may appear even in the presence of small perturbations, e.g. kink and antikink may collide inelastically producing a long-lived breather mode, the total topological charge of the system being conserved.

For the integrable SG model, any localized excitation can be presented as an *asymptotic superposition* of elementary excitations of three kinds, i.e. kinks, breathers, and phonons. The nonlinear periodic solutions of the SG equation can also be found explicitly, for example, a chain of kinks is given by the following solution,

$$u(x,t) = -\sin^{-1}[\mathrm{cn}(x/k;k)]\,, \tag{2.39}$$

where cn is the Jacobi elliptic function. Eq. (2.39) describes a periodic sequence of kinks with the widths, kd ($k < 1$), separated by the distance,

$$L = 4dk\,K(k)\,, \tag{2.40}$$

$K(k)$ being the complete elliptic integral of the first kind. The nonlinear interaction of a SG kink and large-amplitude (anharmonic) phonons is also elastic, and it is described by an exact solution of the SG equation (Zadrodziński and Jaworski, 1982; Jaworski, 1987). In the small-amplitude limit, this general kink-phonon interaction describes a phase shift in the elastic scattering of linear phonons by a SG kink (Rubinstein, 1970; see also Martinez Alonso, 1986).

As has been mentioned above, in the framework of the exactly integrable SG model collisions of solitons are elastic, i.e. their shapes, velocities and energies remain unchanged after collisions and the only effect produced by the interactions is the phase shifts of the colliding solitons. For example, if we take the initial kink at rest and another kink coming from infinity with the initial velocity $v_{\rm in}$, then after collision the first kink will remain at rest but the kinks' coordinates will be shifted by a constant value, for example, the coordinate of the first kink will be shifted on the value Δx_1, where (see, e.g., Zakharov et al., 1980)

$$\Delta x_1 = \frac{d}{\gamma}\ln\left(\frac{\gamma+1}{\gamma-1}\right), \qquad \gamma = \sqrt{1 - v_{\rm in}^2/c^2}\,.$$

Analogously, collisions of any nonlinear excitations (phonons, kinks, and breathers) in the framework of the SG model are accompanied by phase shifts only. One of the main features of such collisions is their two-particle nature: When several solitons collide, a shift of any soliton involved into the interaction is equal to a sum of the shifts caused by its independent interaction with other solitons. Such a two-particle nature of the soliton interactions is a specific property of integrable systems. When the primary SG system is modified by external (even conservative) perturbations, many- (in particular, three-) particle effects emerge (Kivshar and Malomed, 1989).

2.3. The Peierls–Nabarro potential

Kinks are the only excitations of the FK model which can exist in a static state due to their topological origin. In the framework of the discrete FK model a kink (antikink) is defined as a minimally possible topologically stable compression (expansion) of the initially commensurate ground state of the chain, when the configuration of atoms far from the localized region coincides with the ground state configuration.

Indeed, the existence of kinks (and even their main properties) do not depend crucially on the discreteness of the primary model, so that the SG model considered above looks often as an acceptable approximation of the FK model which allows to keep the basic features of the system dynamics. However, the very specific property of a discrete lattice such as the FK chain is the existence of the so-called Peierls–Nabarro (PN) periodic potential, $V_{\rm PN}(X)$, to the kink motion, X being the coordinate of the kink's center. First, the PN potential and the topics related to its existence, have been discussed in the context of the theory of dislocations in crystals (see, e.g., Peierls, 1940; Nabarro, 1947; Indenbom, 1958; Indenbom and Orlov, 1962). To understand the origin of the PN potential to the kink motion, first we note that in the continuum limit approximation the system is invariant to any translation of the kink along the chain (and such

translations are characterized by the existence of the so-called Goldstone mode). On contrary, in the discrete model this invariance is absent, and only the translation for the lattice spacing a_s and its integer multipliers are allowed. The smallest energy barrier to overcome for a kink to move through a lattice is called the PN barrier, E_{PN}. In that case, the zero-frequency translational Goldstone mode is replaced by a finite-frequency localized mode known as the PN frequency mode. The value E_{PN} is equal to the difference between two values of the kink's potential energy defined for two stationary configurations, stable and unstable (saddle) ones (see Fig. 2). The first state, Fig. 2a, describes the stationary state corresponding to a minimum of the energy of the chain with one kink situated at the minimum of the potential relief $V_{\mathrm{PN}}(X)$, while the second state, shown in Fig. 2b, is the unstable configuration when the kink is placed on the top of the effective PN barrier.

The potential energy of the chain with one kink,

$$U(\dots, u_{n-1}, u_n, u_{n+1}, \dots) ,$$

is a function of the coordinates of all atoms of the chain. The state shown in Fig. 2a corresponds to one of the minima of the function U, whereas the state shown in Fig. 2b corresponds to a saddle point of the function U, which is situated just between two nearest minima in the N-dimension coordinate (configuration) space, N being the number of atoms in the chain ($N \to \infty$). The saddle and nearest minima points can be connected by an "adiabatic trajectory", i.e. by a curve which is a solution of the following system of coupled differential equations,

$$\frac{\mathrm{d}u_n(\tau)}{\mathrm{d}\tau} = -\frac{\partial}{\partial u_n} U(\dots, u_{n-1}, u_n, u_{n+1}, \dots) , \tag{2.41}$$

where τ is a parameter along the trajectory. Such a trajectory is a curve with the steepest descent, and it describes the adiabatically slow motion of the kink through the chain. Note that when the system is subjected to a thermostat with low temperature, the kink will predominantly move along the adiabatic trajectory. Of course, at a finite velocity, the kink's motion slightly differs from the adiabatic trajectory.

Thus, the PN potential of the kink moving along the chain can be presented in the form,

$$V_{\mathrm{PN}}(X) = U(\dots, u_{n-1}, u_n, u_{n+1}, \dots)|_{x \in \mathrm{ad.tr.}} . \tag{2.42}$$

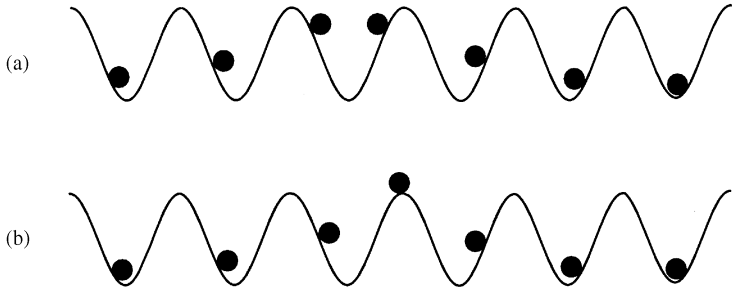

Fig. 2. Stationary configurations of particles in the FK model which correspond to a single kink in the chain: (a) stable, corresponding to a minimum, and (b) unstable, corresponding to a saddle point.

To introduce the collective coordinate describing the motion of the kink's center, X, we present the atomic coordinates as

$$u_n = f(na_s - X) \,, \tag{2.43}$$

where the function $f(x)$ describes the kink's shape. In the continuum limit approximation, i.e. when $g \gg 1$, the function $f(x)$ coincides with the function (2.31) for the SG kink. In the discrete case, the function $f(x)$ differs from the SG shape,

$$f(x) = u_{\mathrm{k}}^{(\mathrm{SG})}(x) + \Delta u_{\mathrm{ad}}(x) \,. \tag{2.44}$$

The function $\Delta u_{\mathrm{ad}}(x)$ is usually called "adiabatic dressing" of the kink. Using Eq. (2.43), the coordinate of the kink's center can be defined as (see Bergman et al., 1983)

$$X = -\frac{\sigma}{a_s}\int \mathrm{d}x\, x f'(x - X) \,, \tag{2.45}$$

where $f'(x) = \mathrm{d}f(x)/\mathrm{d}x$. For numerical simulations with $N < \infty$, it is more convenient to define X integrating Eq. (2.45) by parts to obtain

$$X = \sigma \sum_n u_n + C \,. \tag{2.46}$$

An integration constant C is defined to have the point $X = 0$ corresponding to the kink position at the bottom of the PN potential (at $n = 0$).

The amplitude E_{PN} of the PN potential was calculated in a number of papers for the quasi-continuum limit (Hobart, 1965b, 1966; Pokrovsky, 1981; Ishimori and Munakata, 1982; Ishibashi and Suzuki, 1984; Willis et al., 1986; Lazutkin et al., 1989; Flach and Kladko, 1996), for the weak-bond limit (Joos, 1982; Furuya and Ozorio de Almeida, 1987), as well as by numerical simulations (see, e.g., Hobart and Celli, 1962; Hobart, 1965a; Currie et al., 1977; Sugiyama, 1979; Joos, 1982; Stancioff et al., 1986; Flach and Willis, 1992, 1993; Flach and Kladko, 1996). To estimate the value of the PN potential, we substitute Eq. (2.43) into the expression for the potential energy U and neglect the adiabatic dressing term for the SG kink shape, i.e. take $f(x) = u_{\mathrm{k}}^{(\mathrm{SG})}(x)$. Then, approximating u_{n+1} as

$$u_{n+1} \approx u_n + a_s f'_n \qquad f'_n = \left.\frac{\mathrm{d}f(z)}{\mathrm{d}z}\right|_{z = na_s - X} \,, \tag{2.47}$$

using Poisson summation formulae and keeping only terms corresponding to the first harmonic, we finally obtain (Pokrovsky, 1981)

$$V_{\mathrm{PN}}(X) \approx \sum_{l=0}^{\infty} B_l \cos(lX) \approx \frac{1}{2} E_{\mathrm{PN}}(1 - \cos X) \,, \tag{2.48}$$

where

$$B_l = 16\pi^2 \frac{lg}{\sinh(l\pi^2\sqrt{g})}\left(l^2 + \frac{1}{2\pi^2 g}\right), \quad l \geq 1 \,, \tag{2.49}$$

so that the "bare" PN potential for the case $g \gg 1$ is given by the expression

$$E_{\mathrm{PN}}^{(0)} = 32\pi^2 \frac{g}{\sinh(\pi^2\sqrt{g})}\left(1 + \frac{1}{2\pi^2 g}\right) \approx 64\pi^2 g \mathrm{e}^{-\pi^2\sqrt{g}} . \tag{2.50}$$

For a kink slowly moving with the velocity $v \equiv \mathrm{d}X/\mathrm{d}t \ll c$ along the adiabatic trajectory, the kink's kinetic energy can be calculated as

$$K_{\mathrm{k}} = \frac{1}{2}\sum_n \left(\frac{\mathrm{d}u_n}{\mathrm{d}t}\right)^2 = \frac{1}{2} m \left(\frac{\mathrm{d}X}{\mathrm{d}t}\right)^2 , \tag{2.51}$$

where the effective kink's mass is defined as

$$m(X) \equiv \sum_n \left(\frac{\mathrm{d}u_n}{\mathrm{d}X}\right)^2 = \sum_n (f')^2 . \tag{2.52}$$

Substituting the SG profile $f(x) = u_{\mathrm{k}}^{(\mathrm{SG})}(x)$ into Eq. (2.52), we obtain (see Willis et al., 1986 in the case $g \gg 1$ the following result:

$$m(X) \approx m^{(\mathrm{SG})} + \sum_{l=1}^{\infty} A_l \cos(lX) , \tag{2.53}$$

where

$$A_l = 4l/\sinh(l\pi^2\sqrt{g}) . \tag{2.54}$$

The contribution of the discreteness effects to the kink's shape was investigated numerically, by Currie et al. (1977), Ishimori and Munakata (1982), Willis et al. (1986), Flach and Kladko (1996), and analytically, by Stancioff et al. (1986), De Lillo (1987), Flach and Willis (1993), and Flach and Kladko (1996).

In the case of strong springs, i.e. for $g \gg 1$, the method proposed by Rosenau (1986) leads to the following equation in the first order in the discreteness parameter $\lambda = \frac{1}{12}(a_s/d)^2 \ll 1$,

$$\sin u - u_{xx} = \lambda(u_x^2 \sin u - u_{xx}\cos u) . \tag{2.55}$$

A localized solution of this equation can be easily found by the perturbation theory (see, e.g., Kivshar and Malomed, 1989), and such a correction has the form

$$\Delta u_{\mathrm{ad}}(z) \approx -\lambda\sigma \frac{(3\tanh z - z)}{\cosh z} . \tag{2.56}$$

Thus, the discreteness effects reduce the kink's width, $d \to d_{\mathrm{eff}} = d(1 - \lambda)$. This result coincides with the results of numerical simulations by Currie et al. (1977) and Willis et al. (1986). It is clear that such narrowing of the kink's width should lead to an increasing of the value E_{PN} with respect to that given by Eq. (2.50) which can be estimated as

$$\Delta E_{\mathrm{PN}} \approx \frac{2d\Delta d}{a_s^2}\frac{\mathrm{d}E_{\mathrm{PN}}^{(0)}}{\mathrm{d}g} = -2\lambda g \frac{\mathrm{d}E_{\mathrm{PN}}^{(0)}}{\mathrm{d}g} . \tag{2.57}$$

Analytical calculation of E_{PN} in the continuum limit is a subtle problem, because the kink dressing contributes to E_{PN} through all orders of perturbation in the standard perturbation theory

scheme (Flach and Willis, 1993). An original approach to the problem was proposed by Flach and Kladko (1996). It consists in rewriting the difference equation on discrete variables u_n,

$$g(u_{n+1} + u_{n-1} - 2u_n) - V'_{\rm sub}(u_n) = 0 \,, \tag{2.58}$$

as the differential equation on the continuous function $u(x)$,

$$ga_s^2 u_{xx} - V'_{\rm sub}(u) = [\rho(x) - 1]V'_{\rm sub}(u) \,, \tag{2.59}$$

where

$$\rho(x) = \sum_{n=-\infty}^{\infty} \delta(x - na_s) = a_s\left(1 + 2\sum_{k=1}^{\infty} \cos(2\pi kx/a_s)\right) , \tag{2.60}$$

and then considering the right hand part of Eq. (2.59) as a small perturbation of the SG equation. The result of the first-order perturbation theory is that the kink shape can be obtained by solving the SG equation obtained with the actual substrate potential $V_{\rm sub}$ being replaced by an effective potential

$$V_{\rm eff} = V_{\rm sub} - \frac{1}{24g}\left(\frac{a_s}{2\pi}V'_{\rm sub}\right)^2 . \tag{2.61}$$

As is known, Eq. (2.58) for the stationary configurations can be reduced to the Taylor–Chirikov standard map for an auxiliary two-dimensional dynamical system, so that static solutions of Eq. (2.58) correspond to trajectories (manifolds) of that system. In particular, kink solutions correspond to two homoclinic orbits of the standard map (the stable and unstable manifolds). In the exactly integrable SG model these manifolds overlap. But in the discrete FK system they intersect and are characterized by different energies. The difference between these energies is just the PN energy, and it is determined by the angle of intersection in the point closest to the middle of distance between the fixed points. This angle was calculated by Lazutkin et al. (1989) in the $g \to \infty$ limit, and it results in the PN energy

$$E_{\rm PN} = Ag{\rm e}^{-\pi^2\sqrt{g}} \,, \tag{2.62}$$

where the numerical prefactor is $A = 712.26784\ldots$ Comparing this exact result with the "bare" PN energy (2.50), we see that in the strong coupling limit the kink dressing leads to increasing of the PN energy in 1.13 times only.

In the opposite case of a weak coupling, $g \ll 1$, the kink's parameters in the lowest approximation can be calculated if we neglect the atomic displacements from the bottoms of the substrate potential wells for all the atoms except those in the kink's core. This leads to the following expressions (Joos, 1982; Braun et al., 1990),

$$m \approx 1 \,, \tag{2.63}$$

$$\varepsilon_{\rm k} \approx 2\pi^2 g(1 - 2g) \,, \tag{2.64}$$

$$E_{\rm PN} \approx 2 - \pi^2 g \,. \tag{2.65}$$

Furuya and Ozorio de Almeida (1987) have used the standard map technique to calculate the energies $\varepsilon_{\rm k}$ and $E_{\rm PN}$ in the case $g < 1$. They demonstrated that the minimum energy state shown in

Fig. 2a, is characterized by the energy

$$\varepsilon_{\mathrm{k}} \approx 2\left[1-\cos\left(\frac{2\pi g}{1+3g}\right)\right]+\frac{g}{2}\left[2\pi\frac{(1+g)}{(1+3g)}\right]^2 . \tag{2.66}$$

The "saddle state" shown in Fig. 2b has the energy

$$\varepsilon_{\mathrm{saddle}} = \varepsilon_{\mathrm{k}} + E_{\mathrm{PN}} \approx 2(2-\cos\beta)+\frac{1}{2}g\left[\pi^2+\left(\beta+\frac{1}{\beta}\sin\beta\right)^2\right], \tag{2.67}$$

where

$$\beta = \frac{2\pi g}{(1+2g)+\sqrt{1+4g}}.$$

The dependencies of E_{PN} and ε_{k} on the parameter $d/a_s \equiv \sqrt{g}$ are shown in Figs. 3 and 4, respectively.

The effect of the chain discreteness on the interaction between two kinks was analyzed numerically by Joos (1982), and the exponential law of such an interaction,

$$v_{\mathrm{int}}^{(\mathrm{FK})}(R) = A\mathrm{e}^{-\gamma R/d}\,, \tag{2.68}$$

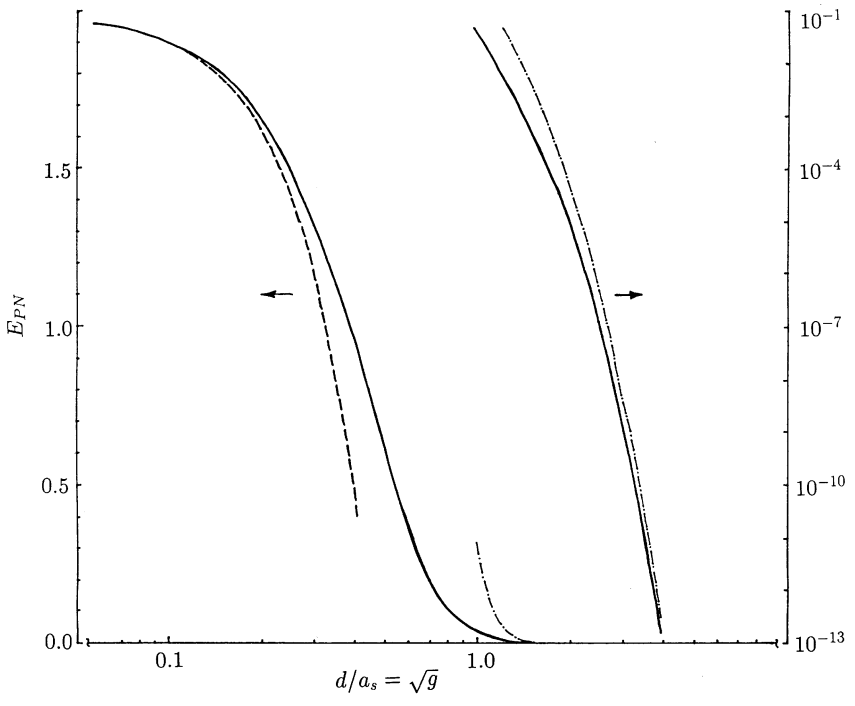

Fig. 3. The maximum (height) of the Peierls–Nabarro potential E_{PN} vs. the normalized kink width $d/a_s = \sqrt{g}$. Solid curve is the numerical results of Joos (1982) and Stancioff et al. (1986), the dashed curve presents the result of the weak coupling analytical approximation, and dashed-dotted curve show the results of the continuum limit approximation.

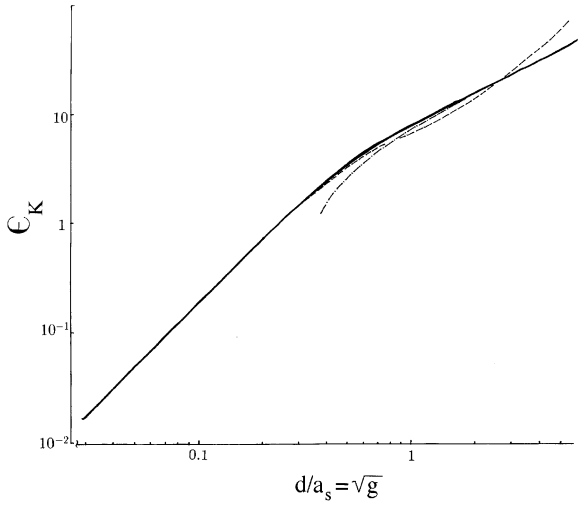

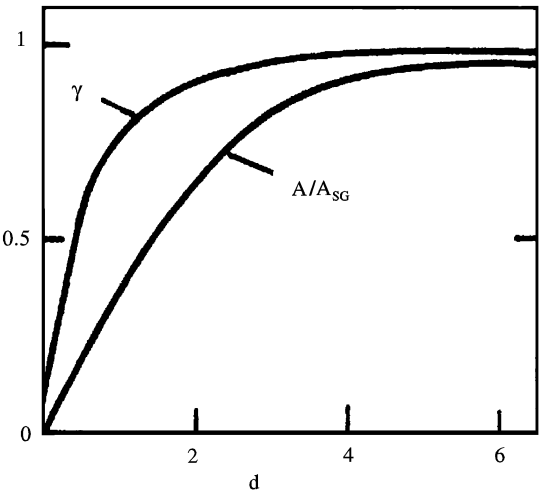

Fig. 4. The kink's rest energy ε_k shown as a function of the parameter $d/a_s = \sqrt{g}$. Solid curve corresponds to the numerical results Joos (1982), the dashed curve presents the results of the weak-coupling approximation, and the dashed-dotted curve, shows the results of the continuum limit approximation.

Fig. 5. The ratio A/A_{SG} (where $A_{SG} = 32\sqrt{g}$) and the parameter γ which determine, according to Eq. (2.63), the kink–kink interaction in the FK chain, as the functions of the kink width d. The numerical curves are based on the data obtained by Joos (1982).

was shown to be valid at $R > 3a_s$ and at any value of the parameter g, although the coefficients A and γ at $g < 5$ depend on g (see Fig. 5); in particular, for $g \to 0$, $A(g) \approx 4\pi^2 g$. Notice also that the presence of a kink in the chain changes the density of the phonon states in the system (Theodorakopoulos et al., 1980).

2.4. Discreteness effects

2.4.1. Kink's equation of motion

In general, there exists no steady-state solutions for a moving kink in the discrete FK model. Due to the lattice discreteness, a moving kink radiates linear waves (phonons). This is one of the main physical effects which explains radiative losses of dislocations calculated for various (more realistic) discrete models (see, e.g., Al'shitz, 1969; Celli and Flytzanis, 1970; Al'shitz et al., 1971; Ishioka, 1973; to cite a few).

For the FK chain, the similar effects were observed numerically by several groups. Here we follow the results by Currie et al. (1977) which allow to make a conclusion about general properties of the FK kink dynamics. If one starts from an initial configuration with kink-type boundary condition, $u_{n\to-\infty} = 0$ and $u_{n\to+\infty} = -\sigma a_s$ (as an initial state, a single kink of the SG equation with some initial velocity is taken usually), such a configuration decays into phonons and a single "dressed" kink, i.e. a kink with the shape modified by the lattice discreteness. Then the FK kink propagates through the chain not freely but with an oscillating velocity, the oscillations being

caused by the lattice discreteness. Moving with a variable velocity, such a kink loses its kinetic energy emitting phonons, so that the kink will be trapped by the PN potential below a certain critical velocity $v_{\rm PN}$. The kink trapped by the PN potential oscillates near a minimum of the potential well continuously emitting phonons, and finally it reaches a stationary state corresponding to a static configuration. Such a behavior can be easily understood in the framework of a simple physical picture of an effective particle with the mass m moving in the periodic PN potential when the total particle's energy is defined as

$$E = \frac{m}{2}\left(\frac{\mathrm{d}X}{\mathrm{d}t}\right)^2 + V_{\rm PN}(X)\,. \tag{2.69}$$

When the energy E is larger than the PN energy, the particle propagates along the chain and a change of its coordinate is described by the equation,

$$X(t) = 2\ \mathrm{am}\,(\omega_{\rm PN}t/k; k)\,, \tag{2.70}$$

where $k = \sqrt{E_{\rm PN}/E}$ is the modulus of the Jacobi elliptic function, and the particle's velocity is varying periodically around its mean value with the frequency

$$\omega_{\rm trav}(E) = \frac{\omega_{\rm PN}}{2kK(k)} = \left\langle\frac{\mathrm{d}X}{\mathrm{d}t}\right\rangle\left(\frac{2\pi}{a_s}\right) \tag{2.71}$$

caused by the periodic PN relief. In the opposite case, when $0 < E < E_{\rm PN}$, the effective particle (kink) gets trapped at a minimum of the PN potential, and the particle's coordinate changes according to the law

$$X(t) = 2\sin^{-1}\left[k\,\mathrm{sn}(\omega_{\rm PN}t; k)\right]\,, \tag{2.72}$$

where this time the modulus of the elliptic function is $\tilde{k} = \sqrt{E/E_{\rm PN}} = k^{-1}$ and the frequency of the kink oscillations is given by the expression

$$\omega_{\rm trap}(E) = \frac{\pi\omega_{\rm PN}}{2K(\tilde{k})}\,, \tag{2.73}$$

so that $0 < \omega_{\rm trap}(E) < \omega_{\rm trap}(0) \equiv \omega_{\rm PN}$, where

$$\omega_{\rm PN}^2 = \frac{1}{m}\frac{\mathrm{d}^2V_{\rm PN}(X)}{\mathrm{d}X^2}\Big|_{X=0} \approx \frac{E_{\rm PN}}{2m} \tag{2.74}$$

is the frequency of harmonic oscillation of the kink near the bottom of the PN potential, the PN frequency.

For the discrete FK chain, the total kink's energy E is not a conserved quantity because of a nonlinearity-induced coupling between different eigenmodes, including phonons. This means that motion of a kink through a chain can be described with the help of an effective particle only approximately, and in reality such a dynamics should be modified by exciting phonon modes. In fact, a kink moving through the lattice with a varying velocity, or a kink trapped by the lattice discreteness and oscillating near the bottom of the PN potential, acts as an effective force on the phonon subsystem with the frequencies $n\omega_{\rm trav}$ or $n\omega_{\rm trap}$ ($n = 1, 2, \ldots$). Such an oscillating force leads

to a generation of phonons, and the kink's energy decreases, being transformed into the energy of the excited phonon modes. As a result, the phenomenology of an effective particle introduced above should be modified by including an effective friction force,

$$F^{(\mathrm{fr})} = -m\eta\frac{\mathrm{d}X}{\mathrm{d}t}\,, \tag{2.75}$$

which causes the final trapping of the kink by the PN potential.

Adiabatic dynamics of a kink in a discrete FK chain was analysed analytically by Ishimori and Munakata (1982) by applying the perturbation theory for solitons developed earlier by McLaughlin and Scott (1978) for the case when the parameter responsible for the discreteness effects is small,

$$\lambda = \frac{1}{12}\left(\frac{a_s}{d}\right)^2 \ll 1\,.$$

Ishimori and Munakata (1982) calculated the effective friction produced by radiation of phonons and they showed that the moving kink radiates phonons predominantly to the backward direction. A more careful study of the kink's dynamics in the discrete chain was carried out by Peyrard and Kruskal (1984) and Boesch et al. (1989) with the help of extended numerical simulations. They showed that the effective friction coefficient η of the kink is a complicated function of the system parameters. Several results are presented in Figs. 6 and 7, which show variations of the kink

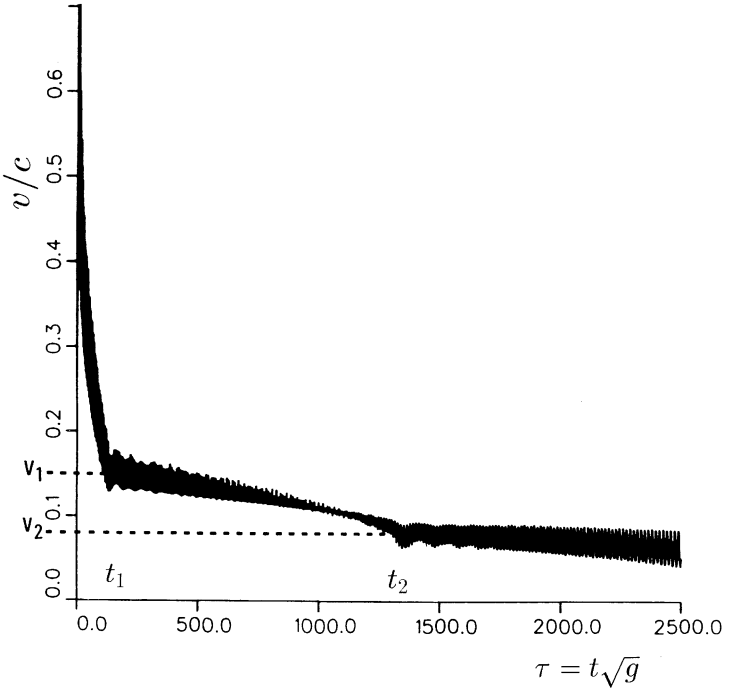

Fig. 6. Evolution of the velocity of a free kink with the initial velocity $v_0 = 0.8c$ in the FK chain with $\sqrt{g} = 0.95$. Arrows show the disappearance of the resonances $k_1 = k_2 = 1$ (at $t = t_1$) and $k_1 = 5$, $k_2 = 1$ (at $t = t_2$) (Peyrard and Kruskal, 1984).

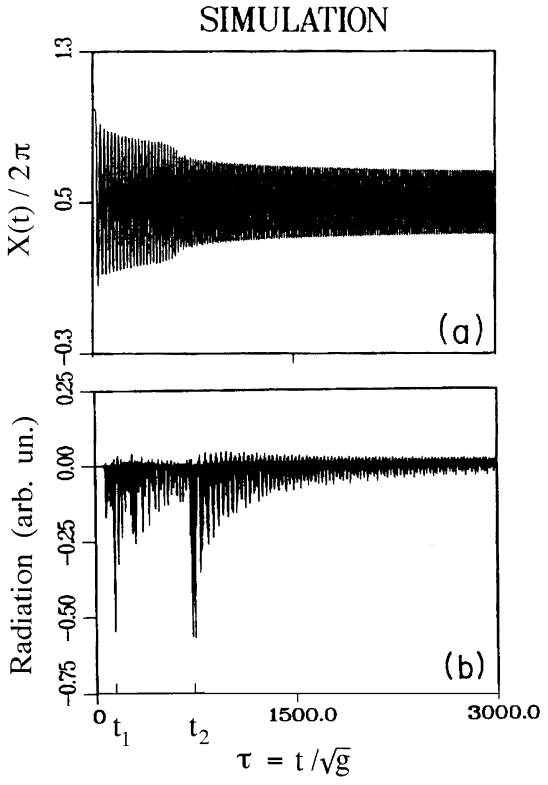

Fig. 7. Simulation results for (a) oscillation of the kink's coordinate $X(t)$ and (b) instantaneous Poynting's flux of phonon radiation away from the kink trapped by the PN potential well, for the FK chain with $g = 0.791$. Arrows indicate the appearance of new resonances with $k_5 = k_2 = 1$ (at $t = t_1$) and $k_1 = 4$, $k_2 = 1$ (at $t = t_2$) (Boesch et al., 1989).

velocity in the moving and trapped states. Before discussing the features observed in numerical simulations in detail, let us introduce the density of the phonon states $\rho(\omega)$ in the one-dimensional lattice (see, e.g., Kosevich, 1972)

$$\rho(\omega) = \frac{2}{\pi} \frac{\omega}{\sqrt{(\omega^2 - \omega_{\min}^2)(\omega_{\max}^2 - \omega^2)}}, \tag{2.76}$$

where the normalization

$$\int_{\omega_{\min}}^{\omega_{\max}} d\omega \, \rho(\omega) = 1$$

has been used. One can see that the function $\rho(\omega)$ tends to infinity at the edges of the phonon spectrum band, $\omega_{\min}$ and $\omega_{\max}$. Besides, the anharmonicity of the lattice vibrations is known to produce higher-order harmonics in the phonon spectrum. As a result, it is clear that the energy exchange between the kink translational or trapped motion is possible provided the following

resonance condition is fulfilled,

$$k_1\omega_{\rm k} = k_2\omega_{\rm ph}(\kappa)\,, \tag{2.77}$$

where $\omega_{\rm k}$ is equal to $\omega_{\rm trav}$ or $\omega_{\rm trap}$ depending on the type of the kink motion, and the integer numbers k_1 and k_2 stand for the order of the resonance. The maximum of the radiative damping produced by the resonant energy transfer to the phonon subsystem is realized for the case $k_1 = k_2 = 1$ and $\omega_{\rm ph}$ being close to the edges of the phonon spectrum where the phonon density takes a maximum value. Below we discuss in more detail the numerical simulation results for the propagating and trapped kink regimes.

2.4.2. Moving kinks

As is seen in Fig. 6 (Peyrard and Kruskal, 1984), a fast kink launched at some velocity, $v_0 < c$, loses immediately its velocity up to the "critical" value v_1 depending on the initial velocity v_0, say during the time interval t_1. For $t < t_1$, the inequality

$$\omega_{\rm min} < \omega_{\rm trav} < \omega_{\rm max} \tag{2.78}$$

is fulfilled, so that this condition does explain a very high rate of the energy losses observed in numerical simulations. However, at the moment $t = t_1$ the first-order resonance disappears and the radiation-induced damping is now caused by the second-order resonance ($k_1 = 2$, $k_2 = 1$), so that the value of the effective friction η is abruptly lowered (see Fig. 6). Correspondingly, the kink radiation becomes drastically smaller, and the mean velocity of the kink translational motion decreases now much slower. At the moment t_2, when $v_{\rm k} = v_2$, the second-order resonance condition becomes not valid, and for $t > t_2$ the velocity decreases even more slowly but subsequently the kink will get trapped by the PN relief at a certain $t = t_{\rm trap}$ when its kinetic energy reaches the value corresponding to the PN energy, $E = E_{\rm PN}$. The numerical simulations show that the time interval $t_{\rm trap}$ is indeed extremely large for the case $g \gg 1$. Nevertheless, this time $t_{\rm trap}$ becomes much smaller for narrow kinks, for example, for $\sqrt{g} = 0.75$ a kink with the initial velocity $v_0 = 0.8c$ cannot propagate through the lattice more than for two lattice spacings and, as a result, it becomes immediately trapped by the lattice discreteness. Very similar behavior of a kink was observed by Combs and Yip (1983) for the so-called ϕ^4 model when simulating the kink propagation in a discrete lattice.

2.4.3. Trapped kinks

The evolution of a trapped kink analyzed numerically by Boesch et al. (1989) and shown in Fig. 7 can be explained in a similar way, taking into account the structure of the phonon spectrum and the density of the phonon states. First of all, we note that the oscillation frequency of a trapped kink, $\omega_{\rm trap}$, increases from zero to its maximum value $\omega_{\rm PN}$. When increasing the frequency $\omega_{\rm trap}$, the order of the resonance is lowered, and for a certain harmonic it becomes possible to cross eventually the edge frequency of the phonon spectrum to satisfy a resonance condition even if this condition was not satisfied earlier. Consequently, emission of phonons by a kink should increase. Besides, the value of the PN frequency,

$$\omega_{\rm PN} \approx \left\{\frac{2\pi^6}{3}\frac{g\sqrt{g}}{\sinh(\pi^2\sqrt{g})}\left(1 + \frac{1}{2\pi^2 g}\right)\right\}^{1/2}, \tag{2.79}$$

is usually much smaller than the edge phonon frequency $\omega_{\min} = 1$, and thus a kink may radiate phonons only due to an excitation of higher-order harmonics, i.e. those corresponding to a large resonance number. For example, at $g = 1$ the PN frequency is calculated to be $\omega_{\rm PN} \approx 0.18$ [the rigorous procedure to calculate $\omega_{\rm PN}$ was suggested by Boesch and Willis (4); see also Braun (1990)] so it is necessary to satisfy the condition $k_2 \geq 6$ in Eq. (2.77) to get a resonant generation of phonons. Slowly changing its frequency, the kink emits suddenly large burst of radiation when its frequency (or frequencies of higher-order harmonics) passes the edges of the phonon spectrum where the density of the phonon states is maximum. This gives peculiarities in the temporal dynamics of the kink's coordinate shown in Fig. 7.

Analytical results to evaluate the radiation-induced friction coefficient η are rather lengthy to be presented here in detail. However, we should mention that the first analytical calculations were made by Ishimori and Munakata (1982) on the basis of the first-order approximation of the soliton perturbation theory, but finally such results did not reproduce well the features of the kink dynamics observed in direct numerical simulations. The rough estimates made by Peyrard and Kruskal (1984) did agree with the corresponding simulation results and they are therefore more satisfactory. The rigorous procedure was proposed by Willis et al. (1986) [see also Boesch et al. (1988), where a projection-operator technique was developed to find the value of the effective friction η, and also the work by Igarashi and Munakata (1989)]. The main idea of this approach is to look for the kink solution in a discrete case in the form

$$u_n(t) = f[na_s - X(t)] + q_n(t) \tag{2.80}$$

and develop a Hamiltonian formalism for the kink coordinate $X(t)$ and its conjugated momentum $P(t) = m(t)(\mathrm{d}X/\mathrm{d}t)$ which are treated as canonical variables *extracted* from the full set of the variables of the discrete FK model. The variables $q_n(t)$ and the corresponding momenta $p_n(t) = \mathrm{d}q_n/\mathrm{d}t$ describe the radiation field as well as the deviation of the kink's shape from its analytical solution calculated in the continuum limit approximation. Introducing the two new canonical variables requires two constraints,

$$C_1 \equiv \sum_n f_n' q_n = 0 \quad \text{and} \quad C_2 \equiv \sum_n f_n' p_n = 0 \,, \tag{2.81}$$

and modifying of the Poisson brackets,

$$\{X, P\} = 1 \quad \text{and} \quad \{q_n, p_{n'}\} = \delta_{n,n'} \,. \tag{2.82}$$

The equations of motion are then obtained according to the Hamiltonian formalism,

$$\frac{\mathrm{d}\theta}{\mathrm{d}t} = \{\theta, H\} \,,$$

θ stands for the canonical variables X, P, q_n, and p_n, and the PN frequency is then found by linearizing those equations for small-amplitude oscillations. The procedure described does give an excellent agreement with numerical simulations taking effectively a renormalization of the kink shape due to a strong discreteness of the model.

2.4.4. Multi-kinks

For a weak interatomic interaction, e.g., $g \leq g_{4\pi} \approx 0.2025$, a repulsion between kinks is weak, and it competes with attractive forces acting from the effective PN potential. Thus, two (or even

more) kinks can be trapped by the lattice discreteness to create a bound state propagating as a single 4π-kink. Moreover, at high velocities, $v \sim c$, such multi-kinks remain stable even for $g \gg g_{2N\pi}$, where $g_{2N\pi}$ is the critical value which depend on the order of such a multi-kink, N being the number of the simple 2π kinks in the multi-kink. The understanding of the existence of this kind of multi-kink is still an open problem, however, it is clear that they become possible due to a Lorentz contraction of the kink's width for large velocities.

Such 4π-kinks, and also 6π-kinks, were discovered numerically by Peyrard and Kruskal (1984), and such multi-kink structures are rather stable to be easily detected in numerical simulations. The results of the numerical simulations for the velocity of 4π-kink and 6π-kink are shown in Fig. 8. Surprisingly, an effective friction coefficient for such types of multi-kink solutions becomes almost negligible allowing them to propagate in the lattice without visible radiative losses. As we have mentioned, there exists no clear analytical explanation of this phenomenon yet.

2.4.5. *Breathers*

Even a weak discreteness does not allow oscillating breather modes exist as dynamical eigenstates of the chain, because it acts as an external perturbation and breaks the integrability of the SG model. As a result, the breathers radiate linear waves and slow decay. In the systems with a very weak coupling between particles in the chain, nonlinear oscillating states are strongly modified due to discreteness. Such "discrete breathers", or nonlinear localized modes, are briefly discussed in Section 6, where is shown that these modes can be strongly localized involving only a few particles into the oscillating dynamics.

For strong coupling between the particles, the breather dynamics can be still considered in the framework of the perturbed SG equation which takes into account the discreteness effects. Then, the breather dynamics and the corresponding lifetime depend on the input energy, and are different for the breathers of small and large amplitudes (see, e.g., Kivshar and Malomed, 1987). In the small-amplitude limit, when the breather width is much larger than the lattice spacing, the effects of

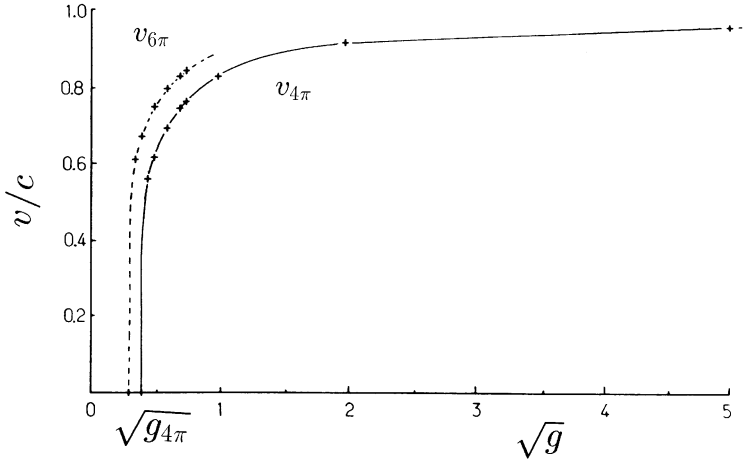

Fig. 8. Velocities $v_{4\pi}$ (solid curve) and $v_{6\pi}$ (dashed curve) of the 4π- and 6π-kinks as functions of the parameter $\sqrt{g} = d/a_s$ in the FK model (Peyrard and Kruskal, 1984).

discreteness are almost negligible, and the radiation-induced losses of the breather energy can be neglected. These losses are usually *exponentially small* in the parameter defined as a ratio between the lattice spacing and the breather's width, and it is "beyond of all order". Neglecting radiation, we can find approximate periodic solutions for the breathers by means of multi-scale asymptotic expansion. The rigorous procedure to find such high-frequency breather modes for general models with on-site potential (arbitrary substrate potential) was suggested by several authors [see, e.g., Kosevich and Kovalev (1974a); Remoissenet (1986), and references therein].

For $g \leq 1$, a low-frequency breather may survive as two separate kink and antikink trapped in the corresponding wells of the PN potential. The effect of discreteness of the breather dynamics and the calculation of the effective PN potential can be found in a paper by Boesch and Peyrard (1991). We will outline some essential ideas here, but the reader is referred to the original work (Boesch and Peyrard, 1991) for the calculational details.

To describe a breather in a discrete chain, we use the ansatz [cf. Eq. (2.36)],

$$u_n^{(\mathrm{br})} = 4\tan^{-1}\left[\frac{\sinh(k_\mathrm{b}Z)}{\cosh[k_\mathrm{b}(n-X)]}\right], \tag{2.83}$$

where X is the center of the breather, which is treated as a parameter, $2Z(t)$ represents the distance between two subkinks which form the breather, and the breather's frequency is defined as $\omega_\mathrm{b} = \sqrt{1-k_\mathrm{b}^2}$. The ansatz (2.83) should be used to calculate the Hamiltonian of the FK chain (Boesch and Peyrard, 1991) which consists of two parts describing, independently, internal and translational dynamics of the breather. If we choose the initial breather profile (2.83) at the time $t=0$ when the subkinks are at their maximum separation $Z(t)|_{t=0} = Z_0$, this yields the initial profile condition

$$\tanh(k_\mathrm{b}Z_0) = k_\mathrm{b}\,. \tag{2.84}$$

Then, the breather's total energy can be simplified keeping the first two terms in the Fourier series [since the coefficients decay exponentially as $1/\sinh(\pi^2/k_\mathrm{b})$], so that the total energy becomes

$$E^{\mathrm{br}}(Z_0, X) = 16k_\mathrm{b}\left[1 + \frac{2\pi^2/k_\mathrm{b}}{\sinh(\pi^2/k_\mathrm{b})}\cos(2\pi Z_0)\cos(2\pi X)\right]. \tag{2.85}$$

Eq. (2.85) must be considered simultaneously with the condition (2.84) which changes the value of k_b for each Z_0. Note that for high-frequency (i.e., small-amplitude) breathers where discreteness effects are small, $k_\mathrm{b} \to 0$ and we recover the well known continuum expression for the SG breather energy, $E^{\mathrm{br}} = 16k_\mathrm{b}$. For large-amplitude breathers, Eq. (2.83) indicates there are *two* PN potentials, one for X and the other for Z_0, and it defines the positions where the initial breather profile will be trapped if started from rest.

3. On-site potential of a general shape

3.1. General properties

The standard FK model (2.1)–(2.5) assumes a sinusoidal shape of the one-site substrate potential. However, in realistic physical models the shape of the substrate potential may deviate from the

sinusoidal one. Indeed, the on-site substrate potential in the FK model is in fact an effective potential produced by the coupling of the atoms in the chain with other degrees of freedom, e.g. with substrate atoms. Then, only in the lowest approximation, i.e., when (i) the substrate atoms constitute a simple lattice with one atom per elementary cell, and (ii) in the Fourier expansion of the interaction potential the main approximation is given by the first harmonic, the simple sinusoidal potential can be derived in a rigorous way. In all other physical situations, the periodic potential $V_{\rm sub}(x)$ deviates from the sinusoidal form. For example, for atoms adsorbed on metal surfaces the substrate potential is usually characterized by sharp bottoms and flat barriers (Braun, 1989). Moreover, if the underlying substrate is characterized by a complex unit cell, the potential $V_{\rm sub}(x)$ should have a quite complicated shape with several minima and maxima.

In the present chapter we discuss a general case when the substrate potential $V_{\rm sub}(x)$ is periodic with the period $a_s = 2\pi$ and for $x \in (0, a_s)$ it has at least one minimum, say at $x = x_0$ [with $V_{\rm sub}(x_0) = 0$], and one maximum, at $x = x_{\rm m}$ [with the normalization $V_{\rm sub}(x_{\rm m}) = \varepsilon_s = 2$]. As above, we consider only the commensurable case when the ground state has only one atom per one period a_s of the substrate potential.

The deviation of the substrate potential from the sinusoidal shape changes the parameters of both linear and nonlinear excitations and, this may lead to appearance of new kink solutions and phonon branches. Nonsinusoidal substrate potential drastically modifies breather solutions. Let us first discuss the problems related to such a modification of the substrate potential from a general point of view.

Phonons in the FK model are characterized by the dispersion relation [see Eq. (2.17)]

$$\omega_{\rm ph}^2(\kappa) = \omega_{\rm min}^2 + 2g(1 - \cos\kappa), \quad |\kappa| < \pi \,, \tag{3.1}$$

where the minimum frequency $\omega_{\rm min}$ is defined as

$$\omega_{\rm min}^2 = V''_{\rm sub}(x_0) \,, \tag{3.2}$$

and it corresponds to the vibration of an isolated atom at the minimum of the substrate potential (recall $m_a = 1$). In the standard FK model this frequency is $\omega_{\rm min} = 1$. Thus, in the case of sharp wells, one has $\omega_{\rm min} > 1$, while for the flat bottoms, $\omega_{\rm min} < 1$. Note that in a generalized FK model it might exist more than one branch in the phonon spectrum if the potential $V_{\rm sub}(x)$ has more than one minimum per the potential period (see below, Section 3.3).

Kinks can be easily described in the continuum limit approximation which is valid provided $g \gg 1$. If the discreteness effect are negligible, the motion equation becomes

$$u_{tt} - d^2 u_{xx} + V'_{\rm sub}(u) = 0 \,. \tag{3.3}$$

Eq. (3.3) is Lorentz invariant and, therefore, it always has a stationary solution $u(x,t) = \phi(y)$, $y = \gamma[x - X(t)]/d$, $\gamma = (1 - v^2/c^2)^{-1/2}$, where the kink coordinate is defined as $X(t) = X_0 + vt$ and its velocity, $v = {\rm d}X/{\rm d}t$ is within the interval $|v| < c$ (recall, in the notations we adopted $c = d$). Equation for the function $\phi(y)$,

$$\frac{{\rm d}^2\phi}{{\rm d}y^2} = V'_{\rm sub}(\phi) \,, \tag{3.4}$$

looks like the equation of motion of an effective particle with the coordinate ϕ in the potential $U(\phi) = -V_{\rm sub}(\phi)$. The periodic oscillation of the particle near the bottom of the potential $U(\phi)$

corresponds to linear waves, the rotation of the particle corresponds to the so-called cnoidal waves, and the separatrix trajectory generates the kink solution, which has the boundary conditions,

$$\phi(y) \to x_0 (\mathrm{mod}\, 2\pi), \ \mathrm{d}\phi(y)/\mathrm{d}y \to 0 \quad \text{as } y \to \pm\infty \ . \tag{3.5}$$

Thus, Eqs. (3.4) and (3.5) yield

$$\left(\frac{\mathrm{d}\phi}{\mathrm{d}y}\right)^2 = 2V_{\mathrm{sub}}(\phi) \ , \tag{3.6}$$

and the shape of the kink can be expressed as

$$y = \mp \int_{x_\mathrm{m}}^{\phi(y)} \frac{\mathrm{d}\phi}{\sqrt{2V_{\mathrm{sub}}(\phi)}} \ . \tag{3.7}$$

Here the upper sign corresponds to a kink solution (local contraction of the chain) and the lower sign corresponds to an antikink, and the value x_m is the coordinate of the substrate potential maximum. Thus, the kink (antikink) solution connects two nearest neighboring minima of the substrate potential, say x_0 and $x_0 + 2\pi$. If the substrate potential has more than two minima per period, one may expect to find more than one type of the kink solutions (see below Section 3.3).

The shape of a stationary kink can be characterized by its asymptotics at infinities. If $u(x) \to x_0$ for $x \to +\infty$ or $x \to -\infty$, then

$$|u_\mathrm{k}(x) - x_0| \propto \exp(-\omega_{\min}|x|/d), \quad |x| \to \infty \ . \tag{3.8}$$

The tails of the kink define the character of interaction between kinks. Therefore, the strength of the kink–kink interaction is weaker in the case $\omega_{\min} > 1$ (i.e. for the substrate potential with sharp bottoms) than is in the case of the SG model. The "core" of the kink is determined by the expression,

$$u_\mathrm{k}(x) \approx x_\mathrm{m} - \left(\frac{\sigma x}{d}\right)\sqrt{2V_{\mathrm{sub}}(x_\mathrm{m})}\left(1 - \frac{x^2}{6d_{\mathrm{eff}}^2}\right), \tag{3.9}$$

for $|u_x(x) - x_\mathrm{m}| \ll d$, so that the kink's effective width becomes

$$d_{\mathrm{eff}} = \frac{d}{\sqrt{-V''_{\mathrm{sub}}(x_\mathrm{m})}} \ . \tag{3.10}$$

According to Eq. (2.53), the kink rest mass can be found as

$$m = \frac{1}{4\pi^2\sqrt{g}} \int_{x'_0}^{x''_0} \mathrm{d}\phi \sqrt{2V_{\mathrm{sub}}(\phi)} \ , \tag{3.11}$$

where x'_0 and x''_0 are the positions of two adjacent successive minima of the substrate potential. The energy associated with a single kink at rest is $\varepsilon_\mathrm{k} = mc^2$, where in our notations $c = d$, and the kink's kinetic energy K_k is defined as $K_\mathrm{k} = mc^2(\gamma - 1) \approx \frac{1}{2}mv^2$.

Unlike the SG kink, a kink in the chain with a nonsinusoidal one-site potential may have internal degrees of freedom, the so-called "shape modes" (see, e.g., Segur, 1983; Campbell et al., 1983; Braun et al., 1997). To explain the existence of such modes, let us linearize the motion

equation (3.3) around the kink's shape substituting $u(x) = u_k(x) + \Psi(x)e^{i\omega t}$. The function $\Psi(x)$ satisfies the linear Schrödinger–type equation

$$-d^2\frac{d^2\Psi}{dx^2} + W(x)\Psi(x) = \omega^2\Psi(x)\,, \tag{3.12}$$

where

$$W(x) = \left|\frac{d^2V_{sub}(u)}{du^2}\right|_{u=u_k(x)}\,. \tag{3.13}$$

Eqs. (3.12) and (3.13) always admit a continuum of the plane wave solutions (phonons) with the frequencies $\omega > \omega_{min}$, and also the so-called Goldstone mode $\Psi(x) = du_k/dx$ with $\omega = 0$. In a discrete FK model the latter mode has a nonzero eigenvalue ω_{PN}. Besides the modes mentioned above, Eq. (3.12) may have one or more eigenfunction with discrete eigenfrequencies within the gap $(0, \omega_{min})$ or, depending on the shape of the substrate potential, with frequencies $\omega > \omega_{max}$ (see details in Braun et al., 1997a). Such modes are localized around the kink and they may be treated as "internal" oscillations of the kink's shape. Such shape modes can be excited during collisions between kinks, or due to interaction of the kinks with impurities, so that they play an important role in the kink dynamics.

Breathers. The important feature of the nonsinusoidal generalization of the FK model is the absence of the exact solutions for the breather modes (dynamical oscillating solitons). In the same time, the breather modes do exist as long-lived nonlinear spatially localized vibrations of the chain, and they may be calculated using an asymptotic procedure (see, e.g., Kosevich and Kovalev, 1974a; Remoissenet, 1986). Let us look for a solution of the nonlinear motion equation in the limit of small amplitudes using the asymptotic expansion,

$$u_{br}(x,t) = \mu\Phi(x,t)e^{i\Omega t} + \text{c.c.}\,, \tag{3.14}$$

where $\mu = (\omega_{min}^2 - \Omega^2)^{1/2}$ is a small parameter of the asymptotic procedure. Substituting Eq. (3.14) into the discrete motion equation and expanding the substrate potential for small u_n,

$$V'_{sub}(u) \approx \omega_{min}^2 u + \beta u^2 + \tilde{\beta}u^3\,, \tag{3.15}$$

we may derive an effective evolution equation for the wave envelope Φ assuming that the latter is changing slowly of the scales of order of the lattice spacing (see details, e.g., in the paper by Remoissenet, 1986),

$$2i\Phi_t - Q\Phi_{zz} + G|\Phi|^2\Phi = 0\,, \tag{3.16}$$

where the variable z is connected with a reference frame moving with the wave group velocity, and the parameters Q and G are functions of the parameters of the effective potential (see Remoissenet, 1986). Eq. (3.16) is the nonlinear Schrödinger (NLS) equation and it has localized soliton solution provided $QG > 0$, the latter condition is that for breathers to exist.

The effective NLS equation (3.16) describes a breather for any type of the substrate potential. However, due to the presence of higher-order harmonics, only the SG model will support nonradiating breathers because the integrability of the SG model implies a cancellation of this kind of higher-order effects. For other type of the substrate potential, it has been rigorously shown that exact breather solutions do not exist (see, e.g., Denzler, 1993; Birnir, 1994) and a breather, being

excited in a chain, radiates slowly energy. This kind of long-lived radiation process has been recently estimated for the breather of the ϕ-model (Geike, 1994).

As will be shown below, the breathers and kink's shape modes play a very important role in kink–antikink collisions. In particular, collision of kinks with internal degrees of freedom may display resonances (Campbell et al., 1983). In a nonintegrable FK model, a breather may be excited in a result of inelastic (destructive) collision between a kink and antikink.

In the sections which follow below, we consider several examples of the non-sinusoidal substrate potential $V_{\rm sub}(u)$. One of the examples is the so-called double SG potential (see Frank and van der Merwe, 1949b; Condat et al., 1983)

$$V_{\rm sub}^{\rm (DSG)}(x) \propto -[\cos x + s\cos(2x)] \,. \tag{3.17}$$

The potential (3.17) is topologically similar to the SG model for $|s| < 1/4$, but it is characterized by flat bottoms for $1/4 < s < 0$ or by sharp wells for $0 < s < 1/4$. Besides, the shape of the potential (3.17) has a double well (DW) structure for $s < -1/4$ and a double-barrier (DB) form for $s > 1/4$. We would like to mention also more general on-site potentials proposed by Peyrard and Remoissenet (1982) (see also Remoissenet and Peyrard, 1984) which will be also analysed below.

3.2. Nonsinusoidal on-site potential

A convenient shape of the on-site potential which describes a realistic situation, e.g., for systems of adsorbed atoms, was suggested by Peyrard and Remoissenet (1982) (in the original paper the parameter $r = -s$ was used),

$$V_{\rm sub}^{(NS)}(x) = \frac{(1+s)^2(1-\cos x)}{(1+s^2-2s\cos x)}, \quad |s| < 1 \,. \tag{3.18}$$

The parameter s describes different shapes of the on-site potential at the unchanged amplitude, including the case of flat bottoms or flat tops (see Fig. 9).

The phonon spectrum for the model (3.18) is characterized by the minimum (gap) frequency

$$\omega_{\rm min} = \frac{(1+s)}{(1-s)} \,, \tag{3.19}$$

the kinks, by a characteristic width,

$$d_{\rm eff} = \omega_{\rm min}\, d \,, \tag{3.20}$$

and the kink mass is equal to (see Fig. 10)

$$m = m^{\rm (SG)}\left(\frac{\omega_{\rm min}}{\omega_*}\right)\begin{cases}\tanh^{-1}\omega_* & \text{if } s<0 \,,\\ \tan^{-1}\omega_* & \text{if } s>0 \,,\end{cases} \tag{3.21}$$

where $\omega_* \equiv \sqrt{|\omega_{\rm min}^2 - 1|}$. The shape of the kink was found numerically in the work by Peyrard and Remoissenet (1982). The kink is narrow, for the case of flat bottoms ($s < 0$), and it is wide, for the opposite case of sharp wells ($s > 0$). The kink rest mass $m_{\rm k}$ tends to zero provided $s \to -1$, i.e. kinks will be more easy to create in the systems with flat bottom potential.

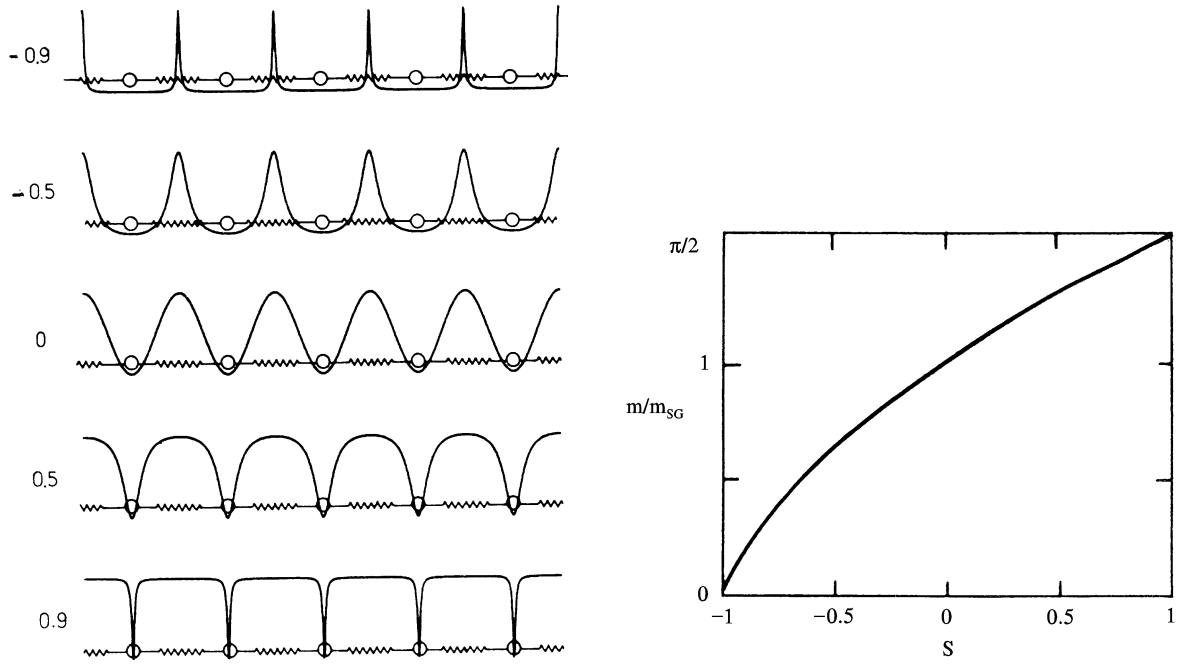

Fig. 9. Schematic presentation of the one-dimensional chain with the variable substrate potential (3.18) for different values of the parameter s (Peyrard and Remoissenet, 1982).

Fig. 10. Relative kink mass as a function of the parameter s determined by the shape of the substrate potential (3.18) (Peyrard and Remoissenet, 1982).

Considering properties of the discrete chain with the substrate potential (3.18), we may naturally expect that the change of the potential shape will lead to a change of the PN barrier. This has been confirmed in numerical simulations made by Peyrard and Remoissenet (1982) and it is shown in Fig. 11. Analytically, the value E_{PN} for this model was estimated by Ishibashi and Suzuki (1984). They used the kink shape corresponding to the continuum approximation to calculate the system energy for the discrete lattice. The result is given by the following expressions,

$$\frac{E_{\mathrm{PN}}}{E_{\mathrm{PN}}^{(\mathrm{SG})}} \propto \begin{cases} \exp\left(\frac{2\pi^2\sqrt{g|s|}}{1+\sqrt{|s|}}\right) & \text{if } s < 0\,, \\ \left|\cos\left(\frac{2\pi^2\sqrt{gs}}{1+s}\right)\right| \exp\left(\frac{2\pi^2 s\sqrt{g}}{1+s}\right) & \text{if } s > 0\,. \end{cases} \tag{3.22}$$

It is interesting that in the case $s > 0$ (sharp wells) the amplitude of the PN potential E_{PN} depends nonmonotonically on the elastic constant g. We should note here that such a nonmonotonic dependence of the PN energy vs. a variation of the coupling in the lattice had been discovered earlier (Kurosawa, 1962; Sanders, 1962; Kratochvil and Indenbom, 1963; Hobart, 1965b; Ishioka, 1974) for a simplified periodic potential composed of a sequence of pieces of a shifted parabola. In the standard FK model with the sinusoidal substrate potential the PN relief $V_{\mathrm{PN}}(X)$ to the kink motion has its minimum at, e.g., $X = 0$, i.e. for the atoms arrangement with two central particles at

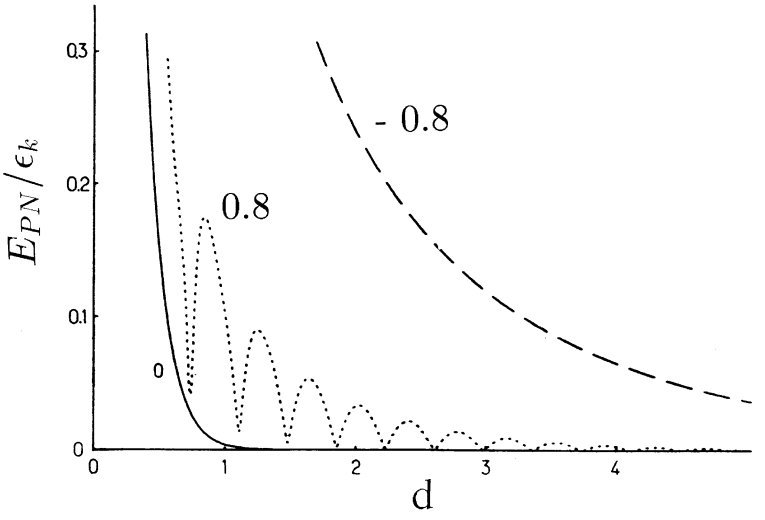

Fig. 11. Ratio of the height of the PN potential, E_{PN}, to the kink rest energy, ε_k, as a function of the kink width, d, for different values of the parameter s (-0.8, 0, and $+0.8$) (Peyrard and Remoissenet, 1982).

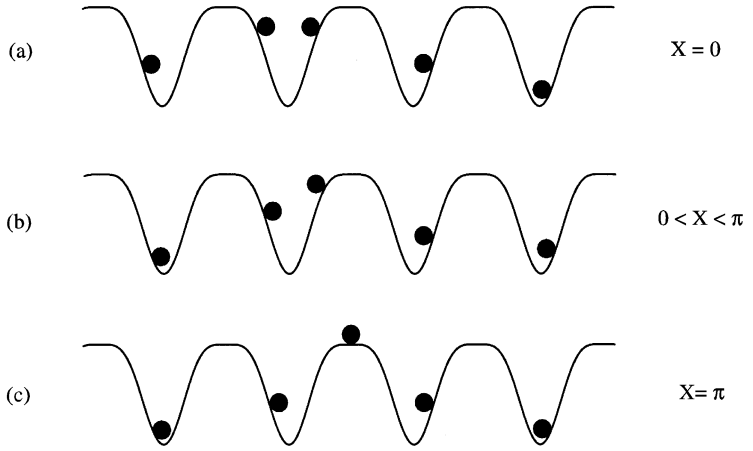

Fig. 12. Kink structure for the substrate potential with sharp wells (see text).

the same potential well (see Fig. 12a), while a maximum of the PN potential is at $X = \pi$ for the atomic configuration shown in Fig. 12c when one of the atoms is at the top of the substrate potential. Let us call this situation as the N- (i.e. *normal*) relief. The case $s < 0$ in the nonsinusoidal substrate (3.18) always corresponds to the N-relief. However, the case $s > 0$ is more complicated. Apart from the N-relief, the so-called I- (i.e. *inverse*) relief may be observed when the configuration shown in Fig. 12a corresponds to a potential maximum, and that shown in Fig. 12c, to a minimum of the function $V_{\mathrm{PN}}(X)$. Such a situation is realized for certain values of g, and the cases of the N- and I-reliefs alternate. In addition, between the regions of the N- and I-relief there exist intermediate regions where both the configurations shown in Fig. 12a and 12c correspond to

maxima of $V_{\rm PN}(x)$ but a minimum is realized at some intermediate configuration (see Fig. 12b) with $0 < X < \pi$. As a result, the dependence $E_{\rm PN}$ vs. g in the intermediate regions has well pronounced local minima (see Fig. 11). It is interesting to note that if the substrate potential consists of a sequence of parabolic, the value $E_{\rm PN}$ in these intermediate regions vanishes (Kratochvil and Indenbom, 1963; Ishioka, 1974). It is rather clear that in the limit $g \to 0$ the features of the PN potential disappear, and it approaches the function $V_{\rm sub}(X)$.

Dynamics of the FK model with nonsinusoidal substrate potential is qualitatively similar to that of the standard FK model described above. The motion of a FK kink is accompanied by radiation of phonons caused by the model discreteness (see, e.g., Peyrard and Remoissenet, 1982). An effective radiation-induced friction coefficient η increases with increasing of $|s|$ due to an increase of the PN barrier, $E_{\rm PN}$. The collisions of kinks with phonons and kink–kink collisions are almost elastic, but the effective phase shift of the kinks now depends on the parameter s. Nevertheless, the FK model with a nonsinusoidal substrate potential displays at least two novel features in the kink dynamics, comparing with the standard FK model. The first feature is the existence of small-amplitude breathers only for a certain interval of the parameter s, namely, the breathers (described approximately by an effective NLS equation for the slowly varying wave envelope) exist for the values lying within the interval $s_0 < s < 1$, where $s_0 = \sqrt{24} - 5 \approx -0.1$. The second new feature of the model is the existence of the internal (shape) modes of the kinks for $s > 0$. These two main features of the nonlinear waves in the generalized FK model with nonsinusoidal substrate significantly modify the dynamics of the kink–antikink collisions.

For the nonsinusoidal potential with $s < 0$ there exists a critical kinetic energy, $K_{\rm cr}$, such that fast kink and antikink with the initial kinetic energy larger than $K_{\rm cr}$ pass through each other almost without changes of their energies. Otherwise, the collision is inelastic and generally the kink and antikink cannot escape from the effective (attractive) interaction potential because of a loss of a part of their energy for radiation. Therefore, the kink and antikink form a bound state as a large-amplitude (LA) breather which loses its energy transforming into a small-amplitude (SA) breather. However, the further evolution of such a bound state differs for the cases $s > s_0$ and $s < s_0$, s_0 is defined above. In the former case, the LA breather slowly evolves into a SA breather (according to a power law). Otherwise, i.e. for $-1 < s < s_0$, when the LA breathers are not possible in the system, the SA breather decays much more rapidly radiating two bumps (wave packets). Thus, in the latter case the kink–antikink collisions are destructive.

In the case when the substrate potential has sharp wells ($s > 0$), the kink–antikink collisions exhibit novel phenomena caused by the kinks' internal modes. Namely, the final state of the kink–antikink collision below the threshold $K_{\rm cr}$ depends on the initial value of the relative kink velocity, so that such a collision may produce either a breather, as a final state which slowly decays, or it may result in a resonant (nondestructive) collision when the kinks do not annihilate. The resonant elastic interaction between a kink and antikink is due to the resonant energy exchange between the kink translational mode and its internal mode, and such type of resonances has been analysed first for the ϕ^4 model by Campbell et al. (1983) [see also Anninos et al. (1991) and references therein], and later, for the potential (3.18), by Peyrard and Campbell (1983). They found that the regions where the trapping into a decaying bound state takes place (the so-called resonant velocity "windows"), and the regions characterized by almost elastic transmission of kinks, alternate. Numerical simulations showed that if the initial value of the relative kink velocity is selected in the resonant velocity "window", then kink and antikink become coupled just after the

first collision and they start to oscillate. However, after a few oscillations the kinks escape to infinities. The explanation proposed by Campbell et al. (1983) is based on the so-called resonant energy exchange mechanism. Indeed, in this case both kinks possess internal (shape) modes which are excited just after the first collision provided the relative kink velocity is not large enough. When the shape modes are excited, they remove a part of the kinks' kinetic energy from the translational motion of the kinks. The kinks turn back because of a mutual attractive interaction, so that they interact with each other again. The energy stored in the kinks' shape modes may be now realized provided certain resonant conditions are satisfied,

$$\omega_{\mathrm{B}} T_{12} \approx 2n\pi + \delta \,, \tag{3.23}$$

where ω_{B} is the shape mode frequency, T_{12} is the time between the first and the second kink collisions, and δ is the offset phase. The integer number n plays a role of the number of the resonance, and it determines a sequence of the resonant velocities for the kink escape below the critical value of the relative velocity for the capture. In fact, the total number of the resonances (i.e. windows) is limited by radiation. The phenomenological explanation of the resonant effects proposed by Campbell et al. (1983) accurately describes the resonance structures in the kink collisions observed in direct numerical simulations, and the existence of such resonances has been shown for several nonlinear models, including the DSG model and the ϕ^4 model.

Finally, it should be noted that the properties of the FK model with nonsinusoidal substrate potential are rather general. For example, analogous types of the nonlinear dynamics may be observed for the DSG model (Campbell et al., 1986) for $|s| < 1/4$, in particular, the LA breather modes exist provided $s > -1/16$, and the kink shape mode appears for $s > 0$.

To conclude this section, we note that there exist some "exotic" shapes of the substrate potential $V_{\mathrm{sub}}(x)$ which produce an exactly vanishing PN potential to the kink motion, i.e., $E_{\mathrm{PN}} = 0$. A systematic procedure for obtaining these exotic cases was developed by Speight and Ward (1994). In particular, above we have mentioned that such an effect may take place for the substrate potential composed of a sequence of parabolas but only for certain values of the model parameters. Another example was given by Bak (1982), and this potential is defined by its first derivative, as follows:

$$V'_{\mathrm{sub}}(x) = 4\tan^{-1}\left(\frac{\lambda \sin x}{1 - \lambda \cos x}\right), \tag{3.24}$$

where $\lambda = \tanh^2(a_s/d)$. For the potential (3.24) the discrete motion equation has an exact discrete kink solution which coincides with the shape of the SG kink,

$$u_n(t) = 4\tan^{-1}\exp[-(na_s - X)/d] \,.$$

This solution is exact, and the kink moves freely along a discrete chain, so that the kinks energy does not depend on its effective coordinate X. Notice, however, that this model still remains nonintegrable unlike the SG one.

3.3. Multiple-well potential

In this section we investigate the FK model with the substrate potential which possesses more than one absolute minimum per period $a_s = 2\pi$. As a consequence of this shape of the potential,

more than one type of kink solutions are possible, and more than one phonon spectrum branch is observed. As a typical example, let us consider the double-well (DW) potential proposed by Remoissenet and Peyrard (1984) (see Fig. 13)

$$V_{\rm sub}(x) = \frac{(1-s)^4[1-\cos(2x)]}{(1+s^2+2s\sin x)^2}\,, \tag{3.25}$$

where $0 \le s \le +1$. This potential has two distinct minima, one at $x_{01} = 0$ and another at $x_{02} = \pi$, at which the energy values coincide, $V_{\rm sub}(x_{01}) = V_{\rm sub}(x_{02}) = 0$. The minima are separated by two barriers, at x_{m1} and x_{m2}, where the first maximum depends on the parameter s,

$$V_{\rm sub}(x_{m1}) = 2\left(\frac{1-s}{1+s}\right)^4, \tag{3.26}$$

while the second barrier has the fixed value, $V_{\rm sub}(x_{m2}) = 2$.

The FK model with the DW substrate potential has two types of ground states (see Fig. 14). In the "left ground state" (LGS) shown in Fig. 14a, all the atoms in the chain occupy the "left" minima of the DW potential, $x_n = x_{01} + 2\pi n$ ($n = 0, \pm 1, \ldots$), and in the "right ground state" (RGS) shown in Fig. 14b, they occupy only the "right" minima, i.e. $x_n = x_{02} + 2\pi n$. Both the ground states are characterized by the same phonon spectrum (3.1) with

$$\omega_{\rm min} = 2\frac{(1-s)^2}{(1+s^2)}\,. \tag{3.27}$$

The standard 2π kink, which connects two equivalent ground states, say LGS and LGS-2π, now splits into two separate subkinks. One subkink connects LGS and RGS (see Fig. 14c), and it is called *large kink* (LK) because it overcome the largest barrier. Another subkink, *small kink* (SK), connects the states RGS and LGS-2π, and it overcome the lower energy barrier (see Fig. 14f). Analogously, large and small antikinks may be defined in the system, $\overline{\rm LK}$ and $\overline{\rm SK}$ shown in Fig. 14d and e.

It is clear that the chain can support a single LK and single SK which are, as a matter of fact, independent topological excitations of the chain. The LKs and SKs have the properties similar to those of the kinks in the standard SG model, however, their parameters are naturally different from the corresponding parameters of the SG kink (see Remoissenet and Peyrard, 1984). For example,

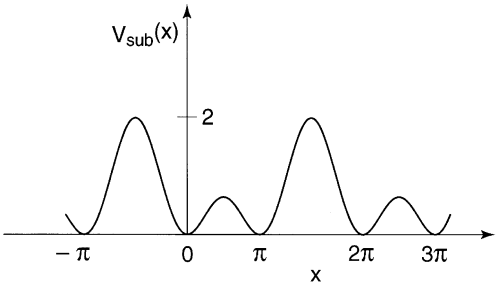

Fig. 13. Schematic presentation of a double-well substrate potential (3.25).

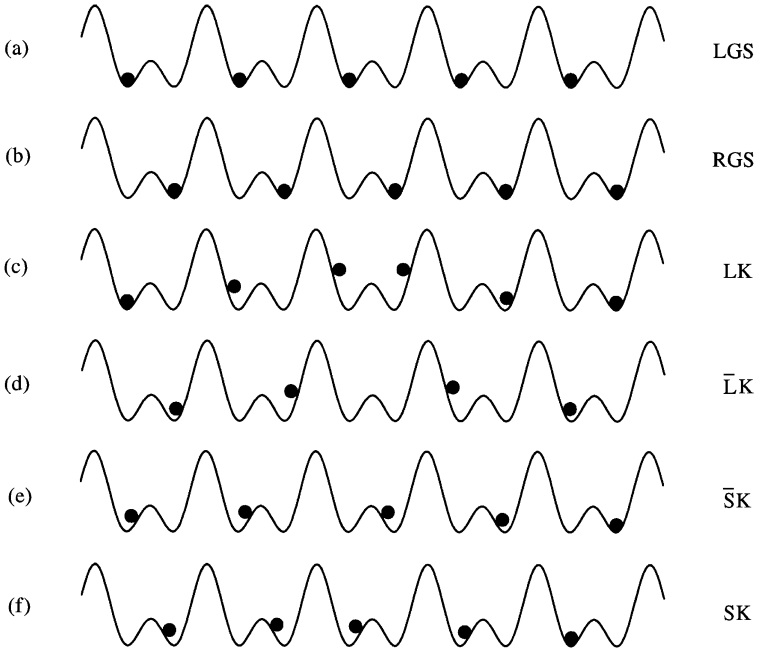

Fig. 14. Structures of the ground states and kinks in the FK model with the double-well substrate potential: (a) "left" GS, (b) "right" GS, (c) large kink, (d) large antikink, (e) small antikink, and (f) small kink.

the kink masses coincide at $s = 0$ and tends to zero for $s \to +1$, but generally they are different so that $m_{\text{SK}} < m_{\text{LK}}$. Besides, these two types of the kinks are different, namely the SK has an internal (shape) mode whereas the LK has no such an extra degree of freedom. The latter difference makes some dynamical effects related to the kink collisions different for SKs and LKs as well.

The standard FK model allows an arbitrary sequence of the kinks and/or antikinks. In the DW model, however, some of the kink combinations are forbidden due to topological constrains. For example, in a periodic train of kinks SKs and LKs should alternate because the situation when one "extra" atom is installed into the chain corresponds to a pair LK + SK. In fact, the DW model allows only *four* sequences of the kink and antikink combinations, SK + LK, $\overline{\text{SK}} + \overline{\text{LK}}$, LK + $\overline{\text{LK}}$, and SK + $\overline{\text{SK}}$. Therefore, only collisions between those kinks is possible in the DW model.

SK + LK (or $\overline{\text{SK}} + \overline{\text{LK}}$) *kink collision*. As usual, two kinks of the same topological charge repel each other, and in the present case two different kinks cannot pass through each other because of topological constrains. Therefore, the kink collision should display a reflection, and such a reflection is almost elastic for $g \gg 1$ (Remoissenet and Peyrard, 1984).

LK + $\overline{\text{LK}}$ *collision*. Numerical simulations by Remoissenet and Peyrard (1984) have shown that this type of kink and antikink pass through each other transforming into a pair $\overline{\text{SK}}$ + SK as should follow from the viewpoint of topological constrains. Such an effect of the kink transformation was analysed earlier by Maki and Kumar (1976) and Schiefman and Kumar (1979) in the framework of the DSG equation. The difference in the kink rest energies, $\Delta\varepsilon = 2(m_{\text{LK}} - m_{\text{SK}})c^2 > 0$, is converted

into the kinetic energy of the small kinks according to the energy conservation which, as has been verified, holds with a good accuracy even when the effect of radiation is not taken into account. However, in a highly discrete chain when $g \sim 1$, the energy excess $\Delta\varepsilon$ may be taken out by radiation leading to a decay of the kink–antikink pair with formation of a breather state.

SK + $\overline{\text{SK}}$ *collision.* When the initial kinetic energy K_{in} of small kinks is large enough, namely $K_{\text{in}} > 2(m_{\text{LK}} - m_{\text{SK}})c^2$, they can pass through each other converting into a slowly moving $\overline{\text{LK}}$ + LK pair. Otherwise, small kinks behave similar to those of the ϕ^4 model, i.e. they may be trapped into a breather state provided the initial velocity is smaller than a certain critical value.

Campbell et al. (1986) have studied in detail the kink collisions in the DSG model (3.18), which has the DW shape for $s < -1/4$. Unlike the model with the potential (3.25) considered above, the DSG subkinks have different amplitudes, $\Delta u_{\text{SK}} < \Delta u_{\text{LK}}$, where $\Delta u = |u_{\text{k}}(+\infty) - u_{\text{k}}(-\infty)|$, so that the SK disappears when the lower barrier vanishes, i.e. for $s \to -1/4$. Besides, SK in the DSG model has an internal (shape) mode. Therefore, the SK + $\overline{\text{SK}}$ collisions at small kinetic energies exhibit resonance phenomena caused by the energy exchange between the kinks translational modes and their internal modes similar to the case described in the previous section (see Campbell et al., 1983, 1986; Peyrard and Campbell, 1983).

Model with a more general shape of the substrate potential has been introduced in the theory of solitons in hydrogen-bonded chains, where topological solitons characterize different types of defects in such a system (Zolotaryuk and Pnevmatikos, 1990),

$$V_{\alpha,\beta}(x) \propto \left[\frac{\cos x - \alpha}{1 - \beta(\cos x - \alpha)}\right]^2 . \tag{3.28}$$

Here the parameter α ($|\alpha| < 1$) describes a relative width of two barriers as well as it controls the distance between the neighboring minima of the substrate potential. The second parameter β describes the relative height of the barriers. The potential reduces to the sinusoidal form for the case $\alpha = \beta = 0$, and to the DSG potential, for $\beta = 0$. For the potential (3.28), a mass of the "small" kink may be larger than that of a "large" kink.

The discussion presented above has involved only the case of a symmetric substrate potential. However, in a general case the substrate potential may have wells with different curvatures. As a consequence, there exist more than one branch of the phonon spectrum in the model. For example, for the asymmetric double-well (ADW) potential proposed by Remoissenet and Peyrard (1984) (see Fig. 15),

$$V_{\text{sub}}(x) = \frac{(1 - s^2)^2[1 - \cos(2x)]}{(1 + s^2 + 2s\cos x)^2} , \tag{3.29}$$

where $0 \le s \le 1$, the LGS has the minimum phonon frequency gap

$$\omega_{\text{min}}^{(L)} = \frac{(1 - s)}{(1 + s)} < 1 , \tag{3.30}$$

while the RGS is characterized by the gap

$$\omega_{\text{min}}^{(R)} = \frac{(1 + s)}{(1 - s)} > 1 . \tag{3.31}$$

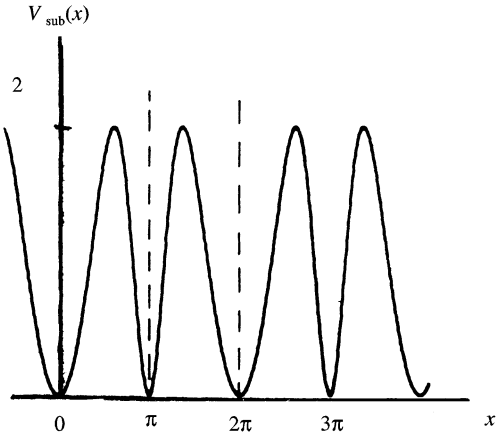

Fig. 15. Schematic presentation of the asymmetric substrate potential (3.29) proposed by Remoissenet and Peyrard (1984).

In this system, there are two subkinks, the "left kink" (LK), which links the LGS and RGS, and the "right kink" (RK) which is just reverse, so that the kinks may be transformed to each other by a mirror transformation. The shape of a kink is asymmetric (i.e. such a kink is oriented) because its tails lie in the wells of different curvatures. For example, the LK has the long-range left-hand tail,

$$u_k(x \to -\infty) \propto -\exp(-\omega_{\min}^{(L)}|x|/d)\,,$$

and the sharp right-hand tail,

$$u_k(x \to +\infty) \propto -\pi + \exp(-\omega_{\min}^{(R)}x/d)\,.$$

The kink's mass is the same for both the kinks,

$$m = m^{(SG)}\frac{(1-s^2)}{4s}\ln\left(\frac{1+s}{1-s}\right),$$

and it varies from $m^{(SG)}/2$, at $s = 0$, to zero, at $s = 1$.

A kink in the FK model with ADW potential (3.29) possesses a shape mode with the frequency ω_B. Remoissenet and Peyrard (1984) have found an interesting phenomenon: For $0 < s < 0.4$ the value of ω_B lies between the frequencies (3.30) and (3.31). Therefore, when the shape mode is excited, e.g., during the kinks collision, it rapidly decays due to radiation of the phonons around the LGS toward the more smooth kink tail. As a natural result, resonance structures may be observed only for RK + $\overline{\text{RK}}$ or $\overline{\text{LK}}$ + LK collisions, when kink and antikink collide by their smooth tails (the "soft" collision), and the chain outside the collision region is in the RGS which is characterized by the phonon frequencies $\omega \geq \omega_{\min}^{(R)} > \omega_B$. Numerical simulations by Remoissenet and Peyrard (1984) demonstrated the existence of the reflection velocity windows for this kind of the kink collisions.

It is clear that each the GS (LGS or RGS) may support its own breather mode in the ADW model. Remoissenet and Peyrard (1984) have shown that the RGS (sharp wells) always supports a SA breathers, while the LGS (flat bottoms) supports LA breather mode provided $0 < s < s_*$,

where $s_* = 2 - \sqrt{3} \approx 0.268$. Therefore, for $s_* < s < 1$ a LA breather cannot be excited in a result of the hard-core kink–antikink collisions (i.e., in collisions $\mathrm{LK} + \overline{\mathrm{LK}}$ or $\overline{\mathrm{RK}} + \mathrm{RK}$ when kinks collide from the side of their short-range tails), and the kinks are destroyed emitting phonons. Other cases of the kink collisions are similar to the standard SG-type model, and such collisions may be treated as those of quasi-particles. However, due to asymmetry of the kink shape, a kink and antikink may collide from the side of by their long-range tails ("soft" collision) and the chain outside the collision region is in the RGS, or the kink and antikink may collide from the side of by their short-range tails (the so-called "hard" collision). As a matter of fact, the soft collisions are almost perfectly elastic, while the hard collisions are inelastic and they are accompanied by strong emission of phonons (Remoissenet and Peyrard, 1984).

3.4. Multiple-barrier potential

In some cases when the FK model is used to describe realistic physical object, e.g., those briefly discussed in the Introduction, the substrate potential may have a complicated structure with additional local minima, for example, the double-barrier (DB) structure as shown in Fig. 16. In this case the system may be observed in a "metastable ground state" (MGS) when all the atoms of the chain occupy the local minima of the substrate potential. Similar to the DW model considered in the previous subsection, the 2π-kink of the DB model will split to give two subkinks connecting GS–MGS and MGS-(GS-2π) which repel each other. However, unlike the case of the DW potential, now the atoms in the region between the subkinks are in the metastable (excited) state (see Fig. 16). This leads to an attraction between two subkinks because the energy of the 2π-kink increases with an increase of the distance between the subkinks, i.e. with a number of atoms occupying the MGS. As a result of a competition of this attraction and the conventional repulsion of the subkinks of the same topological charge, there exists an equilibrium distance R_0 which realizes a minimum of the 2π-kink energy. Thus, the DB kink may be considered as a "molecule" (2π-kink) composed of two "atoms" (subkinks or π-kinks) coupled together by a nonlinear potential $U_{\mathrm{DB}}(R)$ which has a minimum at $R = R_0$. It is clear that the DB kink should always have a shape mode with the frequency ω_{B}, with a natural physical interpretation: Such a mode corresponds to an internal oscillation of the "atoms" in the "molecule".

As an example, let us consider one of the most frequently occurring substrate potentials, the double SG potential (3.17), which has the double-barrier structure provided $s > 1/4$. Introducing the new parameter r according to the relation $s = (\frac{1}{2}\sinh r)^2$, $r > \ln(1 + \sqrt{2}) \approx 0.881$, the DSG potential can be presented as

$$V_r(x) = \frac{4\sinh^2 r}{\cosh^4 r}\left\{(1 - \cos x) + \frac{1}{4}(\sinh^2 r)(1 - \cos 2x)\right\}. \tag{3.32}$$

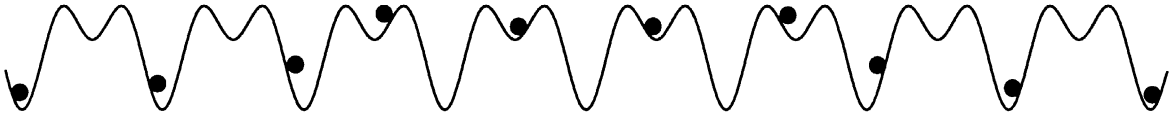

Fig. 16. Structure of the kink in the FK model with the double-barrier substrate potential.

The potential (3.32) has a minimum, at $x_0 = 0$, and two maxima, at $x_m = \pi \pm \cos^{-1}(\cosh^2 r)$, $V_r(x_m) = 2$, and a relative minimum at $x_b = \pi$, $V_r = 8\sinh^2 r/\cosh^4 r$, per one period $a_s = 2\pi$.

In the continuum limit approximation, when $g \gg 1$, the static DB kink (antikink) has a simple form,

$$u^{(\mathrm{DB})}(x) = \mp 2\tan^{-1}\left[\frac{\sinh(y)}{\cosh(r)}\right], \tag{3.33}$$

where

$$y = 2(x - X)/d \tag{3.34}$$

The mass of the kink is defined as

$$m^{(\mathrm{DB})}(r) = m^{(\mathrm{SG})}\frac{\sinh r}{\cosh r}\left[1 + \frac{2r}{\sinh(2r)}\right] > m^{(\mathrm{SG})}\ . \tag{3.35}$$

It is interesting to mention that the static kink (3.33), (3.34) of the DSG equation can be exactly expressed as a sum of the single kink solutions of the standard SG equation (Giachetti et al., 1984; Campbell et al., 1986),

$$u^{(\mathrm{DB})}(x) = \mp\left[u_\pi(\tilde{R} + y) - u_\pi(\tilde{R} - y)\right], \tag{3.36}$$

where $u_\pi(y) = 2\tan^{-1}\exp(y)$, $\tilde{R} = r$ and y is determined by Eq. (3.34). Thus, the parameter X can be considered as the coordinate of the kink center of mass, and the parameter $R = \tilde{R}d$, as the distance between two subkinks of the DB kink. Willis et al. (1987) have analysed a complete Hamiltonian dynamics of a DB kink in the DSG model introducing two collective variables $X(t)$ and $R(t)$, and the corresponding conjugate momenta as canonical variables. Analogously to the Hamiltonian formalism for the SG model, in the present case one should add one more degree of freedom (internal oscillations) and to modify the Poisson brackets. After some lengthy calculations, Willis et al. (1987) have proved that the energy of the DSG kink in such an approach may be presented in the form,

$$H_{\mathrm{DB}} = \frac{1}{2}m^{(\mathrm{DB})}\left(\frac{\mathrm{d}X}{\mathrm{d}t}\right)^2 + \frac{1}{2}m^{(\mathrm{R})}\left(\frac{\mathrm{d}R}{\mathrm{d}t}\right)^2 + U_{\mathrm{DB}}(R)\ , \tag{3.37}$$

where $m^{(\mathrm{DB})}$ is determined by Eq. (3.35),

$$m^{(\mathrm{R})}(r) = \int_{-\infty}^{\infty}\frac{\mathrm{d}x}{2\pi}\left(\frac{\partial u^{(\mathrm{DB})}}{\partial R}\right)^2 = \frac{1}{4}m^{(\mathrm{SG})}\frac{\sinh r}{\cosh r}\left[1 - \frac{2r}{\sinh(2r)}\right], \tag{3.38}$$

$$U_{\mathrm{DB}}(R) = m^{(\mathrm{SG})}c^2\frac{\sinh r}{2\cosh r}\left\{1 + \frac{\tanh^2 r}{\tanh^2\tilde{R}} + 2\tilde{R}\left[\frac{1}{\sinh(2\tilde{R})} + \frac{\coth\tilde{R}}{\cosh^2 r} - \frac{\tanh^2 r\coth\tilde{R}}{2\sinh^2\tilde{R}}\right]\right\}, \tag{3.39}$$

where $\tilde{R} \equiv R/d$. For small-amplitude internal oscillations, the energy $U_{\mathrm{DB}}(R)$ may be expanded to be

$$U_{\mathrm{DB}}(R) \approx m^{(\mathrm{DB})} + \tfrac{1}{2}m^{(\mathrm{R})}\omega_{\mathrm{B}}^2(r)(R - R_0)^2\ , \tag{3.40}$$

where $R_0 = rd$ and $\omega_B(r)$ is the frequency of the internal oscillation,

$$\omega_B^2(r) = \frac{1}{m^{(R)}(r)}\left(\frac{d^2 U_{DB}}{dR^2}\right)\Bigg|_{R=R_0} . \tag{3.41}$$

The value ω_B can be calculated from Eqs. (3.38), (3.39) and (3.41) and also can be found as an eigenvalue of the Schrödinger equations (3.12), (3.13). The latter method leads to the result (Sodano et al., 1986),

$$\omega_B \approx \omega_{min}\sqrt{1-\beta^2} , \tag{3.42}$$

where

$$\beta = \frac{1}{2}\left[\left(1 + \frac{8}{\alpha^2}\tanh^2 r\right)^{1/2} - 1\right], \tag{3.43}$$

$$\alpha = \frac{\tanh^2 r \sinh(2r)}{[\sinh(2r) - 2r]} . \tag{3.44}$$

The potential $U_{DB}(R)$ defined by Eq. (3.39) is anharmonic. Thus, as the amplitude of the "molecule" oscillations increases going to a nonlinear regime, anharmonicity of the potential $U_{DB}(R)$ becomes important, and higher-order harmonics of the fundamental frequency will manifest themselves important in nonlinear dynamics of the kink. However, a coupling of the internal oscillations to the phonons is extremely weak because it is caused only by higher-order resonances. Numerical simulations carried out by Burdick et al. (1987) have shown that an effective damping of the internal oscillations is negligible even when the oscillation become nonlinear.

In the limit $r \to \infty$, the DSG potential (3.32) reduces to the SG one with the period $a = \pi$, the DB kink (3.36) splits into two separate SG π-kinks, and $\omega_B \to 0$. We note also that in the discrete case the Hamiltonian (3.37) should include the PN potential for the subkinks.

Campbell et al. (1986) have studied numerically the DSG kink–antikink collisions, and they demonstrated the existence of the "resonance windows" due to an energy exchange mechanism between the kinks translational and internal modes. The resonance velocity windows correspond to the situation when the kinks collide inelastically with a possibility to form a breather state or to be scattered conserving their identities. For $r > 1/4$ a qualitatively new effect can be also detected, namely, two counter-propagating breathers may emerge as the final result of the kink–antikink collision. The resonant energy exchange can be understood in the framework of an effective collective-coordinate model treating the scattering process as a collision of two "molecules", each consisting of the DB kink and DB antikink.

4. Anharmonic interatomic interaction

4.1. Preliminary remarks

In the classical FK model, a coupling between the neighboring particles in the chain is assumed to be harmonic. However, for describing realistic physical systems, different types of anharmonic interatomic potentials should be taken into account in the FK model. Such generalized FK models

allow to describe qualitatively new physical effects such as breaking of the kink–antikink symmetry, appearance of a new type of dynamical solitons (supersonic waves), a possible breakdown of the solitonic excitations (namely, antikinks) which is followed by a "rupture" of the chain, a change of the ground state of the model, a change of the interaction between the kinks, etc.

There are several ways to introduce anharmonic interparticle interaction into the FK model for modeling realistic physical systems. As an example, we briefly discuss here several mechanisms of interaction between atoms adsorbed on a crystal surface (for details, see, e.g., Einstein, 1978; Braun and Medvedev, 1989).

When adatoms are charged, then the Coulomb repulsion $V_{\rm int}(x) \approx e^2/x$ (e is the adatomic charge) (Vorotyntsev et al., 1979) acts between them for distances $x < a^*$ (a^* being the screening radius which is equal to the Debye screening radius, for a semiconductor substrate, and to the inverse Thomas–Fermi momentum, for a metallic substrate). For a semiconductor substrate, the value a^* is large enough, and the main contribution into the interaction potential is power-law, $V_{\rm int}(x) \propto x^{-1}$. For adsorption on a metallic substrate the value of the screening radius a^* is of order of the lattice constant; for $x > a^*$ the interaction of adatoms has a dipole-dipole character: $V_{\rm int}(x) \approx 2p_A^2/x^3$ (Bolshov et al., 1977), p_A being the dipole moment of an adatom. If adatoms are neutral, then the overlap of their electronic shells gives rise in a direct interaction, which decreases exponentially with the distance, $V_{\rm int}(x) \propto \exp(-\beta x)$ (Einstein, 1978). More complex interaction laws are possible as well, such as for the so-called "indirect" mechanism of adatom interaction (Einstein, 1978; Braun, 1981; Braun and Medvedev, 1989) which may be approximated by the following generalized law:

$$V_{\rm int}(x) \sim x^{-n} \sin(2k_{\rm F}x + \phi) ,$$

where n varies from 1 to 5 depending on the electronic structure of the substrate, ϕ is a constant phase, and $k_{\rm F}$ is the Fermi momentum of the substrate electrons. In the latter case, an attraction (or "effective" attraction) can appear for adatoms at some distances.

To cover a larger class of physically important systems, here we consider the following interaction potentials:

- *exponential*

$$V_{\rm int}(x) = V_0 \exp[-\beta(x - a_s)] , \tag{4.1}$$

  where V_0 is the energy of interaction between adatoms occupying the nearest neighboring minima of this substrate potential, and the parameter β characterizes anharmonicity of the potential;
- *power-law*

$$V_{\rm int}(x) = V_0\left(\frac{a_s}{x}\right)^n , \tag{4.2}$$

  where n is an integer number ($n \geq 1$);
- *Morse potential*

$$V_{\rm int}(x) = V_m[{\rm e}^{-2\beta(x-a_0)} - 2{\rm e}^{-\beta(x-a_0)}] , \tag{4.3}$$

  where a_0 is the equilibrium distance, and V_m is the depth of the potential well, and, at last,

- *double-well potential*

$$V_{\rm int} = V_m[\tfrac{1}{2}\beta^4(x-a_*)^4 - \beta^2(x-a_*)^2] \,. \tag{4.4}$$

The latter potential has two minima at $x = a_* \pm \beta^{-1}$ and it can approximate qualitatively the oscillating potential which appears for the 'indirect' interaction of adatoms.

The potentials (4.1) and (4.2) are repulsive. Of course, one can include also an attractive branch of the form $V_{\rm int} \propto x$ so that the resulting potential will have a minimum at some x_0. Such a modification will produce changes only for the case of the finite chain. In the present survey, however, we consider an infinite FK chain.

The potentials (4.1) and (4.2) are convex, i.e. $V''_{\rm int}(x) > 0$ for all $x > 0$, while the potentials (4.3) and (4.4) are nonconvex. The potential (4.3) is concave for $x > a_0 + \beta^{-1}\ln 2$, and the potential (4.4) is concave for the region $a_* - \beta^{-1}/\sqrt{3} < x < a_* + \beta^{-1}/\sqrt{3}$. As a result, at some values of the parameters a_0 (or a_*), β, and V_m the ground state of the system becomes nontrivial, and its excitation spectrum is changed. The FK model with nonconvex potentials (4.3) and (4.4) is considered in Section 4.3. The exponential potential (4.1) and, especially, the power-law potential (4.2) are long-range potentials. Therefore, the interaction of more neighbors than nearest neighbors should be taken into account. This kind of problems is discussed in Sections 4.3 and 4.4, where we show that the interaction of all neighbors changes the system parameters for the exponential interaction (4.1) while in the case of the power-law interaction (4.2) the motion equation of the system becomes nonlocal even in the continuum limit approximation.

4.2. Short-range interaction

For small anharmonicity of the interatomic interaction, the potential can be expanded into a Taylor series to yield the following motion equation (Braun et al., 1990)

$$\frac{{\rm d}^2 u_n}{{\rm d}t^2} + \sin u_n - V''_{\rm int}(a_s)(u_{n+1} + u_{n-1} - 2u_n)\left[1 + \frac{V''_{\rm int}{}'(a_s)}{2V''_{\rm int}(a_s)}(u_{n+1} - u_{n-1})\right] = 0 \,. \tag{4.5}$$

Neglecting the discreteness effects, i.e. using the continuum limit approximation, Eq. (4.5) can be reduced to the form,

$$u_{tt} + \sin u - {\rm d}^2 u_{xx}(1 + \alpha d u_x) = 0 \,, \tag{4.6}$$

where we have introduced the parameter d, defined according to Eq. (2.29), as

$$d = a_s\sqrt{g} \,, \qquad g = V''_{\rm int}(a_s) \,, \tag{4.7}$$

and the dimensionless anharmonicity parameter α,

$$\alpha = \frac{a_s}{d}\frac{V'''_{\rm int}(a_s)}{V''_{\rm int}(a_s)} \,. \tag{4.8}$$

Anharmonicity does not change the spectrum of linear excitations (phonons) of the chain. However, a kink solution of Eq. (4.6) differs from that in the harmonic FK chain. At small

α a stationary kink solution can be found by the perturbation theory (see, e.g., Kivshar and Malomed, 1989),

$$u_k(z) = u_k^{(SG)}(z) + \alpha u_\alpha(z) , \tag{4.9}$$

where

$$u_\alpha(z) = -\tfrac{4}{3}\tan^{-1}(\sinh z)\operatorname{sech} z \tag{4.10}$$

with $z = x/d$. A simple analysis shows that anharmonicity of interatomic interaction destroys the symmetry between a kink and an antikink because according to Eq. (4.9), the correction u_α is independent on σ. This means that the effective kink width changes by an amount of $\sigma\alpha(\pi d/3)$, i.e.

$$d_{\text{eff}} = d(1 - \pi\sigma\alpha/3) . \tag{4.11}$$

This leads to the corresponding change in other parameters characterizing the properties of the kink and antikink, e.g., the effective mass,

$$m_\sigma \approx m^{(SG)}(1 + \pi\sigma\alpha/6) , \tag{4.12}$$

and the amplitude of the PN potential which may be estimated as

$$E_{PN} \approx E_{PN}^{(SG)}(g) - \frac{2\pi}{3}\sigma\alpha g\frac{\partial E_{PN}^{(SG)}(g)}{\partial g} , \tag{4.13}$$

where the function $E_{PN}^{(SG)}(g)$ is defined by Eq. (2.50). We note also that the energy of kink–antikink pair creation is given by

$$\varepsilon_{\text{pair}} = \varepsilon_{\text{pair}}^{SG}\left(1 - \frac{4}{27}\alpha^2\right), \qquad \varepsilon_{\text{pair}}^{SG} = 2\varepsilon_k^{SG} . \tag{4.14}$$

Such a symmetry breaking between the kink and antikink was firstly found by (Milchev and Markov (1984), see also Markov and Milchev, 1985; Braun et al., 1991). The change of the kink shape may result in the appearance of low-frequency (or high-frequency) shape mode of the kink, as has been shown by Zhang (1996).

For the exponential interatomic potential (3.1) the parameters g and α are calculated to be

$$g = V_0\beta^2, \qquad \alpha = -\beta a_s/d . \tag{4.15}$$

If the anharmonicity parameter α is negative, the effective width of the kink (at $\sigma = +1$) is larger, while that for an antikink ($\sigma = -1$) is lower than for the SG kink. This phenomenon has a simple physical interpretation. Indeed, effective interaction forces for a kink (i.e., in the region of local contraction of a chain) exceed those for an antikink (in the region of local extension of a chain). Because of that, at the same value of the system parameters, V_0 and β, a kink, as compared with an antikink, is characterized by lower values of the effective mass and Peierls energy. These qualitative consideration is substantiated by Fig. 17 adopted from the paper by Braun et al. (1990) which presents the results of calculation of the dependencies $E_{PN}(g)$ and $m(g)$ for the FK model when the interaction between only nearest neighboring atoms is taken into account, but, at the same time, in contrast to the standard FK model, the interaction potential is exponential as in Eq. (3.1). It can be seen that a "splitting" of the curves in Fig. 17 is larger for larger values of β.

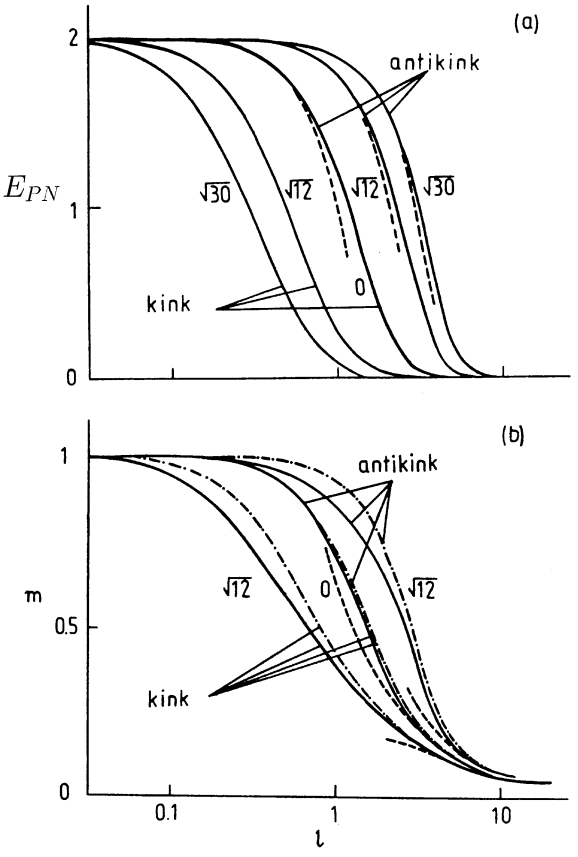

Fig. 17. Amplitude of the PN potential, E_{PN} (a) and the kink's effective mass m (b) for kink and antikink as functions of the parameter $l = \pi\sqrt{g}$ for the case when the nearest neighbors interact via exponential forces defined by Eq. (4.1) at various values of the anharmonicity parameter β: $\beta = 0$ (the classical FK model), $\beta = \sqrt{12}/2\pi$, and $\beta = \sqrt{30}/2\pi$. Dashed lines show analytical asymptotic results (see details in Braun et al., 1990).

Eq. (4.11) indicates that the width of an antikink vanishes with increasing of the anharmonicity parameter β. In order to analyse such an effect in more details, Milchev and Markov (1984) applied the operator relation, $u_{n\pm1} = \exp(\pm a_s\nabla)u_n$ to the discrete version of the FK model with the exponential interaction and they obtained the operator equation

$$2g\exp\{-\beta[\sinh(a_s\nabla)]u\}\sin\{\beta[\cosh(a_s\nabla)-1]u\} = \beta\sin u\ . \tag{4.16}$$

Keeping the lowest-order derivatives in Eq. (4.16), it can be reduced to (Milchev, 1986)

$$\mathrm{d}^2u_{xx}\exp(\alpha du_x) = \sin u\ . \tag{4.17}$$

Integration of Eq. (4.17) yields

$$1-(1-\alpha du_x)\exp(\alpha du_x) = (\beta^2/g)(C-\cos u)\ , \tag{4.18}$$

where C is a constant. The value $C = 1$ corresponds to a separatrix curve on the phase plane (u_x, u), which connects the points $u = 0$, and $u_x = 0$, and this a homoclinic trajectory corresponds to a kink (antikink) solution of Eq. (4.17). Substituting $u = \pi$ into Eq. (4.18), we find

$$(1 - \alpha d u_x)\exp(\alpha d u_x) = 1 - 2\beta^2/g \ , \tag{4.19}$$

which determines the value u_x at the kink center. It is easy to see that Eq. (4.19) has no solution for antikink ($u_x > 0$) for $\beta > \beta_{cr} = \sqrt{g/2}$, i.e. if $\alpha < \alpha_{cr} = -1/\sqrt{2}$. In this case the separatrix corresponding to an antikink (an extra hole) is discontinuous (i.e., $u_x \to \infty$). The latter means that the exponential potential (4.1) cannot withstand the chain extension, and the chain breaks into two disconnected (semi-infinite) parts (Milchev, 1986). The analysis made by Milchev and Mazzucehelli (1988) has shown that the antikink's effective width tends to zero as $d_{eff} = d\sqrt{1 - 2\alpha^2}$ when $\alpha \to \alpha_{cr}$. The energy of the kink–antikink repulsion, $V_{k\bar{k}}(R) \propto \exp(-R/d_{eff})$, also vanishes for $\alpha < \alpha_{cr}$. Thus, for large enough anharmonicity of the interatomic potential, antikinks may come closely to each other creating a cluster of extra holes in the chain, and this explains the effect of the chain "rupture". Such an effect may be clearly observed in collisions of kinks and antikinks as well as in kink interactions with inhomogeneities (such as interfaces). In fact, this phenomenon can be observed for different cases when the antikink changes its effective width interacting with an antikink or an interface (Milchev et al., 1992).

Of course, the continuum limit used above breaks down at $\alpha \to \alpha_{cr}$ even in the case of $g \to \infty$. The predicted "rupture" of the atomic chain is a physical artifact which is explained by nonapplicability of the continuum limit approximation; such a "rupture" indicates only that the effective width of an antikink becomes *smaller* than the lattice spacing a_s, and the energy of disorder of a regular chain of antikinks is rather small. The real rupture of the chain is possible only for nonconvex interatomic potentials such as the Morse potential (3.3) (see Section 4.3 below). In the case when $\alpha \sim \alpha_{cr}$, the antikink's parameters can be calculated with the help of a weak-bond approximation (Joos, 1982; Braun et al., 1990).

For $\alpha < \alpha_{cr}$ the amplitude of the PN potential for the antikink tends to the value of the substrate potential amplitude, $\varepsilon_s = 2$ (see Fig. 17), so that an antikink cannot move freely along the chain and it is strongly pinned at a PN potential well. Otherwise, a kink (a local contraction of the chain) propagates along the anharmonic FK chain more freely than along the harmonic one, because $d_{eff}(\sigma = +1) > d$ and $E_{PN}(\sigma = +1) < (E_{PN})_{harm}$.

Besides the kinks and antikinks, an anharmonic chain supports the so-called *supersonic shock waves*. To show this, let us neglect the substrate potential, then the chain of atoms interacting via the exponential forces coincides with the well-known Toda lattice (Toda, 1967, 1981). The Toda soliton has the following shape,

$$u_n(t) = ma_s + \frac{1}{\beta}\ln\left\{\frac{1 + \exp(-2\kappa)\phi_n(t)}{1 + \phi_n(t)}\right\}, \tag{4.20}$$

where

$$\phi_n(t) = \exp(z_n/d_{eff}), \quad z_n = na_s - vt \ . \tag{4.21}$$

Soliton in the Toda lattice propagates with the velocity $v > c$, and it is characterized by the effective width, $d_{eff} = a_s/2\kappa$, mass, $m = 1/\beta d_{eff}$, momentum, $p = mv$, and energy, $\varepsilon_{Toda} = 2V_0(\sinh\kappa\cosh\kappa - \kappa)$. The parameter $\kappa = \kappa(v)$ used above is determined by the equation

$(\sinh\kappa)/\kappa = v/c$ (recall that we use the units where $c = d = a_s\sqrt{g}$). The Toda soliton is a kink-like excitation which carries a jump of the atomic displacements equal to $\Delta u = -ma_s$ propagating along the chain. Such an excitation is *dynamical* and it cannot be static similar to the topological kink of the FK model.

To the best of our knowledge, propagation of supersonic solitons along the anharmonic FK chain has been not investigated yet. However, we may suppose that a Toda-like soliton can propagate in the FK chain during a finite time. Owing to the periodic substrate potential, a travelling soliton will lose its kinetic energy decreasing its velocity. When the value of v coincides with the critical velocity c, the Toda soliton should decay into FK kinks or/and radiation. The total number of the FK kinks may be estimated from the viewpoint of topological constrains, $n_k = [m - 1/2]$, where $[\dots]$ stands for an integer part.

Recently, the supersonic motion of topological solitons has been studied by Savin (1995) for the ϕ^4-model with anharmonic interatomic interaction. Savin has found that for certain kink velocities, when the jump in the atomic displacements Δu matches exactly the period of the substrate potential, i.e. $n\Delta u = -a_s$, n being integer, the supersonic kink moves almost without radiation of phonons. Thus, the supersonic kink may be considered as n Toda solitons coupled together by the topological constrain due to the external substrate potential.

It is interesting to note that for a special form of the interatomic potential,

$$V_{\rm int}(x) = \tfrac{1}{2}g(x - a_s)^2[1 + \tfrac{1}{48}(x - a_s)^2]\,, \tag{4.22}$$

where the anharmonicity parameter is the certain number, equal to $\frac{1}{48}$, the motion equation of the FK model in the continuum approximation has an exact kink solution of a standard form,

$$u_k(x,t) = 4\tan^{-1}\exp\left\{-\frac{(x - vt)}{d_{\rm eff}}\right\}, \tag{4.23}$$

which can propagate with an *arbitrary* velocity v (Kosevich and Kovalev, 1973; Konno et al., 1974). The effective width of the kink (4.23) is given by the formula

$$d_{\rm eff} = \frac{a_s}{\sqrt{6}}\left\{\left[\left(\frac{v}{c}\right)^2 - 1\right] + \sqrt{\left[\left(\frac{v}{c}\right)^2 - 1\right]^2 + \frac{1}{3}\left(\frac{a_s}{d}\right)^2}\right\}^{-1/2}, \tag{4.24}$$

so that in the limit $|v| \ll c$ the kink's width approaches the value given by the standard SG model, $d_{\rm eff} = d\sqrt{1 - (v/c)^2}$, while in the case of the supersonic motion, when $|v| \gg c$, the kink width is given by the expression $d_{\rm eff} \approx a_s c/\sqrt{12(v^2 - c^2)}$, which looks like the corresponding width of a dynamical Toda soliton.

4.3. Nonconvex interatomic potentials

In the sections above we have assumed that the interatomic interaction in the chain is described by a convex function, i.e. $V''_{\rm int}(x) > 0$ for all $x > 0$. The opposite case of the concave potential, i.e. when $V''_{\rm int}(x) < 0$, is less interesting from the physical point of view because, according to the

inequality

$$V_{\rm int}(a-\Delta a)+V_{\rm int}(a+\Delta a)-2V_{\rm int}(a)<0\,, \tag{4.25}$$

all the atoms will come together to one well of the substrate potential.

In the present section we will consider the so-called nonconvex interatomic interaction potential which has an inflection point a_i defined by the equation $V''_{\rm int}(a_i)=0$. The FK model with such a potential exhibits complicated properties and a rich nonlinear dynamics due to the existence of two competing length scales, the period of the substrate potential, $a_s=2\pi$, and the scale which is given by the inflection point a_i at which the strength of the interatomic bond reaches its maximum. For definiteness, let us suppose that the potential $V_{\rm int}$ is convex beyond the inflection point, i.e. $V''_{\rm int}>0$ for $x<a_i$, and it is concave at larger distances similar to the Morse potential (3.3). The opposite case is reduced to that mentioned if kinks are replaced by antikinks.

The nonconvex potential $V_{\rm int}(x)$ is obviously anharmonic. Thus, when the anharmonicity is large enough, antikinks in the chain may lead to the chain rupture. In contrast to the case of the exponential potential analysed above, now a rupture is a real breaking of the chain into two independent semi-infinite chains, because of attractive interaction between antikinks (Milchev, 1990). More precisely, a coupling of antikinks can lead to a creation of a cluster which consists of n antikinks and makes the system energy *lower* for $n>n_{\rm cr}$. The critical size of the cluster, $n_{\rm cr}$, can be estimated from the inequality

$$V_{\rm int}(n_{\rm cr}a_s)+V_{\rm int}(2a_s)\geq V_{\rm int}(n_{\rm cr}a_s+a_s)+V_{\rm int}(a_s)\,, \tag{4.26}$$

so that $n_{\rm cr}\approx a_i/a_s$. Thus, the chains rupture due to increasing of the number of antikinks in the chain has the nucleation character similar to the first-order phase transitions.

Another feature of the FK model with the nonconvex interatomic interaction is the instability of the trivial ground state (GS). Looking at Eq. (4.25), we may expect that the trivial GS becomes unstable provided $a_i<a_s$ when $V''_{\rm int}(a_s)<0$. Indeed, it is easy to show that for $V''_{\rm int}(a_s)\leq -1/4$ the trivial GS (see Fig. 18a) becomes unstable, and the chain will be dimerized so that short and long bonds alternate as shown in Fig. 18b for the FK chain with the Morse interatomic interaction (Haas, 1978; Markov and Trayanov, 1987). This phenomenon is due to the fact that the average energy of one long and one short bonds is smaller than the energy of a bond with an intermediate length. Decreasing further the value $V''_{\rm int}(a_s)$, the ground state of the chain may be trimerized for $V''_{\rm int}(a_s)\leq -1/3$ (Fig. 18d), tetramerized (Fig. 18d), pentamerized (Fig. 18e), and so on. The simple linear analysis shows that for

$$V''_{\rm int}(a_s)\leq -\frac{1}{2}\left[1-\cos\left(\frac{2\pi}{q}\right)\right], \tag{4.27}$$

the trivial GS becomes unstable with respect to creation of a superstructure with the period $a=qa_s$ [Eq. (4.27) is valid for $q>2$ only].

To find all GS configurations for the FK model with a nonconvex interatomic interaction is a difficult problem because the system of stationary equations, $\partial U/\partial u_n=0$ (where U is the total potential energy), has usually many solutions, only one of them is the ground state while others correspond to metastable and unstable configurations. Griffits and Chou (1986) proposed an algorithm focused directly on the GS and valid for arbitrary interaction potentials $V_{\rm sub}(x)$ and

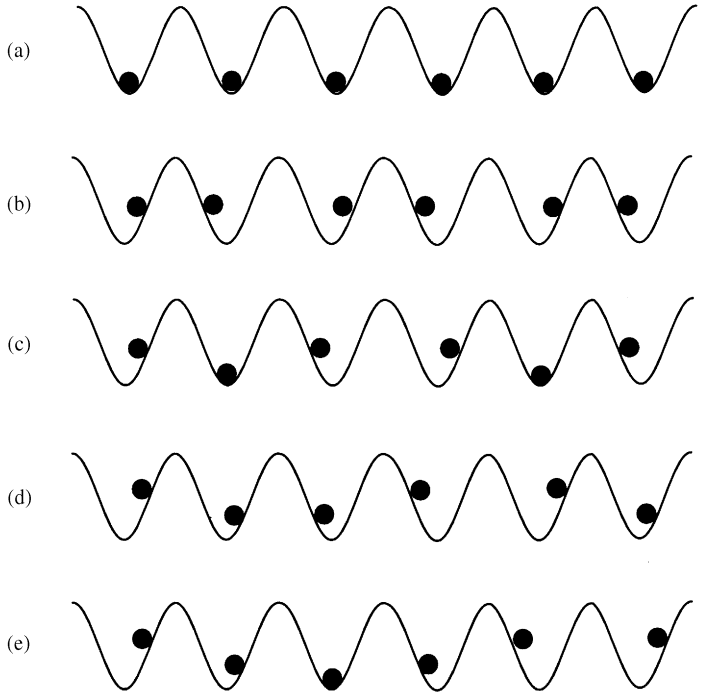

Fig. 18. Ground states of the FK model with the Morse interatomic potential (4.3): (a) undistorted chain, (b) dimerized GS, (c) trimerized GS, (d) tetramerized GS, and (e) pentamerized GS (Markov and Trayanov, 1988).

$V_{\rm int}(x)$. According to these authors, the GS of an infinite chain is found as a solution of the functional eigenvalue equation ($u, u' \in [-a_s/2, +a_s/2]$),

$$\varepsilon_0 + \tilde{V}(u') = V_{\rm sub}(u') + \min_u [V_{\rm int}(u' - u - a_s) + \tilde{V}(u)] \ . \tag{4.28}$$

The function $\tilde{V}(u)$ is called an effective potential [it has the same period as the primary substrate potential, $\tilde{V}(u + a_s) = \tilde{V}(u)$] and the value ε_0 is the average energy per particle in the GS. It was shown (Griffits and Chou, 1986; see also Griffits, 1990) that the function $\tilde{V}(u)$ always exists, and the corresponding value ε_0 is unique to be given by a solution of Eq. (4.28). One can construct the map

$$u = M(u') \ , \tag{4.29}$$

obtained by looking for u which, at a given u', minimizes the r.h.s. of Eq. (4.28). The attraction point of this map, $u_{n+1} = M(u_n)$, generates the corresponding GS configuration, $x_n = na_s + u_n$.

In order to get some physical interpretation of Eqs. (4.28) and (4.29), let us consider a semi-infinite chain of atoms with the edge atom fixed at the position u_0 (Marianer and Floria, 1988). Suppose that we let the rest part of the chain to relax freely reaching a minimum energy configuration corresponding to the boundary condition. Then the value of the derivative, $\partial \tilde{V}(u_0)/\partial u_0$, gives the value of the force which should be applied to hold the edge atoms at the position at $u = u_0$. Then the location of the nth atom is given by the function $M^n(u_0)$.

Usually the functional equation (4.28) is solved numerically by using a grid of a hundred (or more) equally spaced points in an interval around the point $u = 0$ and applying the r.h.s. of Eq. (4.28) to the functions defined at these points. The sequence of the iterations $\tilde{V}^{(n)}$ is stopped when $\tilde{V}^{(n+1)}$ and $\tilde{V}^{(n)}$ differ only by a constant ε_0 within a chosen accuracy. Note that for a hard-core interatomic potential, Eq. (4.28) has an analytic solution (Byrne and Miller, 1989).

As a typical example, let us consider, following to Marchand et al. (1987), the simplified FK model where the sinusoidal on-site potential, $V_{\rm sub}(x)$, is replaced by a sequence of parabolas, $(1 - \cos x_n) \to \frac{1}{2}u_n^2$. For the double-well interatomic potential (3.4) with $\beta = 1$, $a_* = a_s + \delta$, and $V_m = 1/2K$, the Hamiltonian of the model takes the form,

$$H = \sum_n \left[\frac{1}{2}\left(\frac{\mathrm{d}u_n}{\mathrm{d}t}\right)^2 + \frac{1}{2}u_n^2 + \frac{1}{4K}(u_{n+1} - u_n - \delta)^4 - \frac{1}{2K}(u_{n+1} - u_n - \delta)^2 \right]. \tag{4.30}$$

Fig. 19 shows an example of the effective potential $\tilde{V}(u)$ and the associated map $M(u)$ obtained for this model (Marchand et al., 1987). Note that $\tilde{V}(u)$ is continuous but it has a discontinuous first

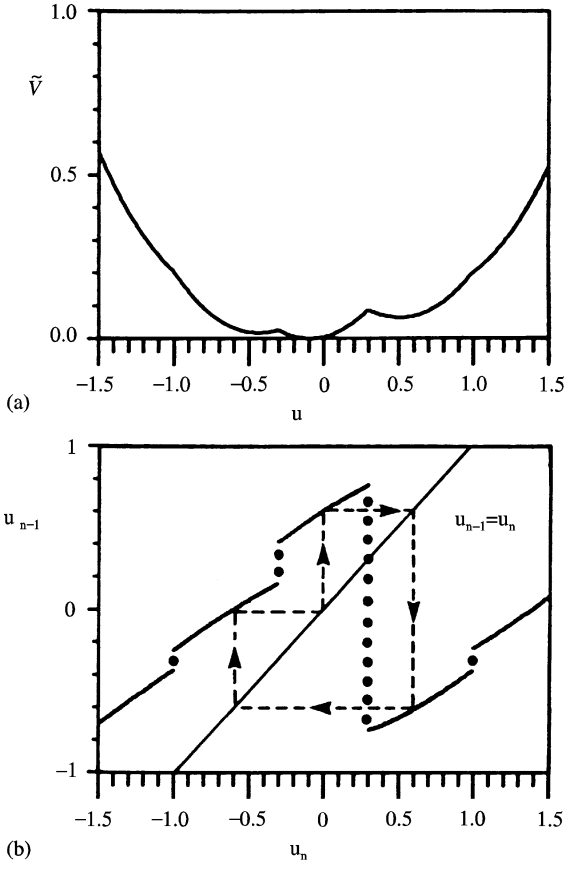

Fig. 19. (a) Effective potential $\tilde{V}(u)$ and (b) associated map $u_{n+1} = M(u_n)$ of the model (4.30) with a double-well interatomic potential for $K = 0.5$ and $\delta = 0.33$. Also shown in (b) are discontinuities (dotted lines), the line $u_{n+1} = u_n$, and the limit cycle of the period $q = 3$ (Marchand et al., 1987).

derivative at the same point where M is discontinuous. This corresponds to a situation when the ground state is "pinned" to the substrate potential, whereas for incommensurate GS configurations, when the chain of atoms can "slide" under zero force, one can expect the functions $\tilde{V}$ and M to be smooth.

Phase diagram obtained by Marchand et al. (1987) for the model (4.30) is shown in Fig. 20. The different GS configurations are labeled by the ratio of two integers, p/q, where q characterizes the period of the modulated structure, $a = qa_s$, and p is the number of long bonds per one unit cell, $p = \sum_1^q \Theta(u_{n+1} - u_n)$ (here the function Θ is the Heaviside function, $\Theta = +1$ for $x \geq 0$, and $\Theta = 0$ for $x < 0$). Numerical results suggest that the model (4.30) exhibits a complete Devil's staircase even through a rigorous proof of this statement is not possible within the framework of the effective potential algorithm. First, all the configurations are structurally stable. Second, the phase characterized by a ratio $\nu = (p + r)/(q + s)$ is always found to be between p/q and r/s phases for sufficiently small values of K. Hence, there is an infinite number of phases between any two given phases (including, probably, incommensurate phases which are characterized by irrational values of ν).

When the system parameters, i.e. γ or K in Eq. (4.30), are adiabatically varying, the phase transitions between different phases should take place. Numerical simulations (Marchand et al., 1987; Marianer and Floria, 1988) show that the transition between the homogeneous (1/1) and any modulated (p/q with $q > 1$) phases is usually a continuous (second-order) phonon-driven

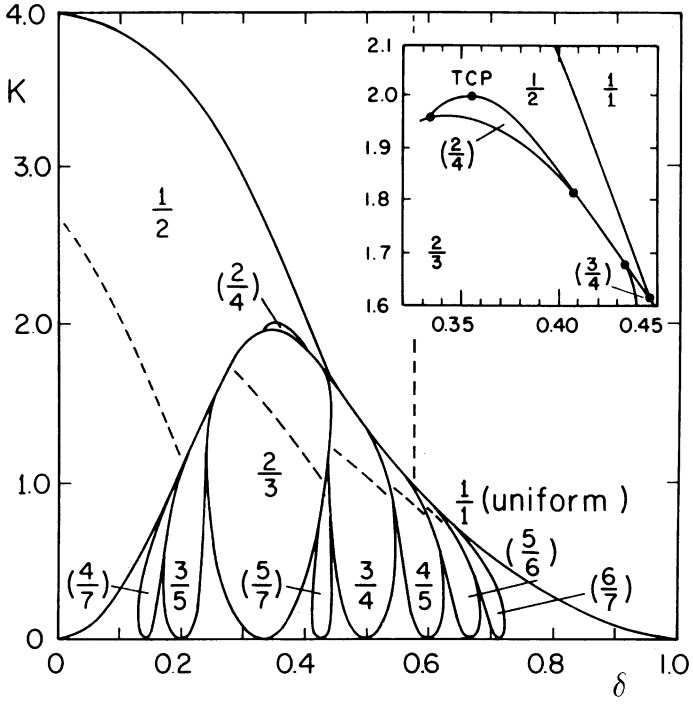

Fig. 20. The phase diagram for the model (4.30). The numbers p/q indicates the structure of modulated phases. The unlabeled regions contain additional commensurate phases. Inset shows the tricritical point (Marchand et al., 1987).

transition, while transitions between the modulated ground states, such as $\frac{1}{2} \to \frac{2}{3}$, $\frac{1}{2} \to \frac{3}{4}$, $\frac{2}{3} \to \frac{3}{4}$, etc., are typically first-order transitions, and they take place via creation of kink-type defects with subsequent nucleation of the defects.

It is worth to mention the work of Byrne and Miller (1989) who considered the FK model with nonconvex Lennard–Jones and double-well interatomic potentials, and the work by Takeno and Homma (1986) and Yokoi et al. (1988) where a sinusoidal interatomic potential was analysed. Marianer and Bishop (1988) investigated the FK model for which, in addition to the double-well interparticle interaction with $a_* = a_s$, the strain gradients are taken into account via next-nearest neighbor interactions, so that the system Hamiltonian is taken to be

$$H = \sum_n \left[\frac{1}{2}\left(\frac{\mathrm{d}u_n}{\mathrm{d}t}\right)^2 + (1 - \cos u_n) + \frac{1}{2} V_m \beta^4 (u_{n+1} - u_n)^4 - V_m \beta^2 (u_{n+1} - u_n)^2 + \frac{1}{2}\gamma (u_{n+1} + u_{n-1} - 2u_n)^2 \right]. \tag{4.31}$$

The model (4.31) can be useful in describing twinning in martensite materials (Barsch et al., 1984, 1987). To apply the effective potential method, Marianer and Floria (1988) transformed the Hamiltonian (4.31) into that with only nearest neighbor interactions but with vector variables defined as $v_n \equiv \{u_{2n}, u_{2n+1}\}$. As a result, the effective potential $\tilde{V}(v_n)$ becomes two-dimensional. The calculated phase diagram consists of various modulated commensurate and incommensurate GS structures.

Let us now briefly discuss an excitation spectrum of the modulated GS. First, we should note that the GS with a complex unit cell (i.e. $q > 1$) may have more than one phonon branch. Second, the modulated GS with the period $a = qa_s$ is q-times degenerated because the shift of all atoms in the chain on the distance which is integer multiplier of the substrate period, $\Delta x = ja_s$, $j = 1, \ldots, q-1$, will transform a GS to a nonequivalent one. Thus, the situation is quite similar to that which arises in the case of a multiple-well substrate potential (see Section 3.3 above). A standard 2π-kink splits into q independent subkinks undergoing repulsive interactions. One of those subkinks (in fact, the largest one) is a SG-like kink which describes a configuration in which atoms occupy neighboring minima of the substrate potential. The other $(q-1)$ subkinks are confined to be in an elementary cell of the substrate; sometimes they are called "interface kinks" or "domain walls". Note, however, that all types of subkinks are topologically stable. Of course, the subkinks as well as the interactions should satisfy some topological constraints.

It is clear that the dynamics of kinks for the modulated GS is much more complicated than that of the original FK model. As a simplest example, let us consider here the FK model with a double-well interatomic potential (3.4) (with $a_* = a_s$ or $\delta = 0$) following the paper by Marianer et al. (1988). As can be seen from Fig. 20, the GS of the chain is dimerized if $V_m\beta^2 > 1/8$, i.e. if $V''_{\mathrm{int}}(a_s) \leq -1/4$. This GS is two-times degenerated, and the first GS describes the "short-long" spring length configuration with the atomic coordinates $x_n = na_s + u_n$, $u_n = (-1)^n b$, where $b \approx (1/2\beta)(1 - 1/8V_m\beta^2)^{1/2}$ for $\beta \gg 1$. The second GS corresponds to the "long-short" length configuration with $u_n = (-1)^{n+1} b$. To consider a subkink ("interface") which links these two GSs, we introduce a dimensionless variable $v_n = (-1)^n u_n/b$ and use the continuum limit approximation, $v_n \to v(x)$ and $v_{n\pm1} \to v \pm a_s v_x$, so that the Hamiltonian is reduced to the form

(Marianer et al., 1988),

$$H \approx b^2 \int \frac{\mathrm{d}x}{a_s} \left\{ \frac{1}{2} v_t^2 + \frac{1}{2} C(v) v_x^2 + A(v^2 - 1)^2 \right\}, \tag{4.32}$$

where

$$A = 2\left(V_m \beta^2 - \frac{1}{8} \right) \quad \text{and} \quad C(v) = 2V_m \beta^2 \left[1 - 3v^2 \left(1 - \frac{1}{8V_m \beta^2} \right) \right].$$

Hamiltonian (4.32) corresponds to the ϕ^4 model with an effective spring constant $C(v)$ which depends on the variable $v(x,t)$. A kink of the ϕ^4 model (4.32), $v(x) = \tanh(x/d_{\mathrm{eff}})$, has an effective width,

$$d_{\mathrm{eff}} = b\sqrt{2} \left(\frac{1 - 12b^2\beta^2}{1 - 1/8V_m\beta^2} \right)^{1/2}. \tag{4.33}$$

The kink's width becomes infinite at $V_m\beta^2 \to 1/8$ (when the dimerized GS disappears) and it vanishes when $b \to 1/2\beta\sqrt{3}$, or for $V_m\beta^2 \to \frac{1}{8} + \frac{1}{16} = \frac{3}{16}$. The latter case is similar to the case of an antikink in the FK model with exponential interatomic interactions when the nonlinearity parameter α is less than the critical value α_{cr} (see Section 4.3). Analogously to this, continuum limit approximation breaks down and for $V_m\beta^2 \geq 3/16$ the subkink becomes pinned by the substrate potential.

General method to analyze the kinks excited on a modulated GS requires straightforward but rather lengthy calculations. Therefore, we outline here only the main idea of this approach not going into specific details. Atomic coordinates are given by the relation

$$x_n = na_s + X_n + u_n\,, \tag{4.34}$$

where X_n corresponds to the kink coordinate (for an "interface" we take $X_n = 0$) and u_n ($|u_n| < a_s/2$) describes the modulation of the GS. Displacements u_n are expanded into a Fourier series,

$$u_n(t) = v_n(t)\mathrm{e}^{\mathrm{i}Qn} + v_n^*(t)\mathrm{e}^{-\mathrm{i}Qn} + \text{h.h.}\,, \tag{4.35}$$

h.h. stands for higher harmonics, with some wavenumber $Q = 2\pi p/q$ (p and q are integers) characterizing the modulated GSs. (Note that if we restrict ourselves only by the first harmonic terms in Eq. (4.35), the approximate ground state may be infinitely degenerated for $q > 2$, and associated kinks will be not topologically stable.) Then the expressions (4.34) and (4.35) are substituted into the Hamiltonian of the model, the periodic substrate potential is changed to be

$$V_{\mathrm{sub}}(x_n) = 1 - \cos u_n \cos X_n + \sin u_n \sin X_n\,, \tag{4.36}$$

and the functions $\cos u_n$ and $\sin u_n$ are expanded into Taylor series in small u_n. The resulting Hamiltonian can be then considered in the continuum limit approximation in a strightforward way using, for example, the methods described in details by Slot and Janssen (1988a,b) for the frustrated ϕ^4 model. Namely, the variables X_n and v_n are assumed to be slowly varying on the scale of order of the lattice spacing a_s, the latter assumption allows us to use the continuum limit expansions, $na_s \to x$, $S_n \to S(x,t)$, $S_{n\pm1} \to S \pm a_s S_x$, where $S \sim \mathcal{O}(1)$, $S_x = \partial S/\partial x \sim \mathcal{O}(\varepsilon)$, $S_x^2, S_{xx} \sim \mathcal{O}(\varepsilon^2)$, etc., with

$\varepsilon \ll 1$, and S_n stands for X_n or v_n. Substituting these expansions into the Hamiltonian, neglecting fast varying terms, and making some transformations, we can derive an approximate Hamiltonian which yields an effective motion equation which has to be solved together with appropriate boundary conditions. However, the procedure described above is rather lengthy, so that direct numerical simulations with a discrete FK model is usually more straightforward.

To conclude this section, we would like to mention that the FK model with Morse or Lennard–Jones interatomic potentials has *three* characteristic lengths, a_s, a_i, and a_0. The additional spatial scale, a_0, corresponds to a minimum of the interaction potential. For the boundary conditions used above (i.e. the chain's ends are *fixed* at infinities) this fact does not change the results provided $a_0 \geq a_{\mathrm{FM}}$, where the value a_{FM} ($a_{\mathrm{FM}} < a_s$) introduced by Frank and van der Merwe (1949a, b) describes the situation when the ground state of the chain with *free* ends contains kinks with a finite density. For $a_0 < a_{\mathrm{FM}}$ the infinite chain (with fixed ends) will rupture into two semi-infinite chains because this effect leads to a lower system energy in the case $V_{\mathrm{int}}(x) \to 0$ at $x \to \infty$. However, such a rupture is not connected with "extra" antikinks as in the case analysed above.

4.4. Kac–Baker interaction

Now we extend the classical FK model, assuming that not only nearest neighboring atoms interact in the chain. It is natural to consider the interaction potential $V_{\mathrm{int}}(x)$ which remains convex and falls fast enough for $|x| \to \infty$ (e.g., as in the case of exponentially decaying potential). In fact, the dynamics of the FK model in this case is similar to that for the model when the nearest neighbors interact only, but it is characterized by the *renormalized* coupling parameter,

$$g \to g_{\mathrm{eff}} = \sum_{j=1}^{\infty} j^2 V''_{\mathrm{int}}(ja_s) \,. \tag{4.37}$$

As an example, we take the exponential interaction (4.1), for which Eq. (4.37) yields

$$g_{\mathrm{eff}} = g\frac{(1+S)}{(1-S)^3} \,, \tag{4.38}$$

where $g = V_0\beta^2$ is defined above, and

$$S = \mathrm{e}^{-\beta a_s}. \tag{4.39}$$

For the long-range interatomic potential, when $\beta a_s \ll 1$, from Eq. (4.38) it follows

$$g_{\mathrm{eff}} \approx \frac{2g}{(\beta a_s)^3} \gg g \,. \tag{4.40}$$

For an exponential interatomic interaction the results mentioned above may be simply proved with the help of the method firstly proposed by Sarker and Krumhansl (1981) (see also Remoissenet and Flytzanis, 1985; Croitoru, 1989; Braun et al., 1990; Woafo et al., 1993). Following this procedure, we expand the interaction potential (4.1) into a Taylor series keeping the cubic terms, for interaction of the nearest-neighbors, and quadratic terms, for interaction of other atoms. In this

case the interaction energy takes the form

$$H_{\rm int} = \frac{1}{2}\sum_{i\neq j} V_{\rm int}(x_i - x_j) \approx \frac{A}{6}\sum_i (u_i - u_{i-1})^3 + J\frac{(1-S)}{4S}\sum_{i\neq j} S^{|i-j|}(u_i - u_j)^2, \tag{4.41}$$

where we have introduced the following notations,

$$A = \alpha\left(\frac{d}{a_s}\right)^3, \qquad J = \frac{(d/a_s)^2}{(1-S)}, \tag{4.42}$$

and the parameters $d = a_s\sqrt{g}$ and $\alpha = -\beta a_s/d$ are defined above. Thus, Eq. (4.41) describes a one-dimensional chain of atoms interacting via a pair potential of the Kac–Baker form (Baker, 1961; Kac and Helfand, 1973). The equations of motion which correspond to the Hamiltonian (4.41), is

$$\frac{{\rm d}^2 u_i}{{\rm d}t^2} + \sin u_i + \frac{1}{2}A[(u_i - u_{i-1})^2 - (u_{i+1} - u_i)^2] + 2Ju_i = L_i, \tag{4.43}$$

where the auxiliary quantity

$$L_i = J\frac{(1-S)}{S}\sum_{j=-\infty(j\neq 0)}^{+\infty} S^{|j|}u_{i+j} \tag{4.44}$$

satisfies the following recurrence relation (Sarker and Krumhansl, 1981)

$$\left(S + \frac{1}{S}\right)L_i = L_{i+1} + L_{i-1} + J\frac{(1-S)}{S}(u_{i+1} + u_{i-1} - 2Su_i), \tag{4.45}$$

which allows to reduce Eqs. (4.43), (4.44) and (4.45) to an effective problem which includes only interactions of the nearest-neighbor atoms.

In the continuum limit, Eqs. (4.43), (4.44) and (4.45) can be presented in the form,

$$u_{tt} + \sin u - d_{\rm eff}^2 u_{xx} - \alpha d^3 u_x u_{xx} = Sa_s^2(1-S)^{-2}f(u), \tag{4.46}$$

where

$$f(u) = u_{ttxx} - (u_x)^2\sin u - u_{xx}(1 - \cos u), \tag{4.47}$$

$$d_{\rm eff}^2 \equiv d^2\frac{(1 + S + S/J)}{(1-S)^3}. \tag{4.48}$$

Using the dimensionless coordinate, $x \to x/d_{\rm eff}$, we derive the equation

$$u_{tt} + \sin u - u_{xx}(1 + \alpha_{\rm eff}u_x) = \varepsilon f(u), \tag{4.49}$$

where

$$\alpha_{\rm eff} \equiv \alpha\left(\frac{d}{d_{\rm eff}}\right)^3, \qquad \varepsilon = \frac{S}{S + J(1+S)}. \tag{4.50}$$

In the case $d \gg a_s$ we have $J \gg 1$ and $\varepsilon \ll 1$; therefore, the perturbation $\varepsilon f(u)$ in Eq. (4.49) can be neglected. Consequently, a long-range exponential character of the atomic interaction, as compared with the considered-above short-range interactions, results only in an effective renormalization of the kink parameters, e.g. the kink s width increases ($d \to d_{\rm eff} > d$), while its nonlinearity parameter decreases ($\alpha \to \alpha_{\rm eff}$, $|\alpha| < |\alpha_{\rm eff}|$). We would like to note also that interaction between two kinks is always more extended than that for the direct interaction of two extra atoms via the potential (4.1) because $d_{\rm eff}^{-1} \approx \beta(\beta_s/2g)^{1/2} \ll \beta$ for $\beta a_s \ll 1$ and $g \gg 1$.

At last, from Eqs. (4.46), (4.47) and (4.48) it follows that the long-range character of the interatomic interaction changes the dispersion relation for phonons. Indeed, for the wave numbers $|\kappa| \ll \pi$, the dispersion relation can be obtained in the following form:

$$\omega_{\rm ph}^2(\kappa) = \frac{\omega_{\rm min}^2 + g_{\rm eff}\kappa^2}{1 + S(1-S)^{-2}\kappa^2}\,, \tag{4.51}$$

where $g_{\rm eff} = (d_{\rm eff}/a_s)^2$ and $\omega_{\rm min} = 1$. We would like to mention that the double SG model with the Kac–Baker interactions was considered by Croitoru (1989) with qualitatively similar conclusions.

4.5. Long-range interactions

Interaction potentials discussed up to now allow a reduction in the continuum approximation to a SG-type equation with local interaction. In contrast to that case, the motion equation for the FK model with a power-law interatomic interaction,

$$V_{\rm int}(x) = V_0\left(\frac{a_s}{x}\right)^n, \tag{4.52}$$

can be reduced to *a nonlocal integro-differential* SG equation (Kosevich and Kovalev, 1974b; Pokrovsky and Virosztek, 1983; Braun et al., 1990). To derive such an equation, let us use the continuum approximation, $j \to y = ja_s$, $\sum_j \to \int {\rm d}y/a_s$, and change the variable, $y \to x = y + u(y)$, so that approximately, ${\rm d}x = (1 + u_y)\,{\rm d}y \approx (1 + u_x)\,{\rm d}y$ and ${\rm d}y \approx (1 - u_x)\,{\rm d}x$. Then the interaction energy takes the form

$$H_{\rm int} = \frac{1}{2}\int\!\!\int \frac{{\rm d}x\,{\rm d}x'}{a_s^2} u_x(x) u_{x'}(x') V_{\rm int}(x - x')\,. \tag{4.53}$$

The result (4.53) has a simple physical meaning, since the value $\rho(x) \equiv -u_x(x)/a_s$ is the density of the atomic excess (with respect to the initial commensurable structure). For a local potential of the atomic interactions,

$$V_{\rm int}(x) = a\delta(x)d^2\,, \tag{4.54}$$

Eq. (4.53) takes the form of the standard SG equation. For the nonlocal potential (4.52) the integral (4.53) diverges provided $(x - x') \to 0$, and, as a result, one should make a cut of the integration interval at some distance $a^* \approx a_s$ (Braun et al., 1990). Introducing dimensionless variables, we may obtain the Hamiltonian for a nonlocal SG model,

$$H = \frac{1}{\delta}\int {\rm d}x \left\{ \frac{1}{2}u_t^2 + \frac{1}{2}u_x^2 + V_{\rm sub}(u) + \frac{1}{2}Au_x \int_\delta^\infty \frac{{\rm d}x'}{(x')^n}\left[u_x(x + x') + u_x(x - x')\right] \right\}, \tag{4.55}$$

where

$$\delta = a_s/d, \qquad A = V_0\delta^{n+1}/(2\pi)^2. \tag{4.56}$$

If the potential $V_{\rm int}(x)$ is short-range, then, without the last term in Eq. (4.55), the expression for the energy should take the form corresponding to the SG model, for which $d^2 = a_s^2 V''_{\rm int}(a_s) = V_0 n(n+1)$. We use this relation to reduce the number of independent parameters and express V_0 of the potential (4.52) in terms of the parameter d. As a result,

$$A = \frac{V_0\delta^{n-1}}{n(n+1)}\,, \tag{4.57}$$

and the Hamiltonian (4.55) is a function of only two parameters, δ and n. The motion equation corresponding to the Hamiltonian (4.55) has the form

$$u_{tt} - u_{xx} + V'_{\rm sub}(u) = A\frac{\partial}{\partial x}\int_\delta^\infty \frac{{\rm d}x'}{x'^n}[u_x(x+x') + u_x(x-x')]\,, \tag{4.58}$$

and it describes the dynamics of a chain with a nonlocal interaction.

From Eq. (4.58), one can see that the core structure of a kink (i.e. its shape at $|x - X| < d$) is determined mainly by local terms of the motion equation (Pokrovsky and Virosztek, 1983). Therefore, "local" characteristics of a kink, such as its effective mass or amplitude of the PN potential, will not differ significantly from those calculated for the local FK model with the renormalized elastic constant

$$g_{\rm eff} = \sum_{j=1}^{\infty} V''_{\rm int}(ja_s) = gS_{n+2}, \qquad g = n(n+1)\frac{V_0}{a_s^2}\,, \tag{4.59}$$

where $S_{\rm m} = \sum_{j=1}^{\infty} j^{-m}$ (for example, $S_3 \approx 1.202$, $S_5 \approx 1.037$), and the anharmonicity of the interaction is determined by the parameter

$$\alpha_{\rm eff} = \alpha S_{n+2}^{-3/2}, \quad \alpha = -(n+2)/d\,. \tag{4.60}$$

Indeed, the dependencies $E_{\rm PN}(l)$ and $m(l)$ (where $l \equiv \pi\sqrt{g}$) calculated by Braun et al. (1990) for the Coulomb ($n = 1$) and dipole–dipole ($n = 3$) atomic interactions shown in Fig. 21are qualitatively similar to those in Fig. 17 obtained for the local anharmonic interaction in the FK model. The difference between the parameters $E_{\rm PN}$ and m for a kink and an antikink at the same value of the parameter g for the dipole interaction, is much larger than for the Coulomb interaction, which is accounted for by larger anharmonicity of the dipole potential, according to Eq. (4.60). We note that the amplitude of the PN potential for the FK model with the Coulomb interaction ($n = 1$) at some particular values of the system parameters was calculated by Wang and Pickett (1976). Braun et al. (1990) have calculated also the kink's parameters for the power-law FK model with nonsinusoidal substrate potential. The dependencies (see Fig. 22) are similar to those for the local FK model described in Section 3.2. It is interesting to note that for $g \ll 1$ the amplitude of the PN potential for the kink moving in the substrate potential with sharp bottoms may be *lower* than that for the sinusoidal substrate potential.

In spite of the fact that local characteristics of the kink are quite similar to those for the classical FK model, asymptotics of the kink of Eq. (4.58), which are determined by the last term, are very

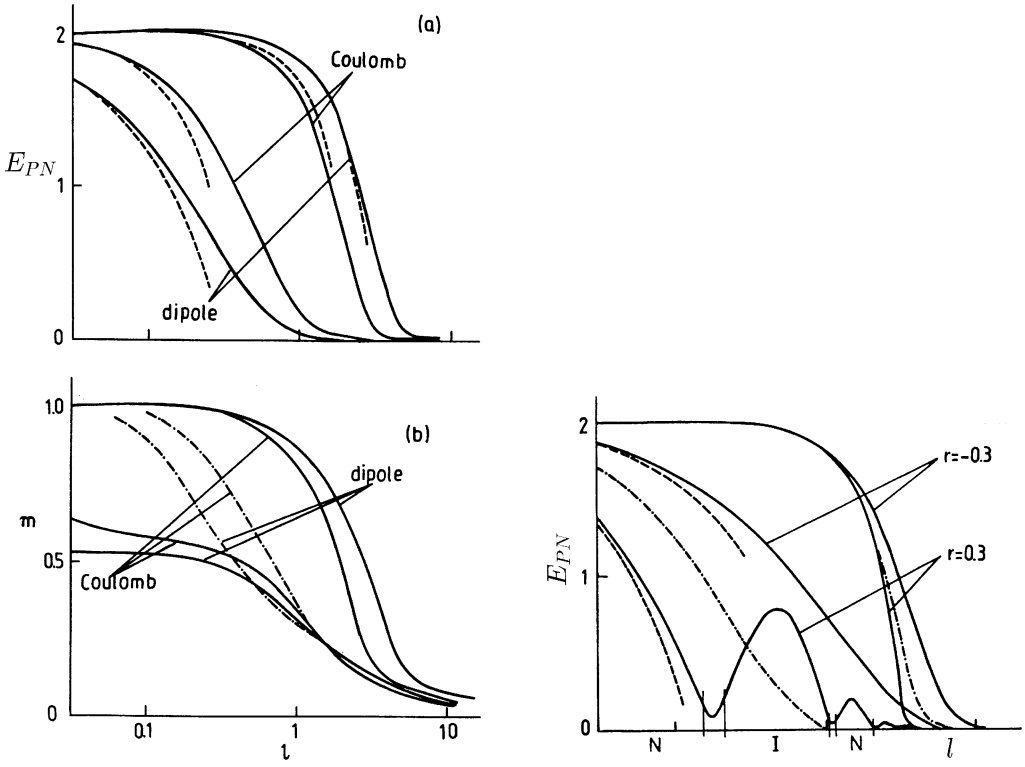

Fig. 21. Dependencies of the PN energy $E_{PN}(l)$ (a) and effective mass $m(l)$ (b) for a kink and antikink in the presence of the Coulomb and dipole mechanisms of interatomic interaction. The parameter $l = \frac{1}{2}\sqrt{V_0 n(n+1)}$ for $n = 1$ or 3, is defined by with the kink width d. Dashed curves show analytical asymptotics (Braun et al., 1990).

Fig. 22. Dependence of the PN energy $E_{PN}(l)$, where $l = \sqrt{3V_0}$, for the dipole repulsion of atoms in the case of the nonsinusoidal substrate potential (3.18) with the parameters $s = \pm 0.3$. For comparison, dash-dotted curves show the kink characteristics for the sinusoidal potential $V_{sub}(x)$. Dashed lines show the results of the weak-bond approximation. Regions of the normal and inverse PN relief are indicated by the letters N and I, respectively (Braun et al., 1990).

different from those of the SG kink, and they are power-like (Kosevich and Kovalev, 1974b; Pokrovsky and Virosztek, 1983). Indeed, linearizing Eq. (4.58) near the asymptotic value $u(\infty)$ and integrating by parts, we obtain

$$|u(x) - u(\infty)| \approx \frac{2\pi n A}{\omega_{\min}^2 |x|^{n+1}}, \quad x \to \pm\infty \ , \tag{4.61}$$

where $\omega_{\min}^2 = V''_{sub}(0)$. It is clear that for the power-law interatomic forces, the interaction between kinks (i.e., between "extra" atoms or holes in the chain) should also be power-like. This has been shown by Kosevich and Kovalev (1974b) for a crowdion moving in a bulk of a crystal, by Gordon and Villain (1979), Lyuksyutov (1982), and Talapov (1982), for elastic interaction of atoms

adsorbed on a crystal surface, and by Haldane and Villain (1981) and Pokrovsky and Virosztek (1983), for dipole–dipole interaction of adatoms. To show this directly, let us consider the chain with two kinks of topological charges σ_1 and σ_2, respectively, which are separated by some distance x_0. In the zero-order approximation, the solution of Eq. (4.58) can be presented as a superposition of two SG kinks,

$$u(x,t) = u_{\mathrm{k}}^{\mathrm{SG}}\left(x - \frac{1}{2}x_0\right) + u_{\mathrm{k}}^{\mathrm{SG}}\left(x + \frac{1}{2}x_0\right). \tag{4.62}$$

Within the framework of the adiabatic perturbation theory (see, e.g., Kivshar and Malomed, 1989) the change of the relative coordinate x_0 due to the kink interaction is given (for large values of x_0) by the following equation (Braun et al., 1990)

$$\frac{\mathrm{d}^2 x_0}{\mathrm{d}t^2} = (2\pi)^2 nA\frac{\sigma_1\sigma_2}{x_0^{n+1}}\,, \tag{4.63}$$

which reduces the problem to a motion of an effective particle in the potential

$$V_{\mathrm{int}}^{(0)}(x_0) = \frac{(2\pi)^2 A\sigma_1\sigma_2}{x_0^n}\,. \tag{4.64}$$

It is interesting to note that after introducing again the dimensional variables we find that the interaction law obtained above is nothing but the interaction of two "extra" atoms (or holes) in the chain. Such a contribution to the kink interaction is absent in the standard FK model where only nearest-neighboring forces are taken into account, i.e. for the classical FK model we always have $V_{\mathrm{int}}^{(0)} \equiv 0$. In the local FK model, however, the kink interaction is caused by an overlapping of their tails, and such an overlapping gives the interaction energy $V_{\mathrm{int}}^{(\mathrm{loc})}(x) \propto u_x(x)$, which is proportional to the density of the "excess" atoms. Of course, the same effect will give a contribution to the kink interaction energy for the power-law forces as well. However, in that case this contribution is *smaller* in comparison with the main interaction described by Eq. (4.64), i.e. $V_{\mathrm{int}}^{(\mathrm{loc})} \propto x^{-(n+2)}$. Indeed, as follows from the numerical simulations of Braun et al. (1990), in the case of the dipole interaction the result $V_{\mathrm{int}}^{(\mathrm{loc})}(x) \propto x^{-5}$ is in a good agreement with numerical data. We should note, however, that in contrast to the case of the Kac–Baker interaction (see Section 4.3), the contribution from the kinks' tails is small and, in particular, for the power-law interactions such a contribution may be neglected.

The phonon spectrum of the nonlocal FK model is described by the expression

$$\omega_{\mathrm{ph}}^2(k) = \omega_{\mathrm{min}}^2 + 2g\sum_{j=1}^{\infty}\frac{[1-\cos(\kappa j)]}{j^{n+2}}\,, \tag{4.65}$$

which is similar to the dispersion relation of a local FK model. However, parameters of the breather excitations differ remarkably from those for the local FK model. For example, the period T_{br} of a large-amplitude (small-frequency) breather, determined from the kink–antikink interaction, is given by (Braun et al., 1990)

$$T_{\mathrm{br}} = \frac{2\pi}{\omega} = A^{-1/2}C_n x_{\mathrm{max}}^{(1+n/2)}, \quad C_n = \frac{\sqrt{2}\Gamma(1/n+1/2)}{\sqrt{\pi}\Gamma(1/n)}\,, \tag{4.66}$$

where $x_{\max}$ is the maximum amplitude of the breather,

$$x_{\max} = \left(\frac{4\pi^2 A}{|\varepsilon_{\rm br}|}\right)^{1/n} \propto \omega^{-2/(n+2)} . \tag{4.67}$$

From Eqs. (4.66) and (4.67), we can make a conclusion that the breather energy is

$$|\varepsilon_{\rm br}| = \frac{(C_n\omega)^{2n/(n+2)}}{(4\pi^2 A)^{2/(n+2)}} . \tag{4.68}$$

The results (4.67) and (4.68) can be compared with those for the standard FK model considered as that formally corresponding to the limit case $n \to \infty$ when $x_{\max} \propto |\ln\omega|$ and $|\varepsilon_{\rm br}| \propto \omega^2$.

Recently, the nonlocal SG equation of the form,

$$u_{tt} + \sin u = \frac{\partial}{\partial x}\int_{-\infty}^{+\infty} {\rm d}x' G(x-x') u_{x'}(x',t) , \tag{4.69}$$

with the exponential kernel, $G(x) = (2\lambda)^{-1}\exp(-|x|/\lambda)$ or the McDonald kernel, $G(x) = (\pi\lambda)^{-1}{\rm K}_0(|x|/\lambda)$, has been derived to describe the nonlocal effects in the electrodynamics of long Josephson junctions (for an overview, see Alfimov, 1996; Aliev et al., 1995; and references therein). For this type of nonlocal models, it has been shown that the nonlocal SG equation (4.69) with the exponential interaction does not support any *moving* 2π-kinks, but instead, it allows the moving 4π-, 6π-, etc. kinks. However, these complex kinks can propagate only with certain velocities (Alfimov et al., 1993).

5. Kink diffusion

5.1. Preliminary remarks

In the previous sections we have investigated the properties of an isolated FK chain, as a Hamiltonian system. In an isolated chain, the kink's effective friction coefficient η corresponds to the "intrinsic" damping $\eta_{\rm int}$ caused by the energy exchange between the kink's translational/vibrational motion and phonon modes excited in the chain. However, to describe realistic physical objects such as dislocations, adsorbed layers, hydrogen-bonded atomic chains and other systems with the help of an effective FK model, we should remember that usually the FK model takes into account only a part of the whole number of degrees of freedom of a physical system while the other part, which corresponds to other types of excitations, should be taken into account effectively. As an example, for adatomic systems an external potential $V_{\rm sub}(x)$ is created by the atoms which form a crystal surface; in the case of a crowdion, the periodic potential is produced by the nearest arrows of metal atoms, etc. In fact, the substrate plays a twofold role: first, it produces an effective external potential to the atoms of the primary chain modelled by the FK model, and second, it creates a mechanism for an energy exchange between the atoms of the FK chain and the substrate degrees of freedom. In other words, the FK chain is usually a nonconservative system, so that the substrate plays a role of a thermostat at a certain temperature T.

Thus, because the positions of the substrate atoms are not fixed, in a general case their motion has to lead to the following effects:

- The substrate atoms should feel and response to the corresponding configurations of atoms in the FK chain. Such a "polaronic effect" will lead to increasing the amplitude of the external potential $V_{\rm sub}(x)$;
- At a nonzero temperature, $T \neq 0$, the substrate atoms are vibrating with some amplitudes. This leads to a dependence of the value ε_s on the temperature (the Debye–Waller effect);
- There always exists an energy exchange between the FK chain and the substrate. This effect leads to an additional damping, i.e. to the "external" friction $\eta_{\rm ext}$. For example, in the case of adatomic chains the external friction is the main damping mechanism ($\eta_{\rm ext} \gg \eta_{\rm int}$) (Braun, 1989).

To describe the energy exchange mechanisms mentioned above, we introduce *an effective friction force* acting on the lth atom of the FK chain. In a general case the friction force $F_l^{\rm (fr)}$ can be taken in the form,

$$F_l^{\rm (fr)}(t) = -m_a \sum_{l'} \int_0^\infty {\rm d}\tau \, \mathcal{N}_{ll'}(\tau) \dot{x}_{l'}(t-\tau) \, , \tag{5.1}$$

where the dot stands for a derivative in time, and the response function

$$\mathcal{N}_{ll'}(\tau) \equiv \mathcal{N}(\dot{x}_l, \ddot{x}_l, \ldots, \dot{x}_{l'}, \ddot{x}_{l'}, \ldots; \tau) \, , \tag{5.2}$$

is, in a general case, nonlocal, nonlinear, and non-Markovian. It is evident that the calculation of this function as well as the solution of the corresponding motion equations is extremely complicated problem. For the sake of simplicity, it is usually assumed that the operator $\mathcal{N}$ is Markovian and local, and, moreover, it does not depend on the position of a given atom relative to the substrate potential, i.e.

$$\mathcal{N}_{ll'}(\tau) = 2\eta \delta_{ll'} \delta(\tau) \, , \tag{5.3}$$

so that the force (5.1) reduces to the standard viscous friction,

$$F_l^{\rm (fr)}(t) = -m_a \eta \dot{x}_l(t) \, . \tag{5.4}$$

However, we should realize that the parameter η in Eq. (5.4) is in fact an "effective" friction coefficient which is calculated by means of a suitable averaging of the response function over all the trajectories of the atomic motion. Thus, because realistic models are quite complicated, the value of η should be estimated rather than calculated with the help of a simplified model.

Besides the energy flux from the FK chain to the substrate caused by the damping force (5.4), it should exist also the backward flux of the energy to the chain which is usually treated as $T \neq 0$. This effect may be modeled by introducing a random force (noise) $\delta F_l(t)$ with zero mean value, $\langle \delta F_l(t) \rangle = 0$, acting on the lth atom of the FK chain from the substrate. Amplitude of the external noise is determined by the fluctuation–dissipation theorem which is based on the assumption of thermal equilibrium, i.e. the equal shearing of the kinetic energy between all degrees of freedom, $\frac{1}{2} m_a \langle \dot{x}_l^2 \rangle = \frac{1}{2} k_{\rm B} T$, at the stationary state. Depending on the physical model under consideration, the external noise may be additive or/and multiplicative. Thus, the problem reduces to the analysis

of the dynamics of the FK chain governed by a system of Langevin-type equations. In the present section we discuss the case when at $T \neq 0$ the chain contains a single kink only. This situation is described by the periodic boundary conditions, $u_{N+1} = u_1 \pm a_s$, when the temperature is assumed to be low enough, $k_B T \ll \varepsilon_k$, so that the probability of the thermal creation of a kink–antikink pair is negligible. So, the problem is to derive and solve a stochastic motion equation for the kink collective coordinate $X(t)$. The kink diffusion coefficient is then obtained as

$$D_k = \lim_{t\to\infty} \frac{1}{2t}\langle [X(t) - X(0)]^2 \rangle \,, \tag{5.5}$$

or, more generally, as

$$D_k(\bar{\omega}) = \int_0^\infty \mathrm{d}t\, \mathrm{e}^{\mathrm{i}\bar{\omega}t}\langle \dot{X}(t)\dot{X}(0)\rangle, \quad \mathrm{Im}(\bar{\omega}) > 0 \,. \tag{5.6}$$

Thus, the physical reason of a diffusional motion for the kink is the effective coupling of the FK chain with the thermostat, i.e. the existence of the nonzero "external" friction coefficient η_{ext}. However, the long-time-scale dynamics of the kinks might be also diffusional for an isolated chain as well. Indeed, as we have shown above, any deviation of the model from the integrable case of the pure SG system such as nonsinusoidal substrate potential, anharmonic interatomic interactions and discreteness of the atomic chain will destroy the exact integrability of the system. Therefore, besides the external chaos induced by the substrate, the dynamics of the FK chain has to exhibit its own "intrinsic chaotization". This effect may be described approximately by introducing an "intrinsic" friction coefficient η_{int}. It is clear that η_{int} cannot be easily calculated, but it can be estimated by a perturbation technique. The intrinsic friction leads to a viscous diffusion of a kink which will be discussed in Section 5.3.

It is interesting that the kink dynamics exhibits two types of diffusion, namely, the *conventional* or *viscous* diffusion and *anomalous* diffusion. To explain the latter mechanism of the kink diffusional motion, we should recall that any collision of a kink with other excitations such as phonons causes a phase shift of the kink, i.e. the displacement of the kink's coordinate. If such collisions occur randomly in time, the kink will undergo a Brownian random walk, however, keeping its averaged velocity unchanged because such collisions are almost elastic or completely elastic for the limit described by the SG equation. It is important that this diffusion mechanism exists even in the integrable SG model where the viscous diffusion is absent (if, of course, we suppose that the mechanism which makes the collisions can be modeled as a random process). A physical reason for the anomalous kink diffusion is based on the fact that a kink is an extended object with its own width, whereas a usual particle cannot exhibit this type of motion being a point-like object which does not suffer a shift of its location after a collision. The coefficient of the anomalous diffusion can be calculated in the random phase approximation as it is usually assumed in the case of the friction for a particle linearly coupled with a thermostat (see, e.g., Haken, 1980). This problem will be analysed in Section 5.4.

In real physical systems the kink diffusion coefficient D_k is determined by all the mechanisms mentioned above, and we expect that it is determined by the anomalous diffusion coefficient D_a for short-time scales, $t \ll \eta$, and by the viscous diffusion coefficient D_η for $t \gg \eta^{-1}$. Besides, in a strongly discrete chain, when the amplitude of the PN potential exceeds the energy of the kink's

thermalized motion, $E_{\rm PN} > k_{\rm B}T$, the kink diffusion becomes thermally activated according to the Arrhenius law, $D_{\rm k} \propto \exp(-E_{\rm PN}/k_{\rm B}T)$.

5.2. Langevin equation

In the presence of the viscous friction (5.4) and the additive stochastic force, the motion equation for the classical FK chain is changed to be

$$m_a \frac{{\rm d}^2 x_l}{{\rm d}t^2} + m_a \eta \frac{{\rm d}x_l}{{\rm d}t} - g(x_{l+1} + x_{l-1} - 2x_l) + V'_{\rm sub}(x_l) = \delta F_l(t) \; . \tag{5.7}$$

The fluctuation–dissipation theorem says that the self-correlation function of the fluctuation force δF_l should satisfy the relation

$$\langle \delta F_l(t)\, \delta F_l(t') \rangle = 2\eta m_a k_{\rm B} T \delta(t - t') \; , \tag{5.8}$$

while the cross-correlation function, $\langle \delta F_l \delta F_{l'} \rangle$ for $l \neq l'$, may be defined in an arbitrary manner. In particular, it is natural to suppose that the spacial correlations decay exponentially with a correlation length $\lambda_{\rm F}$,

$$\langle \delta F_l(t) \delta F_{l'}(t') \rangle = 2\eta m_a k_{\rm B} T {\rm e}^{-|l-l'|a_s/\lambda_{\rm F}} \delta(t - t') \; . \tag{5.9}$$

Below we consider the SG limit, i.e. $g \gg 1$ and $V'_{\rm int}(x) = \sin x$, when we should take $x_l = la_s + u_l$, $la_s \to x$, $u_l(t) \to u(x,t)$, and $\delta F_l(t) \to \delta F(x,t)$, so that the Langevin equation (5.7) becomes (recall $m_a = 1$):

$$u_{tt} + \eta u_t - d^2 u_{xx} + \sin u = \delta F(x,t) \; . \tag{5.10}$$

In order to write Eq. (5.9) in the continuum limit, we have to use additionally the rules $\sum_l \to \int {\rm d}x/a_s$ and $\delta_{ll'} \to a_s \delta(x - x')$, thus obtaining

$$\langle \delta F(x,t) \delta F(x',t') \rangle = 2\eta k_{\rm B} T \frac{\exp(-|x - x'|/\lambda_{\rm F})}{2\lambda_{\rm F}[1 - \exp(-a_s/2\lambda_{\rm F})]} \delta(t - t') \; . \tag{5.11}$$

For a spatially uncorrelated random force, $\lambda_{\rm F} \to 0$, Eq. (5.11) reduces to

$$\langle \delta F(x,t) \delta F(x',t') \rangle = 2\eta k_{\rm B} T a_s \delta(x - x') \delta(t - t') \; , \tag{5.12}$$

while for the coherent external noise, $\lambda_{\rm F} \to \infty$, this leads to the relation,

$$\langle \delta F(x,t) \delta F(x',t') \rangle = 2\eta k_{\rm B} T \delta(t - t') . \tag{5.13}$$

In dimensionless units, when $\tilde{x} = x/d$ and $\tilde{t} = \omega_0 t$, the Langevin equation (5.14) takes the form (we omit all the tildes below),

$$u_{tt} - u_{xx} + \sin u = f(x,t;u,u_t) \equiv \delta F(x,t) - \eta u_t \; . \tag{5.14}$$

If the perturbation f is small, the solution of Eq. (5.14) can be obtained by the perturbation technique (McLaughlin and Scott, 1978; see also Kivshar and Malomed, 1989). Namely, looking

for a solution in the form of a nonrelativistic kink,

$$u(x,t) = 4\tan^{-1}\exp\{-\sigma[x - X(t)]\}\ , \tag{5.15}$$

we obtain the following equation for the kink's coordinate $X(t)$,

$$\frac{\mathrm{d}^2X}{\mathrm{d}t^2} = -\frac{\sigma}{4}\int_{-\infty}^{\infty}\frac{f(x,t;u,u_t)}{\cosh[x - X(t)]}\ . \tag{5.16}$$

Thus, the effect of perturbations reduces to modulations of the kink's coordinate and velocity while the kink's shape is assumed to be unchanged (adiabatic approximation). Eqs. (5.14) and (5.16) lead to the Langevin equation for $X(t)$ (see, e.g., Joergensen et al., 1982; Marchesoni, 1986; Bass et al., 1988)

$$m\frac{\mathrm{d}^2X}{\mathrm{d}t^2} + m\eta\frac{\mathrm{d}X}{\mathrm{d}t} = \delta F_{\mathrm{k}}(t) \tag{5.17}$$

with the kink fluctuation force satisfying the relation

$$\langle \delta F_{\mathrm{k}}(t)\,\delta F_{\mathrm{k}}(t')\rangle = 2\eta m^* k_{\mathrm{B}}T\delta(t - t')\ . \tag{5.18}$$

Here m is the kink's mass, and the effective mass m^* is defined as

$$\begin{aligned} m^* &= \int_{-\infty}^{\infty}\mathrm{d}x\int_{-\infty}^{\infty}\mathrm{d}x'\,u(x)u(x')\langle\delta F(x)\,\delta F(x')\rangle \\ &= \frac{ma_s}{2\lambda_{\mathrm{F}}[1 - \exp(-a_s/2\lambda_{\mathrm{F}})]}\,\xi\left(2, \frac{1 + \lambda_{\mathrm{F}}/a_s}{2\lambda_{\mathrm{F}}/a_s}\right), \end{aligned} \tag{5.19}$$

where

$$\xi(s,v) = \sum_{n=0}^{\infty}(n + v)^{-s} \tag{5.20}$$

is the generalized Riemann zeta-function.

For large-time scales, $t \gg \eta^{-1}$, the Langevin equation (5.17), (5.18) describes the Brownian kink motion,

$$\langle X^2(t)\rangle = 2D_\eta t, \quad D_\eta = \left(\frac{m^*}{m}\right)\frac{k_{\mathrm{B}}T}{m\eta}\ , \tag{5.21}$$

where D_η is the diffusion coefficient.

Thus, if the fluctuation force is spatially uncorrelated, i.e. $\lambda_{\mathrm{F}} \ll d$, from Eq. (5.19) we have $m = m^*$ and the mean kinetic energy of a nonrelativistic kink, $\frac{1}{2}m\langle\dot{X}^2(t)\rangle$, is equal to the thermal energy $\frac{1}{2}k_{\mathrm{B}}T$ in an equilibrium state. In this case the kink diffusion coefficient is equal to (Remoissenet, 1978; Bergman et al., 1983; Marchesoni, 1986)

$$D_\eta = k_{\mathrm{B}}T/m\eta\ . \tag{5.22}$$

In the opposite case of spatially correlated fluctuation force, i.e. for $\lambda_F \gg d$, we find $m^* = (\pi^2/2)m$, and the thermal energy of a single kink is modified to be

$$\frac{1}{2}m\langle \dot{X}^2(t)\rangle = \frac{\pi^2}{4}k_B T \ .$$

The reason for such a renormalization is that a kink is an extended object and, therefore, its coupling to an external source of noise varies to be determined by a ratio of the kink's width d and the noise correlation length λ_F. In the case of a coherent external noise the kink diffusion is determined by the expression (Buttiker and Landauer, 1980; Bergman et al., 1983; Pascual and Vázquez, 1985; Marchesoni, 1986)

$$D_\eta = \frac{\pi^2}{16}\frac{k_B T}{m\eta} \ . \tag{5.23}$$

The result (5.23) has been verified by means of molecular dynamics simulations (Pascual and Vázquez, 1985; Biller and Petruccione, 1990) which showed that the assumption of the preserved kink's shape works with a good accuracy.

In some physical problems the fluctuation force acting on the FK chain from the substrate is modeled by a multiplicative external noise. In this case the corresponding Langevin equation takes the form

$$u_{tt} + \eta u_t - d^2 u_{xx} + \sin u = \delta V(x,t)\sin u \ , \tag{5.24}$$

where $\delta V(x,t)$ is usually assumed to be Gaussian with zero mean value and two-time correlation function,

$$\langle \delta V(x,t)\,\delta V(x',t')\rangle = \mu\delta(x-x')\delta(t-t') \ , \tag{5.25}$$

μ being a measure of the noise intensity, $\mu \propto T$. The perturbation theory applied to this kind of problems shows that the multiplicative noise leads to the very similar Brownian motion of the kink with a diffusion coefficient different from that calculated for an additive noise (Pascual and Vázquez, 1985; Biller and Petruccione, 1990).

5.3. Intrinsic viscosity

In the previous section we have assumed that the viscous friction η has an origin in the energy exchange between the atoms of the chain and substrate, i.e. it corresponds to an external friction η_{ext}. It is clear, however, that a Brownian kink diffusion should exist also in an isolated FK chain as well, and the main reason for that is nonintegrability of the primary model. If the corresponding response function (5.1), (5.2) is approximated by a local function, and the fluctuation force, by an additive uncorrelated noise, the kink diffusion coefficient is calculated to be

$$D_\eta = \frac{k_B T}{m\eta_{int}} \ , \tag{5.26}$$

and the problem itself reduces to the calculation of the intrinsic friction coefficient η_{int}.

Although the value $\eta_{\rm int}$ cannot be calculated exactly, it can be estimated considering the momentum exchange at a kink collision with other excitations such as phonons and/or breathers. These calculations are usually based on perturbation techniques such as the Mori technique and memory-function approach, the inverse scattering transform, the technique in which the kink's coordinate $X(t)$ is treated as a canonical variable, etc. (see, e.g., Ogata and Wada, 1985, 1986; Kunz, 1986a,b; Marchesoni and Willis, 1987; Theodorakopoulos and Weller, 1988; Bar'yakhtar et al., 1988). As an example, let us below briefly describe the approach used by Bar'yakhtar et al. (1988) where the continuum limit of the FK model with nonsinusoidal substrate potential was investigated. As usual, the field variable $u(x,t)$ is presented in the form

$$u(x,t) = u_{\rm k}(x - vt) + \phi(x,t)\ , \tag{5.27}$$

where $u_{\rm k}$ corresponds to a slowly moving unperturbed kink, and $\phi(x,t)$ describes the phonon field accompanying the kink motion. Substituting Eq. (5.27) into the system Hamiltonian and expanding $V_{\rm sub}(u_{\rm k} + \phi)$ into the Taylor series in ϕ, the Hamiltonian can be presented in the form

$$H = H_{\rm k} + H_{\rm ph} + H_{\rm int}\ , \tag{5.28}$$

where $H_{\rm k}$ corresponds to an isolated kink, $H_{\rm ph}$ describes the phonon subsystem, and the third term,

$$H_{\rm int} = \sum_{n=3}^{\infty} H_n, \quad H_n \propto \frac{1}{n!}\int {\rm d}x \left(\frac{\delta^n V_{\rm sub}(u)}{\delta u^n}\right)\Bigg|_{u=u_{\rm k}} \phi^n\ , \tag{5.29}$$

is responsible for inelastic scattering of phonons on the moving kink. Then, let us introduce the complete set of functions $\psi_\alpha(x)$ found as eigenfunctions of the pseudo-Schrödinger equation (3.12); we denote the corresponding eigenvalues as ω_α. The set $\{\psi_\alpha(x)\}$ consists of the Goldstone mode, the shape modes (if any), and the continuum spectrum modes. Using this basis, we introduce new canonical variables ξ_α by the expansion

$$\phi(x,t) = \sum_\alpha \xi_\alpha \psi_\alpha(x) {\rm e}^{{\rm i}\omega_\alpha t}\ , \tag{5.30}$$

and rewrite $H_{\rm int}$ in the terms of ξ_α. Now we can calculate the probability of the n-phonon inelastic scattering process and obtain the corresponding contribution to the rate of the energy exchange $\eta_{\rm int}$. For the pure SG model such a procedure will give the trivial result $\eta_{\rm int} = 0$ because the contributions of all the orders compensate each other, as it should be for an exactly integrable model where the kink motion is not accompanied by radiation (Ogata and Wada, 1985; Bar'yakhtar et al., 1988). Otherwise, for a nonintegrable case, the lowest-order contribution to the inelastic scattering comes from the three-phonon scattering and it leads to a viscous friction coefficient (Bar'yakhtar et al., 1988)

$$\eta_{\rm int} \approx C\omega_0 \left(\frac{k_{\rm B}T}{\varepsilon_{\rm k}}\right)^2\ . \tag{5.31}$$

Substituting Eq. (5.31) into Eq. (5.26), we obtain the diffusion coefficient for a slowly moving kink in the isolated FK chain,

$$D_\eta = C_1 d^2 \omega_0 \left(\frac{\varepsilon_{\rm k}}{k_{\rm B}T}\right). \tag{5.32}$$

The numerical factors C and C_1 in Eqs. (5.31) and (5.32) depend on the particular model under consideration and, for example, in the case of the ϕ^4 model $C_1 \approx 20$ (Ogata and Wada, 1986).

Eqs. (5.31) and (5.32) describe the classical behaviour of the chain. At extremely low temperatures, i.e. for $k_B T \ll \hbar\omega_0$, we should employ the quantum statistics for phonons which leads to the result (Bar'yakhtar et al., 1988),

$$\eta_{\rm int} \propto \exp(-C_2\hbar\omega_0/k_B T) \quad \text{and} \quad D_k \propto T^2 \exp(C_2\hbar\omega_0/k_B T)\,, \tag{5.33}$$

where C_2 is another numerical constant.

5.4. Anomalous diffusion

When a kink collides with other excitations, it suffers a phase shift, or a spatial displacement $\delta(k)$ without a change of its momentum. As a result, the kink's coordinate which has an initial value X_0, evolves according to equation

$$X(t) = X_0 + V_0 t + \delta X(t), \quad \delta X(t) = \int \mathrm{d}k\, \delta(k) v_t(k)\,, \tag{5.34}$$

where V_0 is the initial kink velocity, and $v_t(k)\,\mathrm{d}k$ stands for the number of kink's collisions with excitations having the wavenumbers between k and $k + \mathrm{d}k$. The function $v_t(k) = \rho(k) n_t(k)$, where $\rho(k)$ is the density of the phonon states with the wavenumber k, and $n_t(k)$ is the number of collisions with the mode having the wavenumber k. We would like to note that such an approach can be based on a phonon picture of the low-energy excitations (see Wada and Schrieffer, 1978; Theodorakopoulos and Klein, 1980, 1981; Fesser, 1980; Wada and Ishiuchi, 1982; Ogata and Wada, 1986) as well as on an alternative description in terms of breathers (Sasaki and Maki, 1987a,b; Theodorakopoulos and Weller, 1988); both the approaches lead to identical results (Theodorakopoulos and Weller, 1988). Here we follow the work of Theodorokopoulos and Weller (1988).

Now let us assume that the low-energy excitations constitute a heat bath, i.e. that the kink–phonon collisions occur in a random manner and, moreover, that for the time interval between the collisions the heat bath "regenerate" its equilibrium state. In this case, due to a series of spatial shifts $\{\delta(k)\}$ of the kink, the kink dynamics will be diffusional to be considered as a random walk with the mean velocity V_0,

$$\langle (X(t) - X_0 - V_0 t)^2 \rangle = 2D_a t\,. \tag{5.35}$$

Since the shift $\delta(k)$ is proportional to the squared amplitude of the scattered phonon (or breather), the anomalous diffusion constant D_a is proportional to T^2. Indeed, the fluctuations of the kink's position with respect to the thermal average of $X(t)$ is equal to

$$\delta X(t) = \int \mathrm{d}k\, \delta(k) \delta v_t(k)\,, \tag{5.36}$$

and thus

$$\langle [\delta X(t)]^2 \rangle = \int \mathrm{d}k\, \mathrm{d}k' \delta(k)\delta(k') \langle \delta v_t(k) \delta v_t(k') \rangle\,. \tag{5.37}$$

Taking the phonons as a thermal bath, we obtain

$$\langle \delta v_t(k)\delta v_t(k')\rangle = L^{-1}|v(k)|t\rho_0\delta(k-k')\langle[\delta n(k)]^2\rangle\,, \tag{5.38}$$

where $v(k)$ is the group velocity of phonons with the wavenumber k, $v(k) = \mathrm{d}\omega_{\mathrm{ph}}(k)/\mathrm{d}k$, $\omega_{\mathrm{ph}}(k) = \sqrt{\omega_0^2 + c^2k^2}$, and $\rho_0(k) = \rho_0 \equiv L/2\pi$, L being the chain length. Using the classical limit of the Bose–Einstein statistics,

$$\langle[\delta n(k)]^2\rangle = [k_{\mathrm{B}}T/\hbar\omega_{\mathrm{ph}}(k)]^2\,,$$

we get from Eqs. (5.37) and (5.38) the result

$$\langle[\delta X(t)]^2\rangle = 2D_a t, \quad D_a = \tilde{C}d^2\omega_0\left(\frac{k_{\mathrm{B}}T}{\varepsilon_{\mathrm{k}}}\right)^2. \tag{5.39}$$

Here the numerical factor $\tilde{C}$ depends on the model under consideration, for example, $\tilde{C} = 2/3\pi$ for the SG system, and $\tilde{C} = 8.24/9$, for the ϕ^4 model (Theodorakopoulos, 1979; Ogata and Wada, 1986).

Anomalous (nondissipative) kink diffusion was first investigated by Wada and Schrieffer (1978) for the ϕ^4 model. It should be emphasized that this diffusion mechanism assumes the existence of an "external" thermalization which produces the low-energy heat bath. The only mechanism of such a thermalization is the energy exchange between different degrees of freedom of the system, which appears due to nonintegrability of the isolated FK chain and/or due to a coupling of the chain with the substrate. As a result, the anomalous diffusion defined by Eq. (5.35) exists only on short-time scales, $t \ll \eta^{-1}$, where $\eta = \eta_{\mathrm{ext}} + \eta_{\mathrm{int}}$, while for $t \gg \eta^{-1}$ the kink dynamics should be viscous leading to the standard expression $\langle[X(t) - X_0]^2\rangle = 2D_\eta t$ with $D_\eta = k_{\mathrm{B}}T/m\eta$ (Kunz, 1986b; Ivanov and Kolezhuk, 1989, 1990; Marchesoni and Willis, 1990).

As was verified by Theodorakopoulos and Weller (1988), the dominant contribution to D_a comes from a relatively narrow band of the phonon wavenumbers, $k \sim 0.005\pi/a_s$. Therefore, the continuum approximation yields a correct value of D_a for the discrete FK model as well. Besides, a small number of phonons in the vicinity of the Brillouin-zone edges gives rise to inelastic kink-phonon scattering (Theodorakopoulos and Klein, 1981) leading to a small contribution to the coefficient η. For the SG model the anomalous diffusion was observed in the molecular dynamics simulations by Theodorakopoulos and Weller (1988) (notice, however, that a discretization procedure applied to the continuum equation always destroys integrability of the model and could be a factor for the subsequent viscous diffusion of kinks).

5.5. Kink diffusion coefficient

In a general case, the kink diffusion coefficient $D_{\mathrm{k}}(\omega)$ is determined by Eq. (5.6). Using the Kubo–Mori technique (Mori, 1965; Kubo, 1966), the coefficient $D_{\mathrm{k}}(\omega)$ can be expressed in the form (Marchesoni and Willis, 1990)

$$D_{\mathrm{k}}(\omega) = \left(\frac{k_{\mathrm{B}}T}{m}\right)\frac{1}{[\eta(\omega) - \mathrm{i}\omega]}\,, \tag{5.40}$$

where $\eta(\omega)$ is the total generalized friction coefficient. Expanding $\eta(\omega)$ in ω,

$$\eta(\omega) = \eta_0 - \mathrm{i}\eta_1\left(\frac{\omega}{\omega_0}\right) + \eta_2\left(\frac{\omega}{\omega_0}\right)^2 + \cdots , \tag{5.41}$$

the real part of the diffusion coefficient can be calculated as

$$\mathrm{Re}\, D_{\mathrm{k}}(\omega) \approx \left(\frac{k_{\mathrm{B}}T}{m}\right)\frac{\eta_0 + \eta_2(\omega/\omega_0)^2}{\eta_0^2 + (\omega/\omega_0)^2[(\omega_0 + \eta_1)^2 + 2\eta_0\eta_2]} . \tag{5.42}$$

Thus, the viscous diffusion is characterized by the coefficient

$$D_{\mathrm{k}} \approx \frac{k_{\mathrm{B}}T}{m\eta_0}, \quad \eta_0 = \lim_{\omega\to 0}\eta(\omega) . \tag{5.43}$$

It dominates for low frequencies (or longtime scales), i.e. when

$$\omega \ll \omega^*, \quad \omega^* = \omega_0\sqrt{\frac{\eta_0}{\eta_2}} . \tag{5.44}$$

For the SG model we have the results: $\eta_0 = 0$ and $\omega^* = 0$, so that the viscous diffusion is naturally absent. Otherwise, at high frequencies when $\omega \gg \omega^*$ (or short-time scales) the anomalous diffusion dominates. Comparing $D_{\mathrm{k}}(\omega)$ for $\omega \gg \omega^*$ with the value D_a given by Eq. (5.39), we can estimate the coefficient η_2 as $\eta_2 \sim \omega_0(k_{\mathrm{B}}T/\varepsilon_{\mathrm{k}})$ and then the crossover frequency ω^* is found to be

$$\omega^* \sim \frac{\omega_0\eta_0\varepsilon_{\mathrm{k}}}{k_{\mathrm{B}}\ T} . \tag{5.45}$$

For an isolated FK chain, when, according to Eq. (5.31), $\eta_0 \sim \omega_0(k_{\mathrm{B}}T/\varepsilon_{\mathrm{k}})^2$, we obtain $\omega^* \sim \omega_0(k_{\mathrm{B}}T/\varepsilon_{\mathrm{k}})^{1/2}$. Thus, if $\omega \neq 0$ and the temperature T increases, a crossover from the anomalous diffusion $D_{\mathrm{k}} \approx D_a$ to the standard (viscous) diffusion $D_{\mathrm{k}} \approx D_\eta$ should take place. This effect was investigated by Ogata and Wada (1986) for the ϕ^4 model (see Fig. 23). However, if the FK chain is coupled with a thermostat and $\eta_0 \neq 0$ as $T \to 0$, the inverse consequence should take place.

Up to now we have neglected the existence of the PN relief in the FK chain. In a strongly discrete FK chain, when $g \leq 1$, the amplitude of the PN potential may exceed the kink thermal energy, and the kink diffusion will become activated. Phenomenologically, in such a case the Langevin equation (5.17) for the kink's coordinate $X(t)$ have to be replaced by the equation (Pietronero and Strässler, 1978; Combs and Yip, 1983; Kunz and Combs, 1985)

$$m\frac{\mathrm{d}^2X}{\mathrm{d}t^2} + m\eta\frac{\mathrm{d}X}{\mathrm{d}t} + V'_{\mathrm{PN}}(X) = \delta F_{\mathrm{k}}(t) , \tag{5.46}$$

where $V_{\mathrm{PN}}(X) \approx \frac{1}{2}E_{\mathrm{PN}}(1 - \cos X)$. Eq. (5.46) leads to the Arrhenius form for the diffusion coefficient at $t \to \infty$ $(\omega \to 0)$,

$$D_{\mathrm{k}} = D_0 \exp(-E_{\mathrm{PN}}/k_{\mathrm{B}}T) . \tag{5.47}$$

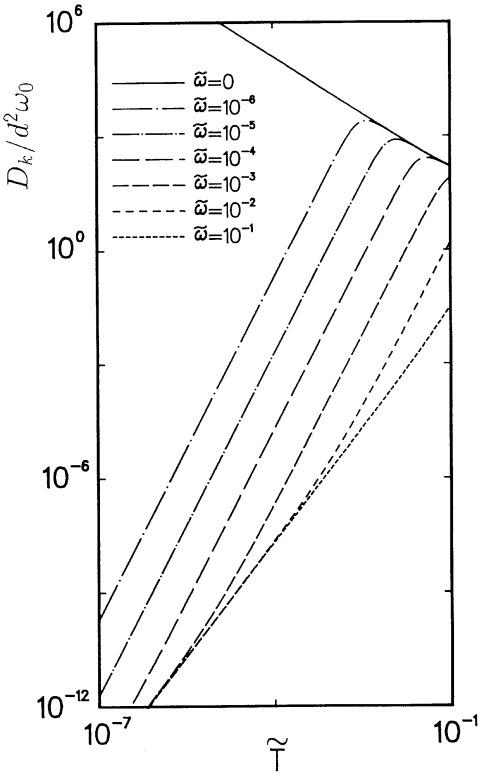

Fig. 23. Log–log plot of the real part of the function $D_k(\omega)/d^2\omega_0$ the dimensionless temperature $\tilde{T} = \frac{2}{3}k_B T/\varepsilon_k$, for several values of the dimensionless frequency $\tilde{\omega} = \omega/\omega_0$. In the region $\tilde{T} < \tilde{\omega}^2$ the diffusion coefficient is approximately given by the estimate $D_a \propto T^2$, while in the region $\tilde{T} > \tilde{\omega}^2$, $D_k(\omega)$ approaches the curve $D_\eta \propto T^{-1}$ (Ogata and Wada, 1986).

Then, the pre-exponential factor D_0 can be calculated approximately with the help of the Kramers theory (Kramers, 1940),

$$D_0 \approx \begin{cases} a_s^2 \omega_{PN}/2\pi & \text{if } \eta^* \ll \eta < \omega_{PN}^* , \\ a_s^2 \omega_{PN}\omega_{PN}^*/2\pi\eta & \text{if } \eta > \omega_{PN}^* , \end{cases} \tag{5.48}$$

where

$$\omega_{PN} = \sqrt{V''_{PN}(0)/m}, \quad \omega_{PN}^* = \sqrt{-V''_{PN}(a_s/2)/m} ,$$

$$\eta^* = \frac{\omega_{PN} k_B T}{2\pi E_{PN}} .$$

The case of a low friction, $\eta < \eta^*$, is rather complicated to be investigated analytically. Numerically, an activated kink diffusion (5.47) was observed in the molecular-dynamics simulations for the ϕ^4 model by Combs and Yip (1984).

Thus, in application of the theory discussed above to real physical objects the following remarks should be taken into account:

(i) The total "generalized" friction coefficient $\eta(\omega)$ consists of the intrinsic contribution $\eta_{\rm int}$ and the external (substrate) contribution $\eta_{\rm ext}$, both $\eta_{\rm int}$ and $\eta_{\rm ext}$ depend, in a general case, on the frequency ω and the temperature T. In some cases, for example, for the chain of atoms chemically adsorbed on a crystal surface, the intrinsic friction is negligible, $\eta_{\rm int} \ll \eta_{\rm ext}$ (Braun, 1989);

(ii) The intrinsic friction $\eta_{\rm int}$ has an origin in radiation-induced effects due to nonintegrability of the FK chain unlike the completely integrable SG equation, and this nonintegrability is caused by all the factors such as a nonsinusoidal substrate potential, anharmonic interatomic interactions, discreteness effects, and the possible presence of impurities, etc.

6. Nonlinear localized modes

6.1. General overview

Up to now the main subject of our discussions related to the properties of nonlinear excitations in the discrete FK model was a kink – a topologically stable excitation which exists in the continuum as well as discrete models. As for the breather modes, we have discussed above the cases when the discreteness effects are actually weak, i.e. when the assumption of strong coupling between the atoms in the chain is valid. However, such breather-like excitations may also exist in discrete lattices, i.e. for the limit of *weak* interparticle coupling. Such nonlinear modes are strongly localized and they exist with the frequencies *below* (similar to a breather in the SG model) or *above* the phonon frequency band.

For an anharmonic lattice without on-site potential, such localized breather-like modes exist in a form of the so-called *intrinsic localized modes* (Dolgov, 1986; Sievers and Takeno, 1988; Page, 1990). In the latter case, the energy localization, which involves only a few particles of the chain, is possible due to nonlinear interparticle interaction itself, but not due to impurities, as is in the theory of linear lattices (see, e.g., Maradudin, 1966). Different properties of the intrinsic localized modes have been discussed in a number of papers (see, e.g., Takeno et al., 1988; Page, 1990; Burlakov et al., 1990a,b; Takeno and Hori, 1990; Bickham and Sievers, 1991; Kivshar, 1991b; Scharf and Bishop, 1991; Bickham et al., 1992; Sandusky et al., 1992; Hori and Takeno, 1992; Dauxois and Peyrard, 1993; Dauxois et al., 1993a,b; Kiselev et al., 1993; Kivshar, 1993a,b; Flach and Willis, 1993; Flach et al., 1994; Bang and Peyrard, 1996; Takeno and Peyrard, 1996; Forinash et al., 1997) and they have been overviewed by Takeno et al. (1988), Sievers and Page (1995), Kiselev et al. (1995), and Flach and Willis (1998). An important theoretical result was a rigorous mathematical proof of the existence of nonlinear localized modes (MacKay and Aubry, 1994) based on the analysis of a system of weakly coupled nonlinear oscillators (the so-called "anti-integrability" limit, see Aubry, 1994; for an overview).

The original model firstly considered to describe intrinsic localized modes (Dolgov, 1986; Sievers and Takeno, 1988) is a chain with anharmonic interatomic interaction, and it describes a one-dimensional lattice without a substrate in which each atom interacts only with its nearest neighbors via a symmetric nonlinear potential. The localized Sievers–Takeno (ST) mode has a symmetric pattern (Sievers and Takeno, 1988) given by $u_n(t) = A(\ldots, 0, -\frac{1}{2}, 1, -\frac{1}{2}, 0, \ldots)\cos\omega t$, whereas the

Page (P) mode has the asymmetric pattern (Page, 1990), $u_n(t) = A(\ldots, 0, -1, 1, 0, \ldots)\cos\omega t$, A being the mode amplitude. These modes can also propagate through the lattice (see, e.g., Bourbonnais and Maynard, 1990a,b) in spite of the fact that their motion is strongly affected by discreteness. Adiabatic motion of the localized mode can be also viewed, till some extend, as the sequential changing between ST and P modes. Due to the lattice discreteness, these two states have different energies (e.g., Claude et al., 1993), viewed as two states of the same mode moving adiabatically through the lattice when its motion is affected by an effective periodic PN-like potential, similar to that introduced earlier for a FK kink. In such a picture, the P mode corresponds to a minimum of the effective PN potential, whereas the ST mode corresponds to a maximum and it displays a dynamical instability (Sandusky et al., 1992).

It is well established that nonlinear localized mode exist not only due to anharmonic coupling between the atoms, but also in a chain with linear coupling when the nonlinearity is introduced only through an on-site substrate potential. The purpose of the present chapter is to describe briefly nonlinear localized modes for the FK model, employing the approximation based on the discrete nonlinear Schrödinger (NLS) equation. The case of the quartic on-site potential was discussed by several authors (Takeno et al., 1988; Kivshar, 1991b; Flach and Willis, 1993; see also the case of the purely cubic on-site potential, (Dauxois et al., 1992) and highly localized modes with the frequencies *below* the minimum frequency of the linear spectrum have been found. The existence of moving localized modes in such a model has been discussed by several authors, but this issue is still not completely clarified. However, we would like to mention several papers (Kivshar and Campbell, 1993; Cai et al., 1994), where the existence of an effective PN potential for moving localized mode, similar to that for the FK kink, was demonstrated, and the height of the PN potential was estimated analytically for two limit cases. Additionally, we would like to note that the spectrum of a linear discrete FK chain is limited from above by an upper cut-off frequency existing due to discreteness, so that one naturally expects to find localized modes with the frequencies *above* the cut-off frequency similar to the odd-parity ST modes (see Sievers and Takeno, 1988) or even-parity P modes (see Page, 1990; Sandusky et al., 1992) in a chain with anharmonic interatomic interactions. The physically important problem related to these localized nonlinear modes is to prove that they are long-lived excitations which can contribute to many properties of nonlinear discrete systems. Additionally, there exists a variety of other modes such as "dark-soliton" nonlinear localized modes with nonvanishing asymptotics which have no simple analog in the continuum limit approximation.

We would like to emphasize that this section has a purpose to complete the picture of the kink dynamics discussed above by a few illustrative examples of nontopological nonlinear modes in the FK model, and the specific features introduced by discreteness. A more comprehensive discussion of the intrinsic localized modes (called also *discrete breathers*) can be found in the papers by Flach and Willis (1998) and Hennig and Tsironis (1999).

6.2. Discrete NLS equation

We consider the dynamics of a one-dimensional FK chain with an on-site potential of a general shape. Taking into account relatively small amplitudes of the modes, one can expand the substrate potential keeping terms up to the quartic one. For the standard FK model, the coefficient α in front of the cubic term is zero, but the case considered below is more general to treat, for example, the

situation of a small dc field applied to the FK chain. Denoting by $u_n(t)$ the displacement of the nth particle, its equation of motion is

$$\frac{\mathrm{d}^2 u_n}{\mathrm{d}t^2} - g(u_{n+1} + u_{n-1} - 2u_n) + \omega_0^2 u_n + \alpha u_n^2 + \beta u_n^3 = 0 \,, \tag{6.1}$$

where g is the coupling constant, ω_0 is the frequency of small-amplitude on-site vibrations in the substrate potential, α and β are the anharmonicity parameters of the potential. Linear waves of the frequency ω and wavenumber k are described by the dispersion relation

$$\omega^2 = \omega_0^2 + 4g \sin^2\left(\frac{ka_s}{2}\right), \tag{6.2}$$

a_s being the lattice spacing. As shown by Eq. (6.2), the linear spectrum has a gap ω_0 and it is limited by the cut-off frequency $\omega_{\max} = (\omega_0^2 + 4g)^{1/2}$ due to discreteness.

Analysing slow temporal variations of the wave envelope, we will try to keep the discreteness of the primary model *completely*. In fact, this is possible only under the condition $\omega_0^2 \gg g$, i.e. when a coupling force between the neighboring particles is weak. Looking for a solution in the form

$$u_n = \phi_n + \psi_n \mathrm{e}^{-\mathrm{i}\omega_0 t} + \psi_n^* \mathrm{e}^{\mathrm{i}\omega_0 t} + \xi_n \mathrm{e}^{-2\mathrm{i}\omega_0 t} + \xi_n^* \mathrm{e}^{2\mathrm{i}\omega_0 t} + \cdots \,, \tag{6.3}$$

we assume the following relations (similar to the continuum case, see, e.g., Remoissenet, 1986), $\phi_n \sim \varepsilon^2$, $\xi_n \sim \varepsilon^2$, $\psi_n \sim \varepsilon$, and also the following relations between the model parameters, $g \sim \varepsilon^2$, ω_0^2, α, $\beta \sim 1$, $(\mathrm{d}/\mathrm{d}t) \sim \varepsilon^2$. It is clear that this choice of the parameters corresponds to large values of ω_0^2 (we may simply divide all the terms by the frequency gap value).

Substituting Eq. (6.3) into Eq. (6.1) and keeping only the lowest order terms in ε, we obtain the equation for ψ_n,

$$2\mathrm{i}\omega_0 \frac{\mathrm{d}\psi_n}{\mathrm{d}t} + g(\psi_{n+1} + \psi_{n-1} - 2\psi_n) - 2\alpha(\phi_n \psi_n + \psi_n^* \xi_n) - 3\beta|\psi_n|^2 \psi_n = 0 \,, \tag{6.4}$$

and two algebraic relations for ϕ_n and ξ_n,

$$\phi_n \approx -\frac{2\alpha}{\omega_0^2}|\psi_n|^2, \qquad \xi_n \approx \frac{\alpha}{3\omega_0^2}\psi_n^2 \,. \tag{6.5}$$

The results (6.4) and (6.5) are generalizations of the well known ones for the continuum case (Remoissenet, 1986). Thus, the final discrete NLS (or DNLS) equation stands,

$$\mathrm{i}\frac{\mathrm{d}\psi_n}{\mathrm{d}t} + K(\psi_{n+1} + \psi_{n-1} - 2\psi_n) + \lambda|\psi_n|^2 \psi_n = 0 \,, \tag{6.6}$$

where

$$K = \frac{g}{2\omega_0}, \qquad \lambda = \frac{1}{2\omega_0}\left(\frac{10\alpha^2}{3\omega_0^2} - 3\beta\right). \tag{6.7}$$

Eq. (6.6) is used below to analyse different types of localized modes in the FK chain. In fact, the DNLS equation (6.6), also known as the discrete self-trapping equation (e.g., Eilbeck et al., 1985;

Carr and Eilbeck, 1985), is rather known to have numerous physical applications, and it describes the self-trapping phenomenon in a variety of coupled-field theories, from the self-trapping of vibron modes in natural and synthetic biomolecules (Eilbeck et al., 1985; Scott, 1985) to the dynamics of a linear array of vortices, being a special limit of the discrete Ginzburg–Landau equation (see, e.g., Willaime et al., 1991). Generalized version of the DNLS equation with arbitrary degree of the nonlinearity has been considered to study the influence of the nonlinearity on the structure and stability of localized modes (see, e.g., Scott and Christiansen, 1990; Bang et al., 1993, 1994; Malomed and Weinstein, 1996; Gupta and Kundu, 1997).

We would like to point out again that in the present context Eq. (6.6) emerges as an approximate equation under the assumption of slow (temporal) variation of the envelopes as well as the neglecting of higher-order harmonics, and the latter means that we assume the gap frequency ω_0 large with respect to the other frequencies in the system, i.e. $\omega_0^2 \gg 4g$, and $\omega_0^2 \gg \alpha u_0$, βu_0^2, u_0 being the wave amplitude. The former inequality is valid in a weakly dispersive system where ω_0 is close to $\omega_{\max}$, while the latter one means that the nonlinearity of the substrate potential is not large. These are usual conditions to get the NLS equation, but in the lattice, the condition $\omega_0^2 \gg 4g$ means also that discreteness effects are considered strong pointing out the interest to the discrete modes localized on a few particles.

First of all, we analyze modulational instability for the DNLS equation (6.6). As is well known, nonlinear physical systems may exhibit an instability that leads to a self-induced modulation of the steady state as a result of an interplay between nonlinear and dispersive effects. This phenomenon, referred to as modulational instability, has been studied in continuum models (see, e.g., Bespalov and Talanov, 1966; Benjamin and Feir, 1967; Ostrovskii, 1966; Hasegawa, 1970) and, only recently, in discrete models (Kivshar and Peyrard, 1992). As has been pointed out, modulational instability is responsible for energy localization and formation of localized pulses.

For the DNLS equation (6.6), derived in the single-frequency approximation, modulational instability in the lattice can be easily analyzed. Eq. (6.6) has the exact continuous wave (cw) solution

$$\psi_n(t) = \psi_0 e^{i\theta_n}, \quad \text{with } \theta_n = ka_s n - \omega t \ , \tag{6.8}$$

where the frequency ω obeys the *nonlinear* dispersion relation

$$\omega = 4K \sin^2\left(\frac{ka_s}{2}\right) - \lambda\psi_0^2 \ . \tag{6.9}$$

The linear stability of the wave (6.8) and (6.9) can be investigated by looking for the perturbed solution of the form $\psi_n(t) = (\psi_0 + b_n)\exp(i\theta_n + i\chi_n)$, where $b_n = b_n(t)$ and $\chi_n = \chi_n(t)$ are assumed to be small in comparison with the parameters of the carrier wave. In the linear approximation two coupled equations for these functions yield the dispersion relation

$$[\Omega - 2K \sin(Qa_s)\sin(ka_s)]^2 = 4K \sin^2(Qa_s/2)\cos(ka_s)\,[4K \sin^2(Qa_s/2)\cos(ka_s) - 2\lambda\psi_0^2] \tag{6.10}$$

for the wavenumber Q and frequency Ω of the linear modulation waves. In the long wavelength limit, when $Qa_s \ll 1$ and $ka_s \ll 1$, Eq. (6.10) reduces to the usual expression obtained for the continuous NLS equation (see, e.g., Benjamin and Feir, 1967).

Eq. (6.10) determines the condition for the stability of a plane wave with the wave-number k in the lattice. Contrary to what would be found in the continuum limit, now the stability depends

on k. An instability region appears only if (Kivshar and Peyrard, 1992)

$$\lambda \cos(ka_s) > 0 \ . \tag{6.11}$$

For positive λ and a given k, i.e. $k < \pi/2a_s$, a plane wave will be *unstable* to modulations in all this region provided $\psi_0^2 > 2K/\lambda$. The stability of the plane wave solutions to modulations of the wave parameters allows to conclude on possible types of nonlinear localized modes which may exist in the chain.

Modulational instability was shown to be an effective mean to generate localized modes in discrete lattices, because the lattice discreteness modifies drastically the stability condition. Daumont et al. (1997) have analyzed, following the technique suggested by Kivshar and Peyrard (1992), the modulational instability of a linear wave in the presence of noise in a lattice with qubic and quintic on-site potential, and they have demonstrated that the modulational instability is the first step towards energy localization (see also Kivshar and Salerno, 1994; for the case of the deformable discrete NLS model).

6.3. Spatially localized modes

As has been mentioned above, one of the main effects of modulational instability is the creation of localized pulses (see, e.g., Karpman, 1967). In the present case, this means that for $\lambda > 0$ the region of small k is unstable, and, therefore, nonlinearity can lead to a generation of localized modes *below* the smallest frequency of the nonlinear spectrum band (6.9). Such a localized mode can be found in an explicit form, from the DNLS equation (6.6) following the method by Page (1990). Looking for the stationary solutions of Eq. (6.6) in the form, $\psi_n(t) = Af_n e^{-i\omega t}$, we obtain a set of coupled algebraic equations for the real functions f_n,

$$\omega f_n + K(f_{n+1} + f_{n-1} - 2f_n) + \lambda A^2 f_n^3 = 0 \ . \tag{6.12}$$

We seek now two kinds of strongly localized solutions of Eq. (6.12), which are centered *at* and *between* the particle sites. First, let us assume that the mode is centered at the site $n = 0$ and take $f_0 = 1, f_{-n} = f_n, |f_n| \ll f_1$ for $|n| > 1$. Simple calculations yield the pattern of the so-called "A-modes" (see Fig. 24a),

$$\psi_n^{(A)}(t) = A(\ldots, 0, \xi_1, 1, \xi_1, 0, \ldots)e^{-i\omega t} \ , \tag{6.13}$$

where the parameter $\xi_1 = K/\lambda A^2$ is assumed to be small (i.e., terms of order of ξ_1^2 are neglected). The frequency ω in Eq. (6.13) is $\omega = -\lambda A^2$, and it indeed lies below the lowest band frequency.

The second type of the localized modes, the "B- modes", may be found assuming that the mode oscillation is centered symmetrically between two neighboring particles (see Fig. 24b),

$$\psi_n^{(B)}(t) = B(\ldots, 0, \xi_2, 1, 1, \xi_2, 0, \ldots)e^{-i\omega t} \ , \tag{6.14}$$

where the values ω and ξ_2 are defined as $\xi_2 = K/\lambda B^2$, and $\omega = -\lambda B^2$.

The calculation of the effective PN potential for localized mode is much more difficult task than that for the kinks, because the localized modes possess more parameters and the PN potential cannot be defined rigorously (Flach and Willis, 1994). However, the existence of a kind of PN potential affecting the motion of a nonlinear localized mode through the lattice can be easily

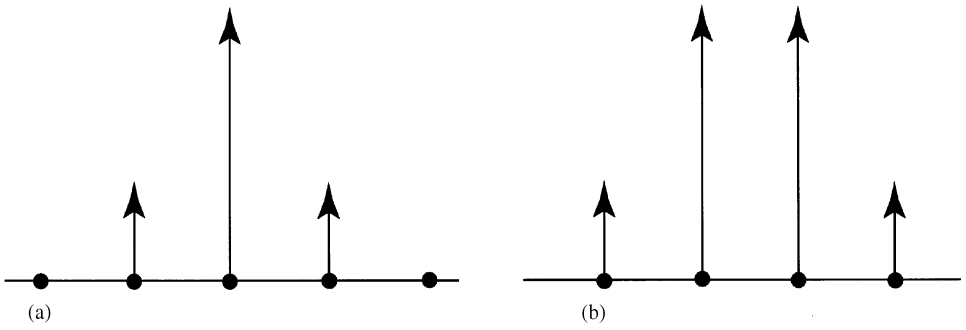

Fig. 24. Schematic shapes of strongly localized low-frequency nonlinear mode: (a) odd-parity mode, and (b) even-parity mode. The former mode may be considered as excited at the particle site whereas the latter one, between two nearest particles.

demonstrated. First, following the paper by Kivshar and Campbell (1993) we can imagine a localized wave form *of a fixed shape* being translated rigidly through the lattice. Then, it is clear that when the peak is centered on a lattice site, the symmetry is of the "A" form, whereas when the peak is centered halfway between the sites, the symmetry is of the "B" form. This observation motivates a comparison between the energies of these two modes provided, for the case of the NLS equation, the integral of motion $N = \sum_n |\psi_n|^2$ is conserved. Such a comparison of the integrals N calculated for A- and B-modes gives the relations between the amplitudes A and B in the lowest order in the small parameter ξ_1 and ξ_2, $A^2 = 2B^2$. With this condition on A and B, we can interpret now the two modes as stationary states of *the same* localized mode, calculating a difference in the energy between these two stationary states, $\Delta E_{AB} = E_A - E_B = -\frac{1}{2}\lambda A^4 + \lambda B^4 = -\frac{1}{4}\lambda A^4$.

From this simple estimate, it follows an important conclusion that there exists an effective energy barrier (the height of the effective PN potential) between these two stationary states of the discrete NLS equation, also meaning that any translation of nonlinear localized modes through the lattice will be affected by a periodic energy relief. In particular, a localized mode may be *captured* by the potential (i.e. trapped by the lattice discreteness). A simple way to observe this effect is "to push" the localized mode to move through the lattice by variation of the mode initial phase (Krolikowski and Kivshar, 1996). The B-mode, corresponding to a maximum of the potential, starts to move almost immediately, whereas it is clear that a certain energy barrier must be overcome to move through the lattice (Krolikowski and Kivshar, 1996). This is an indirect manifestation of the effective barrier due to the lattice discreteness, in spite of the fact it cannot be defined in a rigorous way.

Importantly, the analysis presented above is somewhat related to the stability properties of the nonlinear localized modes: the stationary localized mode corresponding to a local *maximum* of the PN potential should display an instability whereas the mode corresponding to a *minimum* should be stable. This qualitative observation made on the basis of the analysis of the PN barrier is in an agreement with the work by Sandusky et al. (1992) who have shown numerically and analytically (using other arguments and not referring to the PN potential) that for the case of interatomic quartic anharmonicity the ST localized mode (shown in Fig. 25a) is in fact unstable, but the P mode (shown in Fig. 25b) is extremely stable.

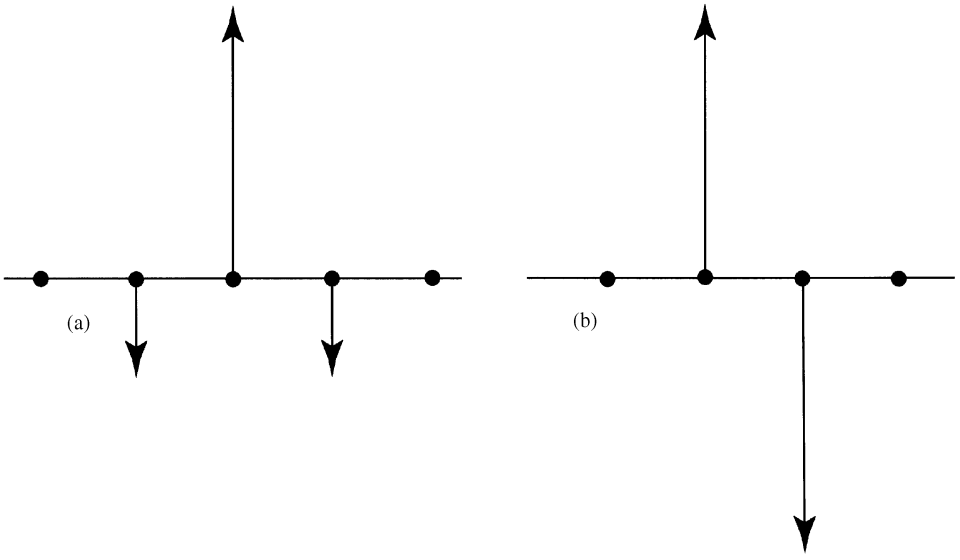

Fig. 25. The same as in Fig. 24a and b but for high-frequency nonlinear modes. However, the properties of such a mode may become reverse so that the mode (a) may have a lower energy than the mode (b).

One of the simple way to calculate the shape of the PN potential in the case of the NLS equation is to use the integrable version of the lattice equation, i.e. the Ablowitz–Ladik (AL) model (Ablowitz and Ladik, 1976), and to take the difference between these two models as a perturbation [see also Salerno (1992a,b) and Cai et al. (1994), where the perturbed AL chain has been considered as a novel physically important model]. To do so, we present the primary discrete NLS equation (6.6) in the form

$$\mathrm{i}\frac{\mathrm{d}\psi_n}{\mathrm{d}t} + K(\psi_{n+1} + \psi_{n-1} - 2\psi_n) + \frac{1}{2}\lambda(\psi_{n+1} + \psi_{n-1})|\psi_n|^2 = R(\psi_n)\,, \tag{6.15}$$

where

$$R(\psi_n) = \tfrac{1}{2}\lambda|\psi_n|^2(\psi_{n+1} + \psi_{n-1} - 2\psi_n)\,. \tag{6.16}$$

We start from the exact solution of the AL model (Ablowitz and Ladik, 1976) for the unperturbed case ($R = 0$) which we present in the form

$$\psi_n(t) = \frac{\sinh\mu\exp[\mathrm{i}v(n - x_0) + \mathrm{i}\alpha]}{\cosh[\mu(n - x_0)]}\,, \tag{6.17}$$

where $\mathrm{d}\mu/\mathrm{d}t = 0$, $\mathrm{d}v/\mathrm{d}t = 0$, $\mathrm{d}x_0/\mathrm{d}t = (2/\mu)\sinh\mu\sin v$, and $\mathrm{d}\alpha/\mathrm{d}t = 2[\cosh(\mu)\cos(v) - 1]$. In Eq. (6.17) and the subsequent calculations related to Eqs. (6.15) and (6.16) we use the normalized variables: $t \to t/K$ and $|\psi_n|^2 \to (2K/\lambda)|\psi_n|^2$.

Considering now the right-hand side of Eq. (6.15) as a perturbation (that is certainly valid for not too strongly localized modes), we may use the perturbation theory based on the inverse scattering

transform (Kivshar and Malomed, 1989). For the case of the AL model, the corresponding version of the soliton perturbation theory was elaborated by Vakhnenko and Gaididei (1986). According to this approach, the parameters of the localized solution (6.17), i.e. μ, v, α and x_0, are assumed to be slowly varying in time. The equations describing their evolution in the presence of perturbations were obtained by Vakhnenko and Gaididei (1986). Substituting Eq. (6.16) into those equations and applying the Poisson formula to evaluate the sums appearing as a result of discreteness of the primary AL model, we obtain two coupled equations for the soliton parameters v and x_0:

$$\frac{\mathrm{d}x_0}{\mathrm{d}t} = \frac{2}{\mu}\sinh\mu\sin v\ , \tag{6.18}$$

$$\frac{\mathrm{d}v}{\mathrm{d}t} = -\frac{2\pi^3\sinh^2\mu\sin(2\pi x_0)}{\mu^3\sinh(\pi^2/\mu)}\ , \tag{6.19}$$

and also $\mathrm{d}\mu/\mathrm{d}t = 0$. In Eq. (6.19) we took into account only the contribution of the first harmonic because the higher ones, of the order of s, will always appear with the additional factor $\sim \exp(-\pi^2 s/\mu)$ which is assumed to be small.

The system (6.18), (6.19) is a Hamiltonian one, the corresponding Hamiltonian is given by the expression,

$$H = -\frac{2}{\mu}\sinh\mu\cos v - \frac{\pi^2\sinh^2\mu}{\mu^3}\frac{\cos(2\pi x_0)}{\sinh(\pi^2/\mu)}\ , \tag{6.20}$$

where the parameters x_0 and v have the sense of the generalized coordinate and momentum, respectively. The first term is the kinetic energy of the effective particle, the second one is the periodic potential, which is, as a matter of fact, the effective periodic PN relief. In the approach assuming the difference between the two models to be small, i.e. the parameter μ small, the amplitude of the PN potential defined as

$$U_{\max} = \frac{\pi^2\sinh^2\mu}{\mu^3\sinh(\pi^2/\mu)}\ , \tag{6.21}$$

is exponentially small in the parameter μ^{-1}. As we can see, the dependence (6.21) and the periodic potential $U_{\max}\cos(2\pi x_0)$ are similar to those in the problem for the topological kink in the FK model discussed above. As a result, all types of motion of the effective particle remain the same as in the case of the kink, in particular, the nonlinear mode may be trapped by discreteness similar to a trapping of a kink.

The approach based on the perturbations of the integrable AL lattice model have been examined by Bang and Peyrard (1995) who found only qualitative agreement with numerical results on nonlinear localized modes in the generalized FK models. One of the possible reason for this is the strong assumption in the derivation of the adiabatic equations (6.18) and (6.19) which is valid only in the case of very small perturbation. In a general case, all higher harmonics in the Poisson sums give a contribution of the same order and the quantitative agreement should be no longer expected. However, the theory based on the AL model may serve as a simple example explaining how the effective periodic dependence of the mode parameters appears due to lattice discreteness when the lattice model becomes nonintegrable.

6.4. Dark-soliton modes

As is well known, in the continuum limit approximation the DNLS equation (6.6) supports two different kinds of soliton solutions, *bright* and *dark* solitons. The bright solitons are similar to spatially localized modes discussed above, whereas localized structures which are similar to dark solitons are less discussed in literature. It is the purpose of this section to present two types of these structures in the FK type lattice following the paper by Kivshar (1992), see also Putterman and Roberts (1993), Huang et al. (1993) and Kivshar et al. (1994). This type of structures has been observed experimentally by Denardo et al. (1992) in an array of parametrically driven pendulums (see also Lou and Huang, 1995; for the case of a diatomic lattice). Similar types of dark-soliton localized modes for a chain with anharmonic interatomic coupling has been recently analyzed by Bortolani et al. (1997).

First, we notice that for positive λ, the continuous wave solution is stable only for $k > \pi/2a_s$, so that dark-profile structures are possible, for example, near the cut-off frequency $\omega_m = 4K$. Substituting $\psi_n = (-1)^n \Psi(x,t) e^{i\omega_m t}$ into Eq. (6.6), where the slowly varying envelope Ψ is found to be a solution of the continuous NLS equation, it is easy to obtain the dark soliton solution in the continuum approximation,

$$\psi_n = (-1)^n A \tanh(Ax) e^{-i\Omega t} , \tag{6.22}$$

where $\Omega = 4K - \lambda A^2$, and $x = n a_s \sqrt{K}$ is considered as a continuous variable.

Looking now for the similar structures in the discrete NLS equation (6.6), we find that they are possible, for example, in the form

$$\psi_n = A e^{-i\Omega t} (\ldots, 1, -1, 1, -\xi_1, 0, \xi_1, -1, 1, \ldots) , \tag{6.23}$$

where $\Omega = 4K - \lambda A^2$, and

$$\xi_1 = 1 - \Delta_1 \quad \text{and} \quad \Delta_1 = \frac{K}{\lambda A^2} \ll 1 . \tag{6.24}$$

The structure (6.23) is a solution of the NLS equation with the accuracy better for smaller Δ_1, and it is a phase-kink excitation with the width localized on a few particles in the lattice (see Fig. 26a). Because the frequency Ω coincides with the cut-off frequency of the nonlinear spectrum, we call these solutions "cutoff kinks".

Another type of dark-profile nonlinear localized structures which may be also described analytically in continuum as well as discrete models, is realized in the case when the mode frequency is just at the middle of the spectrum band, i.e. the wavenumber is equal to $\pi/2a_s$. In this case we may separate the particles in the chain into two subsets, odd and even ones, and describe their dynamics separately, introducing the new variables, i.e. $\psi_n = v_n$, for $n = 2l$, and $\psi_n = w_n$, for $n = 2l + 1$. The main idea of such an approach is to use the continuum approximation for *two* envelopes, v_n and w_n (see Kivshar, 1992).

Looking now for solutions in the vicinity of the point $k = \pi/2a_s$, we may use the following ansatz:

$$v_{2l} = (-1)^l V(2l,t) e^{-i\omega_1 t}, \qquad w_{2l+1} = (-1)^l W(2l+1,t) e^{-i\omega_1 t} , \tag{6.25}$$

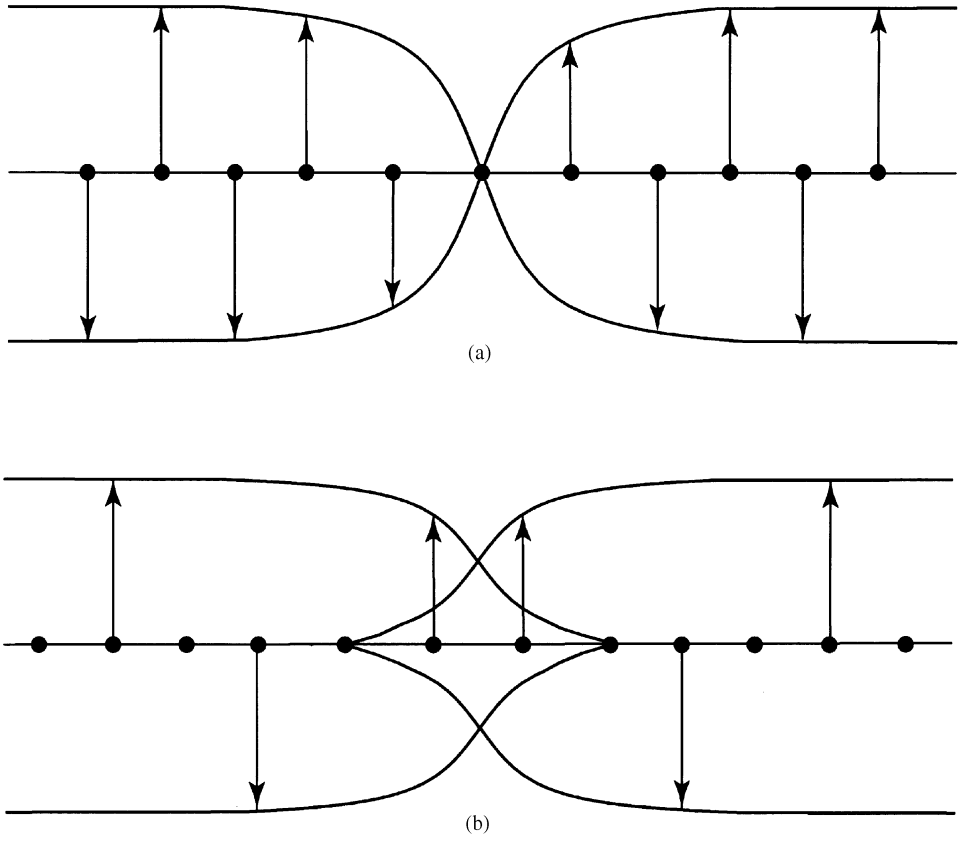

Fig. 26. Dark-soliton localized nonlinear modes: (a) cut-off and (b) non-cut-off kinks.

where $\omega_1 = 2K$ is the frequency of the wavelength-four linear mode, assuming that the functions $V(2l,t)$ and $W(2l+1,t)$ are slowly varying in space. Substituting Eq. (6.25) into Eq. (6.6), we finally get the system of two coupled equations,

$$\mathrm{i}\frac{\partial V}{\partial t} + 2a_s K\frac{\partial W}{\partial x} + \lambda|V|^2 V = 0\,, \tag{6.26}$$

$$\mathrm{i}\frac{\partial W}{\partial t} - 2a_s K\frac{\partial V}{\partial x} + \lambda|W|^2 W = 0\,, \tag{6.27}$$

where the variable x is treated as continuous one. Analysing localized structures, we look for stationary solutions of Eqs. (6.26) and (6.27) in the form

$$(V,W) \propto (f_1,f_2)\mathrm{e}^{\mathrm{i}\Omega t}\,, \tag{6.28}$$

assuming, for simplicity, the functions f_1 and f_2 to be real. Then, the stationary solutions of Eqs. (6.26) and (6.27) are described by the system of two ordinary differential equations of the

first order,

$$\frac{df_1}{dz} = -\Omega f_2 + \lambda f_2^3 , \tag{6.29}$$

$$\frac{df_2}{dz} = \Omega f_1 - \lambda f_1^3 , \tag{6.30}$$

where $z = x/2a_sK$. Eqs. (6.29) and (6.30) represent the dynamics of a Hamiltonian system with one degree of freedom and the conserved energy, $E = -\frac{1}{2}\Omega(f_1^2 + f_2^2) + \frac{1}{4}\lambda(f_1^4 + f_2^4)$, and they may be easily integrated with the help of the auxiliary function $\phi = (f_1/f_2)$, for which the following equation is valid,

$$\left(\frac{d\phi}{dz}\right)^2 = \omega_1^2\Omega^2(1 + \phi^2)^2 + 4\lambda E(1 + \phi^4) . \tag{6.31}$$

Different kinds of solutions of Eq. (6.31) may be characterized by different values of the energy E (Kivshar, 1992). On the phase plane (f_1, f_2) soliton solutions correspond to the separatrix curves connecting a pair of the neighboring saddle points $(0, f_0)$, $(0, -f_0)$, $(f_0, 0)$, or $(-f_0, 0)$, where $f_0^2 = \Omega/\lambda$. Calculating the value of E for these separatrix solutions, $E = -\Omega^2/4\lambda$, it is possible to integrate Eq. (6.31) in elementary functions and to find the soliton solutions,

$$\phi(z) = \exp(\pm\sqrt{2}\Omega z) , \tag{6.32}$$

$$f_2^2 = \frac{\Omega e^{\mp\sqrt{2}\Omega z}[2\cosh(\sqrt{2}\Omega z) \pm \sqrt{2}]}{2\lambda\cosh(2\sqrt{2}\Omega z)}, \quad f_1 = \phi f_2 . \tag{6.33}$$

The solutions (6.32), (6.33), but for negative Ω, exist also for defocusing nonlinearity when $\lambda < 0$.

The results (6.32), (6.33) together with (6.28) and (6.25) give the shapes of the localized structures in the discrete nonlinear lattice. The whole localized structure represents two kinks in the odd and even oscillating modes which are composed to have opposite polarities (see the envelopes in Fig. 26b).

Highly localized nonlinear structures in the lattice corresponding to the solutions (6.32), (6.33) may be also found, and one of these structures has the following form:

$$\psi_n = Ae^{-i\Omega t}(\ldots, 1, 0, -1, 0, \xi_2, \xi_2, 0. -1, 0, 1, \ldots) , \tag{6.34}$$

where $\Omega = 2K - \lambda A^2$ is the frequency at the middle of the nonlinear spectrum, and $\xi_2 = 1 - \Delta_2$, $\Delta_2 = K/2\lambda A^2 \ll 1$. The approximation is better for smaller values of the parameter Δ_2.

7. Effects of disorder

7.1. Models of disorder

For realistic physical models, the interaction of nonlinear excitations with impurities should play an important role in the transport properties because kinks (or breathers) can be trapped or

reflected by local impurities. Additionally, a breather captured by an impurity becomes *a nonlinear impurity mode*, and this observation makes a link between the theory of nonlinear chains and the theory of harmonic lattices with defects (see, e.g., Lifshitz, 1943, 1944; Krivoglaz, 1961; Maradudin, 1966).

Many features of the soliton-impurity interactions have been already discussed in review papers by Kivshar and Malomed (1989) and Gredeskul and Kivshar (1992) in the framework of the SG model with local or extended inhomogeneities. For the discrete FK model, two new features of the soliton-impurity interactions appear and they should be discussed. First, in a discrete chain, a kink moves in the presence of an effective PN potential whose amplitude is always less than the amplitude of the substrate potential. Thus, the kink parameters are varying periodically and this simple mechanism generates phonons leading to the subsequent rapid pinning of the kink by the lattice discreteness. As a result, the discreteness effects which are absent in the SG model may significantly modify the adiabatic kink scattering (see, e.g., Braun and Kivshar, 1991a). Second, the important feature of the kink scattering by impurities in a discrete chain is the possible excitation of impurity modes during the scattering. In fact, such an effect is also possible for continuous models provided one considers strong disorder (see below), but the discreteness modifies the impurity mode frequency making the process of its excitation more easier (see, e.g., Forinash et al., 1994).

A simple generalization of the FK model to include defects of different kind was discussed by Braun and Kivshar (1991a). The FK model with disorder is described by the following Hamiltonian [cf. Eqs. (2.1), (2.2), (2.3), (2.4), (2.5), (2.6), (2.7), (2.8), (2.9) and (2.10)]

$$\mathscr{H} = \sum_j \left\{ \frac{1}{2} m_j \left(\frac{\mathrm{d}x_j}{\mathrm{d}t} \right)^2 + \frac{1}{2} g_j (x_{j+1} - x_j - a_0)^2 + \varepsilon_j \left[1 - \cos\left(\frac{2\pi x_j}{a_s} \right) \right] + v(x_j) \right\}, \tag{7.1}$$

where impurities are taken into account through the parameters m_j (change of the particle mass), g_j (change of the interparticle interaction), ε_j (local distortion of the substrate potential), and $v(x_j)$ (an additional change of on-site potential created by impurities). The motion equation for the atomic displacements $u_j = x_j - ja_s$ takes the form [we select the simplest case when $a_0 = a_s$, cf. Eq. (2.20)]

$$m_j \frac{\mathrm{d}^2 u_j}{\mathrm{d}t^2} + g_j(u_j - u_{j+1}) + g_{j-1}(u_j - u_{j-1}) + \varepsilon_j \sin u_j + v'(ja_s + u_j) = 0 \,. \tag{7.2}$$

When one of the atoms of the chain, say at $j = 0$, has properties which are different from those of the lattice atoms, it may be characterized by a local change of the parameters (in dimensionless units adopted in Section 2), $\varepsilon_0 = 1 + \Delta\varepsilon$, $m_0 = 1 + \Delta m$, and $g_0 = g_{-1} = g + \Delta g$, so that the perturbation-induced correction $\delta\mathscr{H}$ to the Hamiltonian of the FK chain is written as

$$\delta\mathscr{H} = \frac{1}{2}\Delta m \left(\frac{\mathrm{d}u_0}{\mathrm{d}t} \right)^2 + \frac{1}{2}\Delta g[(u_1 - u_0)^2 + (u_0 - u_{-1})^2] + \Delta\varepsilon(1 - \cos u_0) \,. \tag{7.3}$$

In the continuum approximation such an impurity is introduced by the changes like $\varepsilon_j \to \varepsilon(x) = 1 + \Delta\varepsilon a_s \delta(x)$, and so on.

7.2. Kinks

7.2.1. Static properties

First of all, the combined effect of nonlinearity and disorder can modify the kinks properties even in the static case. This problem is easier to be analysed for the SG model, i.e. for the continuous version of the FK chain. In fact, the SG model with defects was introduced by Baeriswyl and Bishop (1980) who analysed the linear properties of that model. For the case of the delta-like impurities, a number of exact results to the SG model can be obtained for defect stationary states, nonlinear static structures created by the effect of kink's pinning due to impurities. Several cases where such stationary structures may be treated analytically have been considered for both the linear coupling between the defect and the wave field, i.e. when $v(x) \sim \lambda\delta(x - x_0)$ (see, e.g., Reisinger and Schwabl, 1983), and for nonlinear coupling (when, e.g., $\varepsilon(x) \sim \lambda\delta(x - x_0)$, see Galpern and Filippov, 1984). The derivative mismatch introduced by such a δ-function allows to get (for isolated defects) the nonlinear stationary conditions which can be solved analytically. With the help of those exact results, the correlation function in the presence of defects can be calculated, as well as the free energy of the various possible configurations. This program can be realized not only for one or two impurities but also for a random distribution of defects in the limit of small concentration (see, e.g., Reisinger and Schwabl, 1983).

More complicated behavior is observed in a generalized FK model where, e.g., an extension of the model beyond the limits of the harmonic approximation for the interatomic potential leads to some qualitatively novel results such as the existence of distortion chain configurations (Markov and Trayanov, 1987) or formation of cracks when the tensile strength of the chain exceeds a certain critical value (see, e.g., Milchev, 1986, 1990). When local impurities are inserted into the chain, they may act as traps in both pinning the antikinks and increasing the threshold for a chain breakup. Such an effect was analysed for the FK chain with nonconvex interaction between neighboring atoms by Malomed and Milchev (1990) who showed that the breakup threshold for an antikink pinned by an inhomogeneity which locally decreases the substrate potential is higher than for a free antikink, the effect they related to the observed formation of cracks out of misfit dislocations in III–V heterostructures (Franzosi et al., 1988).

7.2.2. Effective equation of motion

First we consider the continuum approximation of the FK model described by the SG equation with inhomogeneous parameters. In this case, the effective equation for the kink's coordinate can be derived by a simplified version of the collective-coordinate approach (see, e.g., Fogel et al., 1976, 1977; Kivshar and Malomed, 1989; and references therein). As an example, we consider the simplest case of the inhomogeneous SG model,

$$u_{tt} - u_{xx} + \sin u = \varepsilon f(x) \sin u \ , \tag{7.4}$$

when the impurity is modelled by introducing the external potential

$$U_{\text{ext}}(x) = \int_x \mathrm{d}x f(x) \ .$$

Analysing the kink dynamics in the framework of the collective-coordinate approach, we can obtain, in a simple way, an effective equation of motion for the kink's coordinate (see, e.g., Currie et al., 1977; McLaughlin and Scott, 1978). To derive such an equation, we note that the unperturbed SG system has an infinite number of quantities (system invariants) that are conserved during the evolution, among which there is the momentum,

$$P \equiv -\int_{-\infty}^{\infty} \mathrm{d}x\, u_t u_x \,. \tag{7.5}$$

For the SG kink, Eq. (7.5) takes the form of the well-known relativistic expression $P = mV/\sqrt{1-V^2}$, V being the kink velocity. In the presence of perturbations, the momentum is no longer conserved; using Eq. (7.4) it is possible to show that it varies according to the equation

$$\frac{\mathrm{d}P}{\mathrm{d}t} = \varepsilon \int_{-\infty}^{\infty} \mathrm{d}x f(x)(\cos u)_x \,,$$

provided the boundary conditions $u \to 0(2\pi)$ at $x \to \pm\infty$ holds. The adiabatic approach is now defined by the assumption that, for ε small enough, the kink shape is not affected and only the kink's coordinate X becomes a slowly varying function of time. Within this hypothesis it can be shown that, in the non-relativistic limit, the kink center obeys the following equation of motion $m\,\mathrm{d}^2X/\mathrm{d}t^2 = -U'(X)$, where

$$U(X) \equiv -2\varepsilon \int_{-\infty}^{\infty} \mathrm{d}x \frac{f(x)}{\cosh^2(x-X)} \,, \tag{7.6}$$

and we have used the approximate expression $P \approx m_k(\mathrm{d}X/\mathrm{d}t)$, valid for small velocities. Thus, in the framework of such an adiabatic approach, the motion of the SG kink can be thought of as that of a particle with (kink) mass m in the external potential $U(X)$ defined by Eq. (7.6). The similar properties can be shown for relativistic kinks (Bergman et al., 1983).

The following two cases arise naturally from Eq. (7.6). If $f(x)$ changes rapidly over distances of the order of the kink length, then ε has to be small for our approximation to hold. For example, in the case $f(x) = \delta(x)$, we have (McLaughlin and Scott, 1978): $U(X) = -2\varepsilon\,\mathrm{sech}^2 X$. On the other hand, if $f(x)$ changes slowly, i.e., its characteristic length (say L) is much larger than the kink width, it is not necessary for ε to be small, because all the parameters of the perturbation theory are of the order of L^{-1}, and we are left with $U(X) \approx 4\varepsilon f(X/L)$.

The approximation involved in the derivation presented above is based on the assumption that the kink moves slow through the region of inhomogeneity. In this case, the kink's width does not change much and its variation can be neglected. This corresponds to the so-called 'nonrelativistic' interaction of the kink with an impurity. However, relativistic effects can be taken into account by introducing one more collective coordinate associated with kink's width (Rice, 1984; Fernandez et al., 1986). A more detailed analysis of this effect was presented by Woafo and Kofané (1994) who observed that a kink is shortened in the attractive potential and extended in the repulsive potential of the impurity.

The adiabatic theory presented above becomes not valid in the case when a localized impurity can support an impurity mode, an oscillating linear mode at the impurity site. In this latter case, the kink's position and the impurity mode amplitude are two effective collective coordinates as discussed in detail below. Different types of the so-called resonant interactions of solitons and kinks with impurities have been recently overviewed by Belova and Kudryavtsev (1997), and the simplest example of such an interaction can be found below in Section 7.4.

In a discrete FK lattice, the motion equation for the kink's coordinate is modified by the PN relief. One of the ways to derive the effective equation of motion for the kink has been already mentioned in Section 2.3 and it is based on the projection-technique approach developed by the group of Willis. Another approach is based on the Lagrangian formalism which we will apply here just to mention the example how such a method really works (see, e.g., Pouget et al., 1989; Braun and Kivshar, 1991a; Salerno and Kivshar, 1994).

Let us start from the Lagrangian of the inhomogeneous FK chain

$$L = \sum_j \left\{ \frac{1}{2} m_j \left(\frac{\mathrm{d}u_j}{\mathrm{d}t} \right)^2 - \frac{1}{2} g_j (u_{j+1} - u_j)^2 - \varepsilon_j \left[1 - \cos\left(\frac{2\pi u_j}{a_s} \right) \right] \right\} . \tag{7.7}$$

Considering now the simplest case of a single-point defect at the site $n = 0$ (the case of several impurities can be treated in a similar manner) we put $\varepsilon_j = \varepsilon_s + \Delta\varepsilon\delta_{j0}$, $m_j = m_a + \Delta m\delta_{j0}$, and $g_j = g + \Delta g\delta_{j0}$. Introducing the dimensionless variables, $\tau = (c/a_s)t$ and $\phi_j = (2\pi/a_s)u_j$ and setting $\mu = a_s/l$, $c^2 = ga_s^2/m_a$, $l = c/\omega_0$, where $\omega_0^2 = 2\pi^2\varepsilon_s/m_a a_s^2$, the Lagrangian (7.7) becomes

$$L = A\sum_j \left\{ \frac{1}{2} \left(\frac{\mathrm{d}\phi_j}{\mathrm{d}t} \right)^2 \left(1 + \frac{\Delta m}{m_a} \delta_{j0} \right) - \frac{1}{2} (\phi_{j+1} - \phi_j)^2 \left(1 + \frac{\Delta g}{g} \delta_{j0} \right) - \mu^2 (1 - \cos\phi_j) \left(1 + \frac{\Delta\varepsilon}{\varepsilon_s} \right) \right\} , \tag{7.8}$$

where $A = m_a(c/2\pi)^2$. In the notations adopted above, the parameter μ has the meaning of a ratio of the lattice spacing to the kink's width. We now assume that the value μ is small, so that distorted kink in the discrete chain may be approximated by the SG kink ansatz

$$\phi_j(\tau) = 4\tan^{-1} \mathrm{e}^{\mu\xi_j} , \tag{7.9}$$

where $\xi_j = j - Y(\tau)$, where $Y(\tau)$ is a collective coordinate of the kink. Substituting Eq. (7.9) into the system Lagrangian and evaluating the sums with the help of the Poisson sum formula:

$$\sum_{n=-\infty}^{\infty} f(nh)h = \int_{-\infty}^{\infty} \mathrm{d}f f(x) \left[1 + 2\sum_{s=1}^{\infty} \cos\left(\frac{2\pi s x}{h} \right) \right] ,$$

we obtain the effective Lagrangian in the following reduced form (Braun and Kivshar, 1991a)

$$L/A = 4\mu \left\{ \left(\frac{\mathrm{d}Y}{\mathrm{d}t} \right)^2 - \frac{4\pi^2}{\sinh(\pi^2/\mu)} \cos(2\pi Y) \right\} + \frac{2\mu^2}{\cosh^2(\mu Y)} \left\{ \left(\frac{\mathrm{d}Y}{\mathrm{d}t} \right)^2 \left(\frac{\Delta m}{m_s} \right) - \left(\frac{\Delta g}{g} - \frac{\Delta\varepsilon}{\varepsilon_s} \right) \right\} . \tag{7.10}$$

The equation of motion for the kink's coordinate $X = \mu Y$ can be obtained from Eq. (7.10) in a straightforward manner. The simple analysis shows that the discreteness yields an additional potential field associated with the PN relief so that the kink may be treated as an effective particle of a variable mass moving in an effective potential

$$U_{\rm eff}(X) = U_{\rm PN}(X) + U_{\rm im}(X)\,, \tag{7.11}$$

where

$$U_{\rm PN}(X) = \frac{2\pi^2\mu}{\sinh(\pi^2/\mu)}\cos\left(\frac{2\pi X}{\mu}\right), \tag{7.12}$$

and

$$U_{\rm im}(X) = \frac{1}{4}\left(\frac{\Delta g}{g} + \frac{\Delta\varepsilon}{\varepsilon_s}\right)\frac{\mu^3}{\cosh^2 X}\,. \tag{7.13}$$

The analysis of the kink motion in the vicinity of the impurity can be found in the paper by Braun and Kivshar (1991a), but a qualitative physical picture of such an interaction is rather simple: The kink's motion is affected by the potentials of two kinds, localized, from the impurity, and nonlocalized from the periodic PN relief. In particular, if the kink is pinned by the discreteness not far from the impurity, its PN frequency is renormalized to be

$$\omega_j^2 = \omega_{\rm PN}^2 - \mu^3\frac{1}{2}\left(\frac{\Delta g}{g} + \frac{\Delta\varepsilon}{\varepsilon}\right)\frac{(1 - 2\sinh 2X_j)}{\cosh^4 X_j}\,, \tag{7.14}$$

where $\omega_{\rm PN}^2 = [8\pi^4/\mu\sinh(\pi^2/\mu)]$ is the PN frequency, $X_j = \mu(j + \frac{1}{2})$, and ja_s is the distance from the impurity. It is important to note that the local impurity potential $U_{\rm im}$ acts on a kink and antikink in the same way.

The similar technique can be applied to the problem of the DNA promoters to explain its role as dynamical activators of transport processes of the RNA polymerase along DNA macromolecules. By introducing an effective potential for the kink in a disordered FK model, suggested as a simplest model of the DNA chain (Englander et al., 1980; Yomosa, 1983, 1984; Homma and Takeno, 1984; Zhang, 1987; Yakushevich, 1989; Salerno, 1991, 1992b), Salerno and Kivshar (1994) have demonstrated the existence of a dynamically 'active' region inside of a DNA promoter, in a qualitative agreement with experimental data (Ricchetty et al., 1988).

Several interesting effects can be observed for a multi-kink dynamics when more than one kink interact near the impurity. In particular, when a moving kink collides with a kink trapped by at an impurity site, three different outcomes of the collision are possible: depinning, capture, and exchange (Malomed and Nepomnyashchy, 1992). For the kinks of different polarities, such collisions may result also in annihilation of the kinks at the impurity. The scattering of a SG breather can be treated as that of a coupled pair of kinks, at least in the case of low-frequency breathers. A complex dynamics of the breather-impurity scattering has been demonstrated by Kenfack and Kofané (1994) and Zhang (1998).

The adiabatic effects discussed above are based on the approximation when radiative losses are negligible. However, during the scattering by impurities, the kink radiates phonons which may

change the general pictures of the scattering by introducing an effective radiative losses (see, e.g., Kivshar and Malomed, 1989). In fact, radiative losses in the inhomogeneous FK model may be of *three* types.

- *The first type* of radiation effects arises due to the PN potential: Moving in a discrete lattice with a variable velocity, the kink generates phonons (see Ishimori and Munakata, 1982; Peyrard and Kruskal, 1984; Boesch et al., 1989). Such an emission of radiation is strongly connected with the structure of the spectrum band of linear phonons and, for example, in the case of extreme discreteness ($g \sim 1$), the emission of the moving kink exhibits well-defined changes at some critical velocities (Peyrard and Kruskal, 1984). The trapped kink oscillating in the PN potential emits large and sudden bursts of radiation when the frequency of the kink oscillation reaches certain resonant values (Boesch et al., 1989).
- *The second type* of the resonant effects is related to the change of the kink's velocity caused by impurities. This kind of the kink's emission can be calculated in the lowest order as emission of the SG kink. A number of such problems was mentioned in a review paper on the soliton perturbation theory (Kivshar and Malomed, 1989). The importance of this type of radiative effects has been demonstrated for the case of the kink scattering by two impurities by Kivshar et al. (1992), who demonstrated that, for low kink's velocities, the reflection coefficient of the kink depends oscillatory on the distance between impurities, the effect caused by an interference of the radiation emitted by the kink.
- At last, *the third type* of inelastic effect which are not taken into account by the adiabatic approach is the excitation of impurity modes by the scattering kink, and in the limit of the SG model such a problem will be discussed below (see Section 7.4).

7.2.3. Point impurities

When the function $f(x)$ in Eq. (7.4) describes random impurities, we may consider the simplest case of delta-like inhomogeneities,

$$\varepsilon f(x) = \sum_n \varepsilon_n \delta(x - a_n) \,, \tag{7.15}$$

where the numbers ε_n and a_n are chosen to be random, and it is assumed that the distances $b_n = a_{n+1} - a_n$ are identically distributed random numbers with the probability density

$$p(b) = b_0^{-1} \mathrm{e}^{-b/b_0} \,. \tag{7.16}$$

Then, the equation for the kink coordinate X takes the form, $m\,\mathrm{d}^2X/\mathrm{d}t^2 = -U'(X)$, where

$$U(X) = \sum_n u_n(X), \quad u_n(X) \equiv u(X - a_n), \quad u(X) \equiv -\frac{2\varepsilon}{\cosh^2 X} \,. \tag{7.17}$$

Here, as above, we have approximated $P \simeq mV \simeq m\,\mathrm{d}X/\mathrm{d}t$. Thus, in the collective coordinate framework, the motion of the SG kink can be interpreted as the motion of a nonrelativistic particle with the unit mass m in an effective, random potential defined in Eq. (7.17).

In the paper by Gredeskul et al. (1992) the kink scattering was analysed for the case when disorder appears as randomly distributed point impurities with equal intensities, i.e. for $\varepsilon_n = \varepsilon$. The general methods usually used for time-dependent random perturbations [see, e.g., Pascual and

Vázquez (1985), Biller and Petruccione (1990) and also the review papers by Bass et al. (1988); Gredeskul and Kivshar (1992) and Sánchez and Vázquez (1992)] cannot be directly applied to the problem because for randomly distributed spatial impurities we cannot derive the Fokker–Plank equation [notice that the potential (7.17) is not Markovian]. Gredeskul et al. (1992) elaborated a statistical procedure to compute the mean characteristics of the kink propagation, e.g. the kink's mean velocity, assuming the velocity is rather large and the strength of impurities small.

One of the important problems related to the FK chain dynamics is the influence of disorder on the dislocation motion in crystals with a high PN potential. The basic concepts of the dislocation dynamics in crystals with a high PN relief were formulated by Lothe and Hirth (1959) and Kazantsev and Pokrovsky (1968). Transversal displacement of the dislocation line is treated as creation of kink–antikink pairs by thermal fluctuations under the action of the applied constant force. Experimental data show that the dislocation mobility is also significantly affected by point defects, e.g. doping of crystals can give rise to an increase in the dislocation speed (Patel and Chandhuri, 1966; Erofeev and Nikitenko, 1971). This effect can be explained in the framework of the FK model as a consequence of local lowering of the PN barrier due to the interaction between the dislocation and impurities (Petukhov, 1971, 1983) and we would like to mention that such conclusions were confirmed by extensive numerical simulations which showed that point defects in crystal lattice have an extremely profound effect on dislocation mobility (Vinokur, 1986; Sagdeev and Vinokur, 1987). This kind of effects is caused by the force-activated dynamics of the kinks in the FK model, but the detailed analysis of such effects is out of the content of the present survey.

7.2.4. Kink diffusion in a disordered chain

For many applications of the FK model, for example, in the surface physics, the analyzing of mass transport along the chain is a very important problem. As distinct from two- and three-dimensional systems, in the one-dimensional atomic chain impurities cannot be bypassed, and therefore impurities may drastically modify the transport properties of such systems.

In the FK model, the chemical diffusion along the chain is determined by the motion of kinks (see, e.g., Gillan, 1985; Gillan and Holloway, 1985; Braun et al., 1990). For the system temperature T, lower then the amplitude of the PN potential E_{PN}, the kink's motion has an activated character, so that, for a homogeneous FK chain the kink diffusion coefficient is equal to (Gillan, 1985) $D_0 = Ra_s^2$, where the escape rate R is determined by the Kramers theory (Kramers, 1940; see also Section 5 above),

$$R \approx \frac{\omega_{\mathrm{PN}}}{2\pi} \exp\left(-\frac{E_{\mathrm{PN}}}{k_{\mathrm{B}}T} \right). \tag{7.18}$$

Note that here we have taken into account the energy exchange between the FK chain and the substrate, and assume that the friction coefficient η has an intermediate value (see details in Section 5, and also Braun, 1989; Braun et al., 1990).

In the presence of impurities, the external potential for the kink motion is modified as well. According to Eq. (7.11), the minima of the effective potential are equal to (we suppose $\Delta m = 0$, for simplicity) $U_j = U_{\mathrm{eff}}(\mu_j + \mu/2)$, and the maxima are determined by the expression

$U_{j,j-1} = E_{\mathrm{PN}} + U_{\mathrm{eff}}(\mu_j)$. Thus, the escape rate for the kink from the jth well to the $(j+1)$th well takes the form

$$R_{j+1,j} \approx \frac{\omega_j}{2\pi} \exp\left(-\frac{E_{j+1,j}}{k_{\mathrm{B}}T} \right), \tag{7.19}$$

where the frequency ω_j is determined by Eq. (7.14), and the activation energy for the jump $j \to (j+1)$ is given by

$$E_{j+1,j} \approx E_{\mathrm{PN}} - mu^4 \frac{1}{4} \left(\frac{\Delta g}{g} + \frac{\Delta \varepsilon}{\varepsilon_s} \right) \frac{\sinh(\mu j)}{\cosh^3(\mu j)} . \tag{7.20}$$

Let us suppose that the average distance between impurities in Na_s. Then the kink diffusion coefficient may be presented as $D_k = D_0 K$, where the value of K is determined by the escape rates (7.19) (see, e.g., Haus and Kehr, 1987). The expression for K is simplified if all the minima are equivalent (when, for example, there is no external force), so that $R_{j+1,j} = R_{j,j+1} \equiv R_j$, or if all the maxima of the potential have the same value E_{PN}, so that $R_{j+1,j} = R_{j-1,j} \equiv R_j$. According to Kehr et al. (1978), in these cases $K = \langle R \rangle / R$, where

$$\frac{1}{\langle R \rangle} = \frac{1}{N} \sum_{j=1}^{N} \frac{1}{R_j} . \tag{7.21}$$

As follows from estimations for adsystems (see Braun, 1989; Braun et al., 1990), it is usually valid $g \sim 1$, so that the kink width $d \sim a_s$, and only one well or barrier, say at $j = 0$, is changed significantly. In this case,

$$K = \frac{NR_0}{(N-1)R_0 + R} . \tag{7.22}$$

If $R_0 \sim R$ for $N \gg 1$, then $K \approx 1 - (R - R_0)/NR_0$. For $R_0 \gg R$, we obtain $K \approx N/(N-1) \approx 1$ and for $NR_0 \ll R$, $K \approx NR_0/R \ll 1$. Therefore, the estimate shows that impurities may drastically change the value of the diffusion coefficient of the kink, and, therefore, modify transport properties of the kink-bearing nonlinear systems.

7.3. Nonlinear impurity modes

Localized modes created by impurities are well known in the linear theory of crystal lattices (see, e.g., Maradudin, 1966). To investigate such kind of localized excitations in the framework of the linearized FK model, we consider small-amplitude oscillations of the impurity atoms making the expansion $\sin u_j \approx u_j$. Then the localized modes of the linear lattice can be easily found analytically with the help of the Green-function technique (see, e.g., Maradudin, 1966; Kosevich, 1972). Such an analysis for the case of the linearized FK model can be found in the paper by Braun and Kivshar (1991a). The Green function of the chain with impurities satisfies the Dyson equation, and a simple analysis of the corresponding solutions of that equation gives the conditions for the impurity modes to exist. As a result, the impurity-induced localized modes are possible with the frequencies lying either *above* or *below* the phonon frequency band defined as $(\omega_{\min}, \omega_{\max})$, where $\omega_{\min} = 1$ and $\omega_{\max} = \sqrt{1 + 4g}$. For example, in the case of an isotopic defect (firstly analysed for another type of

lattices by Lifshitz, 1943), when $\Delta m \neq 0$ but $\Delta g = \Delta\varepsilon = 0$, the localized impurity mode exists for $\Delta m > 0$ (heavy mass) below the frequency band, $0 < \omega < \omega_{\min}$, and for $\Delta m < 0$ (light mass), it exists above the frequency band, $\omega > \omega_{\max}$. The mode frequency is given by

$$\omega_l^2 = \frac{(1+2g) \mp \sqrt{4g^2 + \Delta m^2(1+4g)}}{(1-\Delta m^2)}\,, \tag{7.23}$$

for the cases $\Delta m > 0$ or $\Delta m < 0$, respectively.

The impurity-induced localized modes can be also described in the nonlinear FK chain in the long-wavelength limit when the effective SG equation is valid. In such a case nonlinear impurity modes may be obtained as breather modes captured by impurities (Kosevich and Kovalev, 1975; Braun and Kivshar, 1991a; Boardman et al., 1995). Analogously to the linear approximation discussed above, the nonlinear impurity modes may exist with the frequencies lying either below or above the phonon spectrum band. However, the shape of the nonlinear mode is modified by nonlinearity giving rise several new features. In particular, the nonlinearity itself may extend the condition for the nonlinear modes to exist (see, e.g., Kosevich and Kovalev, 1975; Kivshar and Malomed, 1988; Braun and Kivshar, 1991a; Kovalev et al., 1995), however, the stability analysis shows that such nonlinear localized modes excited near local impurities are stable only in the regions of existence of corresponding linear modes (Kivshar and Malomed, 1988; Braun and Kivshar, 1991a).

As an example, let us consider the case when only $\Delta\varepsilon \neq 0$ so that the corresponding continuous version of the FK model is described by the perturbed SG equation

$$u_{tt} - u_{zz} + \sin u = -\varepsilon_1(z)\sin u\,, \tag{7.24}$$

where $z = x/l$, $l = a_s\sqrt{g}$, and $\varepsilon_1 = \Delta\varepsilon/2\sqrt{g}$. In the linear approximation, the impurity mode for Eq. (7.24) is given by the expression $u = A\exp(\varepsilon|z|/2)\cos(\omega_l t)$, where $\omega_l = \sqrt{1-\varepsilon^2/4}$ and such a mode exist only provided $\varepsilon < 0$. To analyse the impurity mode in the nonlinear case, it is convenient to derive an effective envelope equation instead of Eq. (7.24) making the transformation

$$u = \Psi\,\mathrm{e}^{\mathrm{i}t} + \Psi^*\mathrm{e}^{-\mathrm{i}t} \tag{7.25}$$

(the asterisk stands for the complex conjugation), where the envelope function Ψ is assumed to be slowly varying and small enough to take the nonlinearity in the lowest order. Then, it is possible to reduce the problem to the effective nonlinear Schrödinger equation

$$2\mathrm{i}\Psi_t - \Psi_{zz} - \tfrac{1}{2}|\Psi|^2\Psi = 0\,, \tag{7.26}$$

with the matching condition at $z = 0$

$$\Psi_z|_{0+} - \Psi_z|_{0-} = \varepsilon_1\Psi(0)\,. \tag{7.27}$$

Matching two soliton solutions of the NLS equation (7.26), (7.27) we may find the approximate solution for the nonlinear impurity mode,

$$u(z,t) = 4\beta\,\mathrm{sech}[\beta(|z| + z_0)]\cos(\Omega_l t)\,, \tag{7.28}$$

where the impurity mode frequency Ω_l is determined by the relation $\Omega_l = \sqrt{1-\beta^2/2}$, and unlike the linear case, now it depends on the mode amplitude β. The equation which follows from the

matching condition (7.27) takes the form

$$\tanh(\beta z_0) = -\varepsilon_1/2\beta \,, \tag{7.29}$$

and it determines the structure of the nonlinear impurity mode which has different shapes for different signs of ε_1. For $\varepsilon_1 < 0$, Eq. (7.29) yields $z_0 > 0$, and the impurity mode has a shape similar to the harmonic case (see Fig. 27a), and, moreover, for $z_0 \to \infty$ it recovers the linear case. In the case of $\varepsilon_1 > 0$, Eq. (7.29) leads to the solution with $z_0 < 0$, and the impurity mode has two maxima (see Fig. 27b): The latter case shows that, in principle, impurity localized mode may be supported by nonlinearity in the cases when it is not possible in the linear limit, however, as a matter of fact, this new kind of localized impurity modes does not give stable solutions (Kivshar and Malomed, 1988; Braun and Kivshar, 1991a).

Analogously, we may find the impurity modes with the frequencies lying above the cut-off frequency of the linear lattice $\omega_{\max}$, using again the approximation of the slowly varying mode envelope. In this case we start from the FK model looking for a solution which describes out-of-phase oscillations of the atoms. The approximate solution is found to be (Braun and Kivshar, 1991a)

$$u_j = 4(-1)^j \beta \,\mathrm{cosech}[\beta(|ja_s| + z_0)] \cos(\Omega_l t) \,, \tag{7.30}$$

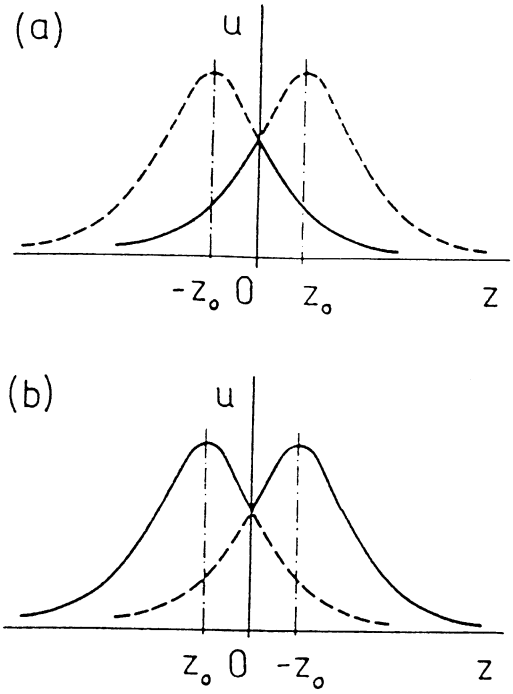

Fig. 27. Shape of a low-frequency nonlinear impurity mode for (a) $\varepsilon_1 < 0$ and (b) $\varepsilon_1 > 0$. The parameter z_0 is defined in the text.

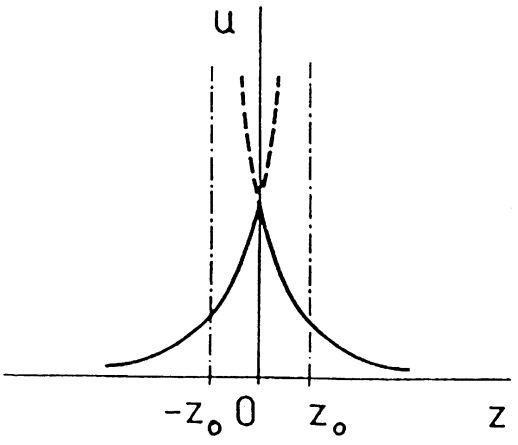

Fig. 28. Shape of a high-frequency nonlinear impurity mode for $\varepsilon_1 > 0$. The parameter z_0 is defined in the text.

and it is shown in Fig. 28. The matching parameter z_0 is determined by the equation

$$\coth(\beta z_0) = \varepsilon_1/2\beta \ . \tag{7.31}$$

and the mode frequency,

$$\Omega_l = \omega_{\max} + (\beta^2/2\omega_{\max}) \ , \tag{7.32}$$

lies above the upper (cut-off) frequency of the spectrum. Such a mode exists only provided $\varepsilon_1 > 0$.

As has been mentioned above, one of the main problems for the nonlinear impurity modes to exist is their stability. Although such impurity modes may exist even for the conditions when the linear impurity modes are forbidden, in most of the cases these new modes are in fact unstable. One of the simplest ways to carry out the stability analysis for the nonlinear modes discussed above is to introduce a small mismatch between two parts of the composed solution (7.28). Then the small-amplitude oscillations around the stationary solution are characterized by the frequency (Braun and Kivshar, 1991a) $\tilde{\omega}^2 = -3\varepsilon_1(\beta + \varepsilon/2)$ which clearly shows that the nonlinear mode is unstable for $\varepsilon_1 > 0$, i.e. just for the condition when the linear problem does not have spatially localized solutions. Thus, even supporting stationary localized solutions of a new form, nonlinearity itself does not extend the conditions for the impurity localized modes to exist.

A rigorous analysis of the stability of a nonlinear impurity mode has been recently developed by Bogdan et al. (1997) for the case of the NLS equation. They employed the analysis similar to that developed by Vakhitov and Kolokolov (1973) for solitary waves of the generalized NLS equation in a homogeneous medium and formulated the stability in terms of the invariant

$$N(\omega_l) = \int_{-\infty}^{\infty} |\Psi(x;\omega_l)|^2 \, \mathrm{d}x \ .$$

As a result, they provided a rigorous proof that the nonlinear modes for $\varepsilon_1 > 0$ is unstable, the instability corresponds to the condition $\mathrm{d}N(\omega_l)/\mathrm{d}\omega_l < 0$. Such an instability manifests itself in an exponential growth of antisymmetric perturbations which shift the soliton to one side from the

impurity mode that finally repel the localized mode due to the repulsive effective interaction with it, as consistent with the prediction based on an effective potential. In the case of negative nonlinearity, i.e. the positive sign in front of the nonlinear term in Eq. (7.26), the nonlinear impurity mode is possible only for $\varepsilon_1 < 0$ and, according to the analysis of Bogdan et al. (1997), it is stable.

In a discrete chain, the potential of the interaction between the localized mode and an impurity is modified by an effective periodic Peierls–Nabarro potential. Due to a complex structure of extremum points of a total effective potential, the mode can be shifted from the impurity site, creating *an asymmetric nonlinear impurity mode*. Such a kind of (high-frequency) nonlinear impurity mode has been recently analyzed for a lattice without a substrate potential but with nonlinear interatomic coupling (Kovalev et al., 1995; Kivshar et al., 1997), and it has been shown that it may exist even for a heavy-mass impurity (i.e. for $\varepsilon_1 > 0$, see above). Even being expected, such modes are not investigated yet for a lattice with on-site potential.

Another very important problem related to the theory of nonlinear impurity modes is the radiative damping of the mode oscillations. For the low-frequency impurity modes such an effective decay is usually power-law (Kivshar and Malomed, 1987; Braun and Kivshar, 1991a) while for the high-frequency nonlinear modes the mode lifetime may be much shorter (see Braun and Kivshar, 1991a, and references therein).

7.4. Resonant interactions with impurities

As has been demonstrated above, the kink–impurity interaction may be described by a simple picture where a local inhomogeneity gives rise to an effective potential to the kink. However, the model of a classical particle is valid only in the case when the impurity does not support an impurity mode, a local oscillating state at the impurity site. Such an impurity mode can be *excited* due to the kink scattering and it may change the result for the kink transmission. The importance of such impurity modes in the kink–impurity interactions has been pointed out in the papers by Fraggis et al. (1989), Kivshar et al. (1991), Zhang et al. (1991, 1992a, 1992b, 1994) Malomed et al. (1993), and Belova and Kudryavtsev (1995). A comprehensive overview of different types of the kink–impurity interactions can be found in a recent review paper by Belova and Kudryavtsev (1997).

An important effect found first numerically (Kivshar et al., 1991) is that a kink may be totally *reflected by an attractive impurity* due to a resonance energy exchange between the kink translational mode and the impurity mode. This resonant phenomenon is quite similar to the resonances observed in the kink–antikink collisions in some nonlinear Klein–Gordon equations (see Campbell et al., 1983, 1986; Peyrard and Campbell, 1983; Anninos et al., 1991).

To demonstrate the origin of the resonant kink–impurity interactions, we start from the SG model (7.4) which includes a local point-like impurity, i.e. $f(x) = \delta(x)$. When the impurity is absent, the model (7.4) displays the kink propagation without any distortion. In the presence of the δ-impurity, the potential (7.6) becomes

$$U(X) = -\frac{2\varepsilon}{\cosh^2 X}\,, \tag{7.33}$$

i.e. for $\varepsilon > 0$ the impurity attracts the kink.

Kivshar et al. (1991) (see also Zhang et al., 1991, 1992a, b) have studied the kink–impurity interactions for $\varepsilon > 0$ by numerical simulations. They found that there are *three* different regions of the initial kink velocity, namely, region of pass, of capture, and of reflection; and a critical velocity V_c (e.g., $V_c \approx 0.2678$ for $\varepsilon = 0.7$) exists such that if the incoming velocity of the kink is larger than V_c, the kink will pass the impurity inelastically and escape without change of the propagation direction, losing a part of its kinetic energy through radiation and exciting an impurity mode. In this case, there is a linear relationship between the squares of the kink initial velocity V_i and its final velocity V_f: $V_f^2 = \alpha(V_i^2 - V_c^2)$, $\alpha \approx 0.887$ being constant. If the incoming velocity of the kink is smaller than V_c, the kink cannot escape to infinity from the impurity after the first collision, but will stop at a certain distance and return back (due to the attracting force of the impurity) to interact with the impurity again. For most of the velocities, the kink will lose energy again in the second interaction and finally it gets trapped by the impurity. However, for some special incoming velocities, the kink may escape to the direction *opposite* to the incident one after the second collision, i.e., the kink may be totally *reflected* by the impurity. The reflection is possible only if the kink initial velocity is taken from certain resonance windows. By numerical simulation, Kivshar et al. (1991a) have found a number of such windows. Using the idea of the resonant energy exchange between the kink translational mode and the impurity mode, it is possible to analytically predict the positions of the resonance windows (Kivshar et al., 1991),

$$V_n^2 = V_c^2 - \frac{11.0153}{(nT_{im} + 0.3)^2}, \quad n = 2, 3, \dots , \tag{7.34}$$

where T_{im} is the period of the impurity mode oscillation, and V_c is the critical velocity. This formula has been shown to provide a very good prediction [see the corresponding data in the table presented by Kivshar et al. (1991)].

Let us give a brief explanation of the resonance structures in the kink–impurity interactions. The main point is the observation that the nonlinear system (7.4) supports a localized mode. By linearizing Eq. (7.4) in small u, the shape of the impurity mode can be found analytically to be

$$u_{im}(x, t) = a(t)e^{-\varepsilon|x|/2} , \tag{7.35}$$

where $a(t) = a_0 \cos(\Omega t + \theta_0)$, Ω is the frequency of the impurity mode,

$$\Omega = \sqrt{1 - \varepsilon^2/4} , \tag{7.36}$$

and θ_0 is an initial phase. As a matter of fact, the impurity mode (7.35) can be considered as a small-amplitude oscillating mode trapped by the impurity, with energy $E_{im} = \Omega^2 a_0^2/\varepsilon$.

Now we may analyze the kink–impurity interactions through the collective-coordinate method taking into account two dynamical variables, namely the kink coordinate $X(t)$ and the amplitude of the impurity mode oscillation $a(t)$ [see Eq. (7.35)]. Substituting the ansatz

$$u = u_k + u_{im} = 4 \tan^{-1} e^{[x - X(t)]} + a(t)e^{-\varepsilon|x|/2} \tag{7.37}$$

into the Lagrangian of the system, and assuming that a and ε are small enough so that the higher-order terms can be neglected, it is possible to derive the following (reduced) effective

Lagrangian

$$L_{\text{eff}} = \frac{1}{2}m\left(\frac{\mathrm{d}X}{\mathrm{d}t}\right)^2 + \frac{1}{\varepsilon}\left[\left(\frac{\mathrm{d}a}{\mathrm{d}t}\right)^2 - \Omega^2 a^2\right] - U(X) - aF(X)\,, \tag{7.38}$$

where $U(X)$ is given by Eq. (7.33), and $F(X) = -2\varepsilon \tanh X \operatorname{sech} X$. The equations of motion for the two dynamical variables become

$$m\frac{\mathrm{d}^2X}{\mathrm{d}t^2} + U'(X) + aF'(X) = 0, \qquad \frac{\mathrm{d}^2a}{\mathrm{d}t^2} + \Omega^2 a + \frac{\varepsilon}{2}F(X) = 0\,. \tag{7.39}$$

System (7.39) describes a particle (kink) with coordinate $X(t)$ and effective mass m placed in an attractive potential $U(X)$ ($\varepsilon > 0$), and "weakly" coupled with a harmonic oscillator $a(t)$ (the impurity mode). Here we say "weakly" because the coupling term $aF(X)$ is of order $O(\varepsilon)$ and it falls off exponentially. The system (7.39) is a generalization of the well-known equation

$$m_k\frac{\mathrm{d}^2X}{\mathrm{d}t^2} = -U'(X)$$

describing the kink–impurity interactions in the adiabatic approximation.

The dynamical system (7.39) can describe all features of the kink–impurity interactions. First, it may be used to calculate the threshold velocity of kink capture, which is given by the equation (Zhang et al., 1992a, b),

$$V_{\text{thr}} = \frac{\pi\varepsilon}{\sqrt{2}}\frac{\sinh[\Omega Z(V_{\text{thr}})/2V_{\text{thr}}]}{\cosh(\Omega\pi/2V_{\text{thr}})}\,, \tag{7.40}$$

where $Z(V) = \cos^{-1}[(2V^2 - \varepsilon)/(2V^2 + \varepsilon)]$. Comparing the analytical results with the direct numerical simulations of Eq. (7.4), Zhang et al. (1991a) found that the perturbation theory is valid only for very small ε ($\varepsilon \leq 0.05$), while formula (7.40) gives good estimations of $V_{\text{thr}}(\varepsilon)$ for ε over the region $(0.2, 0.7)$.

As was pointed out by Kivshar et al. (1991) and Zhang et al. (1992a), Eq. (7.39) can be used as a qualitative model to explain the mechanism of resonant energy exchange between the classical particle and the oscillator. The resonant reflection of the particle by the potential well corresponds to the reflection of the kink by an attractive impurity. Therefore, the collective-coordinate approach can give a qualitative explanation of the resonance effects in the kink–impurity interactions. At the same time, the collective-coordinate model (7.39) is conservative, so that it cannot explain the inelastic effects such as the subsequent kink trapping by the impurity. Such effects are possible to be explained only by introducing other degrees of freedom of the system, for example, an effective coupling to phonons or another subsystem (Malomed et al., 1993).

It is important to note that similar resonance phenomena have been observed in the kink–impurity interactions in the ϕ^4 model (Zhang et al., 1992b; Belova and Kudryavtsev, 1995). However, the resonant structures in the ϕ^4 kink–impurity interactions are more complicated than in the SG model because the ϕ^4 kink has an internal (shape) mode which also can be considered as an effective oscillator. Zhang et al. (1992b) have developed a collective-coordinate approach taking into account three dynamical variables, and they have found that due to the joint effect of the impurity and the kink internal mode oscillation, some resonance windows may disappear.

The resonant interactions described above have been analyzed numerically and analytically for a single impurity, and we can say that the physical mechanism of this effect has been well understood. It is clear that in the case of several impurities the well-defined energy-exchange process will be more difficult to observe (for the case of two impurities, see Zhang et al., 1994). However, increasing the number of impurities, it is likely to expect that the fine structure of resonances will be destroyed, especially for the case of a random lattice. However, the possibility of exciting impurity modes during the kink propagation will lead to an additional and, as we have seen for a single impurity, an efficient source of the energy loss during the kink propagation. So, a possible mechanism of the kink damping in disordered media is the excitation of localized mode vibrations due to impurities but not radiation of small-amplitude waves. This mechanism was mentioned in the earlier paper by Tsurui (1973) who discussed the soliton propagation in a nonlinear lattice with isotopic disorder [see also the paper by Malomed (1992) for the case of the ϕ^4 kink].

When a discrete breather (or nonlinear localized mode) interacts with an impurity, the resonant effects similar to those described above can be observed (Forinash et al., 1994). In particular, due to an overlapping of the breather and impurity mode frequencies, a local change of only 5–10% of the particular mass is already sufficient to trap the breather in a lattice. Forinash et al. (1994) also observed that the lattice discreteness enforce a stronger interaction between the localized breather mode and impurity mode, although they were not able to describe this effect quantitatively within the collective coordinate approach because the form of a breather moving in a discrete lattice is not known even numerically. A number of interesting effects was described by Forinash et al. (1994) for the case of the interaction of breather with an excited impurity. In particular, they noticed that the disorder associated with impurities can act as a catalyst for nonlinear energy localization because it can cause the fusion of two nonlinear excitations into a single larger one.

8. Concluding remarks

To conclude this brief presentation of the nonlinear dynamics of the FK model and its physically important generalizations, it is fitting to mention some other examples of physical systems where the fundamental concepts and results based on the FK model and the analysis of its nonlinear excitations such as kinks and breathers are effectively applied. It would be relevant to mention also possible generalizations of the one-dimensional model to describe more realistic physical situations as well as to apply this model to certain physical objects such as arrays of Josephson junctions, hydrogen-bonded chains, adsorbed atomic layers, etc.

Josephson junctions arrays. As has been already pointed out in the Introduction, the FK model appears in many models of solid state physics describing nonlinear wave phenomena of different physical nature. Among the many systems already mentioned in Introduction, one of the closest correspondence to the pure SG dynamics was found for flux quanta in long quasi-one-dimensional Josephson junctions (JJs) (see, e.g., McLaughlin and Scott, 1978; Pedersen, 1986). The FK model itself does appear in the theory of long JJs when one considers the flux flow in *discrete parallel arrays* of weak links based on low-T_c superconductors (see, e.g., Hontsu and Ishii, 1988) or high-T_c (see, e.g., Hohenwarter et al., 1989). As a matter of fact, the physical model for a discrete array of JJs can be reduced to the same FK chain as has been discussed above, and it displays a number of

peculiarities caused by discreteness which are naturally absent in the continuum model (see, e.g., Ustinov et al., 1993; where the influence of the discreteness effects on the current–voltage characteristics of an array of JJs has been analysed). It is important to mention the recent experiments on the JJ arrays which reported the first measurements of the discreteness effects (van der Zant et al., 1995; Watanabe et al., 1995).

One more interesting (but very unusual) example how the FK model appears in the theory of continuous media is the JJ lattices with inhomogeneities, the latter arise due to a spatially periodic modulation of the critical current density. In the simplest case, the model is described by the SG equation (7.4) with the inhomogeneity of the form,

$$f(x) = 1 + \varepsilon \sum_n \delta(x - na) \,, \tag{8.1}$$

a being the spacing between the impurities. The impurity lattice introduced in this way, gives rise to novel effects, e.g. *superkink* resonances (Ustinov, 1989). To explain briefly the physics of such a phenomenon as the superkink propagation, let us consider a periodic array of kinks interacting with the periodic lattice of delta-like impurities introduced by Eq. (8.1). In the case when the array as a whole remains in a pinned state, it may support propagation of particle-like (or hole-like) defects moving along the pinned chain of kinks. Such defects are called *superkinks*, because they are kink-like excitations of the chain of the primary SG kinks. The superkinks were discovered by Ustinov (1989) in numerical simulations for an annual JJ with a regular lattice of point-like inhomogeneities, and their existence and excitation were experimentally observed as new resonant modes of long JJs (Oboznov and Ustinov, 1989; Vernik et al., 1992). A theoretical model for the superkink propagation was developed by Malomed (1990) who showed that for the collective coordinate of the kink chain with the average spatial period $L = 2kK(k)$, where k $(0 < k < 1)$ is the modulus of a Jacobi elliptic function, the following (effective) equation of motion can be derived,

$$\xi_{tt} - \xi_{xx} + \frac{4\varepsilon}{a\rho k} \mathrm{sn}(\xi/k)\mathrm{cn}(\xi/k)\,\mathrm{dn}(\xi/k) = 0 \,, \tag{8.2}$$

where the standard Jacobi elliptic functions are used, and ρ stands for the "density" of the kink chain. Eq. (8.2) was shown to have a kink solution with the boundary condition $\xi(+\infty) - \xi(-\infty) = 2kK(k) \equiv L$ (Malomed, 1990) which gives, in fact, a nontrivial generalization of the standard SG kink to the case of the elliptic SG equation (8.2). As a matter of fact, Eq. (8.2) is derived as a continuum limit of the discrete motion equations for the kinks' coordinates, so that in such a case the generalized *discrete* elliptic FK model appears from the theory of periodic continuous systems.

Hydrogen-bonded chains. Another interesting version of the FK model arises in the theory of proton transport of hydrogen-bonded chains. These systems are known to consist of two different types of atoms, light hydrogen atoms and heavy oxygen atoms. In the lowest-order approximation the oxygen atoms are assumed to have almost fixed positions producing an effective substrate potential to the mobile hydrogen atoms, for which a kind of the FK model can be derived. The mechanism of the proton conductivity is based on a migration transport of the so-called ionic and bonding (Bjerrum) defects along the hydrogen-bonded chain, the defects

are nothing but *two types of kinks* of the corresponding generalized FK model with the double-barrier substrate potential. This kind of *one-component* model for hydrogen-bonded systems is rather well investigated in the framework of the continuum approximation (see, e.g., Zolotaryuk and Pnevmatikos, 1990; Pnevmatikos et al., 1991; and references therein). In the same time, some recent ideas in the theory of kink-induced proton conductivity involve more general properties of the FK type models like discreteness of the proton chains and thermalized kink motion (Savin and Zolotaryuk, 1991), the effect of the increased proton conductivity due to commensurability–incommensurability phase transitions (Christophorov and Gaididei, 1992), complex chain with a zigzag structure (Christiansen et al., 1997), mass variation along the chain (Kalosakas et al., 1997), etc.

More rigorously, the dynamics of the systems such as hydrogen-bonded chains may be properly described by introducing *two interacting sublattices* for proton and oxygen atoms, respectively. In such a case, we should consider "two-component" generalizations of the FK model which describe two interacting chains of particles, one is subjected into a substrate potential created by the second chain. Several models of this type have been introduced and studied in the continuum limit approximation (see, e.g., Antonchenko et al., 1983; Zolotaryuk et al., 1984; Zolotaryuk, 1986; Hochstrasser et al., 1988; Pnevmatikos, 1988). The dynamics of the two-component models has several new features in comparison with the standard one-component models, for example, a new branch of the phonon spectrum appears in the gap of the linear spectrum band of the standard FK chain, so that the motion of kinks is stable only for small velocities which do not exceed the sound speed of acoustic phonons of the oxygen sublattice (see, e.g., Zolotaryuk et al., 1984). As a matter of fact, this second (acoustic or optical) branch plays an important role in the kink scattering by local impurities as well (Kivshar, 1991a).

The two-component FK model describes more realistically the dynamics of some other physical objects such as crowdions, adatomic chains, chains of ions in superionic conductors, etc. In all such situations the second (heavy atoms) subsystem corresponds to substrate atoms, so that the whole system may be treated again as a FK chain on a deformable substrate. Similar situation appears for the physical models of molecular crystals and polymer chains as well as ferroelectric or ferroelastic chains where rotational and vibrational degrees of freedom are coupled together (see, e.g., Remoissenet, 1981; Pouget and Maugin, 1984, 1985; Maugin and Miled, 1986; Sayadi and Pouget, 1991; to site a few).

Incommensurable chains. One more class of the problems strongly related to the FK model is the chain dynamics in the case of an incommensurate ground state. Namely, in the present survey we have described the nonlinear dynamics of the FK type model considering excitations of the trivial ground state of the chain when the chain has a fixed density of atoms (owing to fixed or periodic boundary conditions) with the coverage parameter $\theta = 1$ for which the mean interatomic distance coincides with the period of the substrate potential. If, however, we consider the free-end boundary conditions and assume that the equilibrium distance introduced by the interatomic interaction potential does not coincide with the substrate period a_s, then we naturally come to one of the simplest physical models with two (or more, if one treats a nonconvex interatomic potentials) competing lengths. The richness of the FK model (and a variety of the corresponding physical problems) drastically increases in this case due to a possibility of two distinct types of the system ground state, commensurate and incommensurate ones, the latter exhibits also such a remarkable phenomena such as the Aubry transition of analyticity breaking

(see, e.g., Bak, 1982; Aubry, 1983). Besides, the FK chain may be subjected to a thermostat at nonzero temperature that naturally leads to a series of physical problems such as the analysis of thermodynamic properties at an equilibrium state (see, e.g., Schneider, 1986; Tsuzuki and Sasaki, 1988; Griffits, 1990), the mass or charge transport along the FK chain (e.g., Gillan and Holloway, 1985), the kink–antikink nucleation, and the dynamics of the FK chain in the presence of external DC or AC fields, etc.

Weakly interacting chains. In fact, one of the important restrictions of the standard FK model is the one-dimensional nature of the chain dynamics. In many physical situations the one-dimensional approximation is rather good. However, usually quasi-one-dimensional chains of atoms do not exist as completely independent, forming a system of parallel chains. For example, a typical situation when atoms are adsorbed on stepped or furrowed surfaces of a crystal can be described as a two-dimensional system of weakly coupled one-dimensional FK chains. Considering kinks of the primary FK chains as quasiparticles subjected to a periodic PN potential, we may analyse collective excitations of such two-dimensional systems. In fact, excitations of the two-dimensional model may be treated as "secondary" kinks which can be again described by a variant of the "super FK model". A system of interacting FK chains was analysed, for example, by Braun et al. (1988) and Braun and Kivshar (1990), and there exist also many papers devoted to the statistical mechanics of adsorbed layers (see, e.g., the book by Lyuksyutov et al., 1988, and references therein).

Two-dimensional lattices. One of the ways to make the FK model more realistic for a broader class of physical applications is to include an additional degree of freedom allowing the atoms to move in the direction perpendicular to the chain. The corresponding FK model with a transverse degree of freedom was proposed by Braun and Kivshar (1991b). Interesting physical effects are possible in this type of models due to the existence of nontrivial zigzag-like ground states and, correspondingly, novel types of topological kink-like excitations. In some sense, this situation is analogous to the case of the FK model with a nonconvex interatomic potential.

More general models describing the particle dynamics in two-dimensional systems correspond to *a vector generalization* of the FK model, which is the most realistic model for two-dimensional arrays of atoms adsorbed on crystal surfaces: each atom has two degrees of freedom to move and it is subjected to a two-dimensional external potential created by atoms of the surface. In fact, a variety of such models is generated by symmetry properties of various substrate potentials (isotropic models with square, triangular, hexagonal lattices or anisotropic models with, e.g., rectangular lattice, etc.). As several examples of these models, we would like to mention here those introduced by van der Merwe (1970), Snyman and van der Merwe (1974), Snyman and Snyman (1981), Abraham et al. (1984), Lomdahl and Srolovitz (1986).

Additionally, the structure and stability of nonlinear localized excitations in two-dimensional lattice is an interesting topic of current research (Fischer, 1993; Pouget et al., 1993) in order to understand the mechanism of the energy localization in discrete lattices.

Forced dynamics. We would like to point out again that in the present review paper we did not discuss a rather wide class of problems related to the effects of external (impulsive, DC, or AC) fields on the dynamics of the FK chain. Such kind of effects is very important from the physical point of view for both one-component and two-component modes, and there exist many corresponding studies for the continuum limit of the FK model, the perturbed SG equation. A number of novel

physical effects which appear in this model when external AC or DC forces are applied is indeed large enough to be reviewed in such a short survey paper. In particular, we mention here the breather stabilization by a direct (Lomdahl and Samuelsen, 1986, 1988) or parametric (Grønbech-Jensen et al., 1991) forces, complicated nonlinear dynamics which includes period-doubling, spatial-temporal complexity, and chaos (see, e.g., Bishop et al., 1983, 1986; Mazor et al., 1986; Mazor and Bishop, 1987; Taki et al., 1989; Grauer and Birnir, 1992, to cite a few), and so on. Similar effects can be found also for discrete chains but they have been not investigated in detail yet. The discreteness itself may give rise to novel features not existing in the continuous SG equation.

The overdamped discrete FK chain driven by an AC force has been recently investigated analytically and numerically (see, e.g., a recent review paper by Mazo and Floria, 1996; and references therein). Besides, in view of possible applications of the FK model to the problems of tribology, a number of papers which appear recently has been devoted to the FK model with dissipation (as well as its generalization known as the FK–Tomlinson model) driven by a DC force (e.g., Weiss and Elmer, 1996, 1997; Braun et al., 1997b,c).

Nonlinear localized modes. At last but not least, during recent years an exponentially growing activity was directed towards understanding the properties of localized modes in discrete lattices with on-site and intersite potentials. In this survey paper we just touched this topic in Section 6. A number of results, including a rigorous proof of the existence and stability, has appeared in the literature which are beyond the scope of our original idea about this work. We would like to mention the most recent review papers by Aubry (1997) and Flach and Willis (1998) where a summary of the recent progress in the theory of nonlinear localized modes (also called *discrete breathers*) is presented.

In conclusion, we believe the understanding of the specific and unusual properties on nonlinear models introduced by discreteness is an active and attractive topic of the current research. Since realistic physical models of solids are rather complicated, it is extremely important to develop the basic concepts with the help of simple physical models such as the FK model.

Acknowledgements

It is a great pleasure for us to thank all the people with whom we have discussed and worked on this subject during the last few years. We would like to name especially Alan Bishop, Thierry Dauxois, Nikos Flytzanis, Alexander Kovalev, Arnold Kosevich, Boris Malomed, Anton Naumovets, Michel Peyrard, Alfred Seeger, Theo Valkering, Chuck Willis, and also our former students Angel Sánchez, Zhang Fei, Irina Zelenskaya, and Oksana Chubykalo.

We are deeply indebted to David Campbell for his continuous and stimulating interest to this topic which encouraged and helped us to complete this work which we actually began a long time ago. We also thank all our colleagues for their permission to use figures from their original papers.

During the long course of the work on this review, Yuri Kivshar was supported by the Institut für Theoretische Physik I and the Alexander-von-Humbold-Stiftung (Germany), and the Australian National University (Australia). Oleg Braun acknowledges the support from the Soros Foundation and the hospitality of the University of Twente (The Netherlands) and Optical Sciences Centre of the Australian National University (Australia).

References

Ablowitz, M.J., Kaup, D., Newell, A.C., Segur, H., 1973. Phys. Rev. Lett. 30, 1262.
Ablowitz, M.J., Ladik, J.F., 1976. J. Math. Phys. 17, 1011.
Abraham, F.F., Rudge, W.E., Auerbach, D.J., Koch, S.W., 1984. Phys. Rev. Lett. 52, 445.
Aliev, Yu.M., Ovchinnikov, K.N., Silin, V.P., Uryupin, S.A., 1995. Zh. Eksp. Teor. Fiz. 107, 972 [JETP 80, 551 (1995)].
Anninos, P., Oliveira, S., Matzner, R.A., 1991. Phys. Rev. D 44, 1147.
Antonchenko, V.Ya., Davydov, A.S., Zolotaryuk, A.V., 1983. Phys. Stat. Sol. (b) 115, 631.
Alfimov, G.L., 1996. In: Vázquez, L., Streit, L., Pérez-Garcia, V.M. (Eds.), Nonlinear Klein–Gordon and Schrödinger Systems: Theory and Applications. World Scientific, Singapore, p. 257.
Alfimov, G.L., Eleonsky, V.M., Kulagin, N.E., Mitzkevich, N.V., 1993. Chaos 3, 405.
Al'shitz, V.I., 1969. Fiz. Tverd. Tela 11, 2405 [Sov. Phys-Solid State 11, 1947 (1970)].
Al'shitz, V.I., Indenbom, V.L., Shtol'berg, A.A., 1971. Zh. Eksp. Teor. Fiz. 60, 2308 [Sov. Phys. JETP 33, 1240 (1971)].
Atkinson, W., Cabrera, N., 1965. Phys. Rev. 138, A763.
Aubry, S., 1983. Physica D 7, 240.
Aubry, S., 1994. Physica D 71, 196.
Aubry, S., 1997. Physica D 103, 201.
Baeriswyl, D., Bishop, A.R., 1980. J. Phys. C 13, 1403.
Bak, P., 1982. Rep. Progr. Phys. 45, 587.
Baker, G.A., 1961. Phys. Rev. 122, 1477.
Bäcklund, A.V., 1882. Om ytor med konstant negative krökning. In: Lunds Universitets Ars-skrift XIX, IV, p. 1.
Bang, O., Rasmussen, J.J., Christiansen, P.L., 1993. Physica D 68, 169.
Bang, O., Rasmussen, J.J., Christiansen, P.L., 1994. Nonlinearity 7, 205.
Bang, O., Peyrard, M., 1995. Physica D 81, 9.
Bang, O., Peyrard, M., 1996. Phys. Rev. E 53, 4143.
Barsch, G.R., Krumhansl, J.A., 1984. Phys. Rev. Lett. 53, 1069.
Barsch, G.R., Horovitz, B., Krumhansl, J.A., 1987. Phys. Rev. Lett. 59, 1251.
Bar'yakhtar, V.G., Ivanov, B.A., Sukstanskii, A.L., Tartakovskaya, E.V., 1988. Teor. Mat. Fiz. 74, 46.
Bass, F.G., Kivshar, Yu.S., Konotop, V.V., Sinitsyn, Yu.A., 1988. Phys. Rep. 157, 63.
Belova, T.I., Kudryavtsev, A.E., 1995. Zh. Eksp. Teor. Fiz. 108, 1489 [JETP 81, 817 (1995)].
Belova, T.I., Kudryavtsev, A.E., 1997. Sov. Phys. Usp. 40, 359.
Becker, R., 1951. J. Phys. Radium 12, 332.
Benjamin, T.B., Feir, J.E., 1967. J. Fluid. Mech. 27, 417.
Bergman, D.J., Ben-Jacob, E., Imry, Y., Maki, K., 1983. Phys. Rev. A 27, 3345.
Bespalov, V.I., Talanov, V.I., 1966. Pis'ma Zh. Eksp. Teor. Fiz. 3, 471 [JETP Lett. 3, 307 (1966)].
Bickham, S.R., Sievers, A.J., 1991. Phys. Rev. B 43, 2339.
Bickham, S.R., Sievers, A.J., Takeno, S., 1992. Phys. Rev. B 45, 10 344.
Biller, P., Petruccione, F., 1990. Phys. Rev. B 41, 2139, 2145.
Birnir, B., 1994. Comm. Pure Appl. Math. 157, 103.
Bishop, A.R., 1978. J. Phys. C 11, L329.
Bishop, A.R., Lewis, W.F., 1979. J. Phys. C 12, 3811.
Bishop, A.R., Fesser, K., Lomdahl, P.S., Trullinger, S.E., 1983. Physica D 7, 259.
Bishop, A.R., Forest, M., McLaughlin, D.W., Overman-II, E.A., 1986. Physica D 23, 293.
Boardman, A.D., Bortolani, V., Willis, R.F., Xie, K., Mehta, H.M., 1995. Phys. Rev. B 52, 12736.
Boesch, R., Willis, C.R., 1989. Phys. Rev. B 39, 361.
Boesch, R., Peyrard, M., 1991. Phys. Rev. B 43, 8491.
Boesch, R., Stancioff, P., Willis, C.R., 1988. Phys. Rev. B 38, 6713.
Boesch, R., Willis, C.R., El-Batanouny, M., 1989. Phys. Rev. B 40, 2284.
Bogdan, M.M., Kovalev, A.S., Gerasimchuk, I.V., 1997. Fiz. Nizk. Temp. 23, 197 [Low Temp. Phys. 23, 145 (1997)].

Bolshov, L.A., Napartovich, A.P., Naumovets, A.G., Fedorus, A.G., 1977. Usp. Fiz. Nauk 122, 125 [Sov. Phys.- Usp. 20, 412 (1977)].
Bortolani, V., Franchini, A., Willis, R.F., 1997. Phys. Rev. B 56, 8047.
Bourbonnais, R., Maynard, R., 1990a. Phys. Rev. Lett. 64, 1397.
Bourbonnais, R., Maynard, R., 1990b. Int. J. Mod. Phys. 1, 233.
Boyce, J.B., Huberman, B.A., 1979. Phys. Rep. 51, 189.
Braun, O.M., 1981. Fiz. Tverd. Tela 23, 2779 [Sov. Phys.- Solid State 23, 1626 (1981)].
Braun, O.M., 1989. Surface Sci. 213, 336.
Braun, O.M., 1990. Surface Sci. 230, 262.
Braun, O.M., Kivshar, Yu.S., Kosevich, A.M., 1988. J. Phys. C 21, 3881.
Braun, O.M., Kivshar, Yu.S., 1990. J. Phys.: Condens. Matter 2, 5961.
Braun, O.M., Kivshar, Yu.S., Zelenskaya, I.I., 1990. Phys. Rev. B 41, 7118.
Braun, O.M., Kivshar, Yu.S., 1991a. Phys. Rev. B 43, 1060.
Braun, O.M., Kivshar, Yu.S., 1991b. Phys. Rev. B 44, 7694.
Braun, O.M., Medvedev, V.K., 1989. Usp. Fiz. Nauk 157, 631 [Sov. Phys.- Usp. 32, 328 (1989)].
Braun, O.M., Zhang, F., Kivshar, Yu.S., Vázquez, L., 1991. Phys. Lett. A 157, 241.
Braun, O.M., Kivshar, Yu.S., Peyrard, M., 1997a. Phys. Rev. E 56, 6050.
Braun, O.M., Dauxois, T., Paliy, M.V., Peyrard, M., 1997b. Phys. Rev. Lett. 78, 1295.
Braun, O.M., Bishop, A.R., Röder, J., 1997c. Phys. Rev. Lett. 79, 3692.
Bruce, D.A., 1981. J. Phys. C 14, 5195.
Burdick, S., Willis, C.R., El-Batanouny, M., 1987. Phys. Rev. B 36, 6920.
Burlakov, V.M., Kiselev, S.A., Pyrkov, V.N., 1990a. Solid State Commun. 74, 327.
Burlakov, V.M., Kiselev, S.A., Pyrkov, V.N., 1990b. Phys. Rev. B 42, 4921.
Büttiker, M., Landauer, R., 1980. J. Phys. C 13, L325.
Byrne, J.E., Miller, M.D., 1989. Phys. Rev. B 39, 374.
Cai, D., Bishop, A.R., Grønbech-Jensen, N., 1994. Phys. Rev. Lett. 72, 591.
Campbell, D.K., Schonfeld, J.F., Wingate, C.A., 1983. Physica D 9, 1.
Campbell, D.K., Peyrard, M., Sodano, P., 1986. Physica D 19, 165.
Carr, J., Eilbeck, J.C., 1985. Phys. Lett. A 109, 201.
Celli, V., Flytzanis, N., 1970. J. Appl. Phys. 41, 4443.
Christiansen, P.L., Savin, A.V., Zolotaryuk, A.V., 1997. J. Comput. Phys. 134, 108.
Christiansen, P.L., Savin, A.V., Zolotaryuk, A.V., 1998. Phys. Rev. B 57, 13564.
Christophorov, L.N., Gaididei, Yu.B., 1992. Phys. Lett. A 167, 367.
Claude, Ch., Kivshar, Yu.S., Kluth, O., Spatschek, K.H., 1993. Phys. Rev. B 47, 14 228.
Combs, J.A., Yip, S., 1983. Phys. Rev. B 28, 6873.
Combs, J.A., Yip, S., 1984. Phys. Rev. B 29, 438.
Condat, C.A., Guyer, R.A., Miller, M.D., 1983. Phys. Rev. B 27, 474.
Cowley, R.A., Axe, J.D., Iizumi, M., 1976. Phys. Rev. Lett. 36, 806.
Croitoru, M., 1989. J. Phys. A 22, 845.
Currie, J.F., Trullinger, S.E., Bishop, A.R., Krumhansl, J.A., 1977. Phys. Rev. B 15, 5567.
Daumont, I., Dauxois, T., Peyrard, M., 1997. Nonlinearity 10, 617.
Dauxois, T., Peyrard, M., 1993. Phys. Rev. Lett. 70, 3935.
Dauxois, T., Peyrard, M., Willis, C.R., 1992. Physica D 57, 267.
Dauxois, T., Peyrard, M., Bishop, A.R., 1993a. Phys. Rev. E 47, 684.
Dauxois, T., Peyrard, M., Willis, C.R., 1993b. Phys. Rev. E 48, 4768.
Dehlinger, U., 1929. Ann. Phys. Lpz. 2, 749.
De Lillo, S., 1987. Nuovo Cimento B 100, 105.
Denardo, B., Galvin, B., Greenfield, A., Larraza, A., Putterman, S., Wright, W., 1992. Phys. Rev. Lett. 68, 1730.
Denzler, J., 1993. Commun. Math. Phys. 158, 397.
Dieterich, W., Fulde, P., Peschel, I., 1980. Adv. Phys. 29, 527.
Dolgov, A.S., 1986. Sov. Phys. Solid State 28, 907.

Döring, W., 1948. Z. Naturf. 3a, 373.
Döttling, R., Esslinger, J., Lay, W., Seeger, A., 1990. in: Barthes, M., Léon, J. (Eds.), Nonlinear Coherent Structures, Lecture Notes in Physics, vol. 353. Springer, Berlin, p. 193.
Eilbeck, J.C., Lomdahl, P.S., Scott, A.C., 1985. Physica D 16, 318.
Einstein, T.L., 1978. CRC Crit. Rev. Solid State Mater. Sci. 7, 261.
Englander, S.W., Kallenback, N., Heeger, A., Krumhansl, J.A., Litwin, S., 1980. Proc. Nat. Acad. Sci. 77, 7222.
Enneper, A., 1870. Über asymptotische Linien. In: Nachr. Königl. Gesellsch. d. Wiss. Göttingen, p. 493.
Enz, U., 1964. Helv. Phys. Acta 37, 245.
Erofeev, V.N., Nikitenko, V.I., 1971. Fiz. Tverd. Tela 13, 146 [Sov. Phys.-Solid State 13, 116 (1971)].
Fernandez, J.C., Goupil, M.J., Legrand, O., Reinish, G., 1986. Phys. Rev. B 34, 6207.
Fesser, K., 1980. Z. Physik B 39, 47.
Fischer, F., 1993. Ann. Physik 2, 296.
Flach, S., Willis, C.R., 1992. Phys. Lett. A 181, 232.
Flach, S., Willis, C.R., 1993. Phys. Rev. E 47, 4447.
Flach, S., Willis, C.R., 1994. Phys. Rev. Lett. 72, 1777.
Flach, S., Kladko, K., 1996. Phys. Rev. E 54, 2912.
Flach, S., Willis, C.R., Olbrich, E., 1994. Phys. Rev. E 49, 836.
Flach, S., Willis, C.R., 1998. Phys. Rep. 295, 181.
Floria, L.M., Mazo, J.J., 1996. Adv. Phys. 45, 505.
Flytzanis, N., Crowley, S., Celli, V., 1977. Phys. Rev. Lett. 39, 891.
Fogel, M.B., Trullinger, S.E., Bishop, A.R., Krumhansl, J.A., 1976. Phys. Rev. Lett. 36, 1411.
Fogel, M.B., Trullinger, S.E., Bishop, A.R., Krumhansl, J.A., 1977. Phys. Rev. B 15, 1578.
Forinash, K., Peyrard, M., Malomed, B., 1994. Phys. Rev. E 49, 3400.
Forinash, K., Cretegny, T., Peyrard, M., 1997. Phys. Rev. E 55, 4740.
Fraggis, T., Pnevmatikos, St., Economou, E.N., 1989. Phys. Lett. A 142, 361.
Frank, F.C., van der Merwe, J.H., 1949a. Proc. Roy. Soc. (London) A 198, 205, 216.
Frank, F.C., van der Merwe, J.H., 1949b. Proc. Roy. Soc. (London) A 200, 125.
Franzosi, P., Salviati, G., Seaffardi, M., Genova, F., Pellegrino, S., Stano, A., 1988. J. Crystal Growth, 88, 135.
Frenkel, Ya., Kontorova, T., 1938. Phys. Z. Sowietunion 13, 1.
Frenkel, Ya., Kontorova, T., 1939. Fiz. Zh. (Moscow) 1, 137 (in Russian).
Frenkel, Ya.I., 1972. Introduction into the Theory of Metals. Nauka, Leningrad (in Russian).
Furuya, K., Ozorio de Almeida, A.M., 1987. J. Phys. A 20, 6211.
Gaeta, G., Reiss, C., Peyrard, M., Dauxois, T., 1994. Rivista Nuovo Cim. 17, 1.
Galpern, Yu., Filippov, A., 1984. Zh. Eksp. Teor. Fiz. 86, 1527 [Sov. Phys. JETP 59, 894 (1984)].
Gardner, C.S., Greene, J.M., Kruskal, M.D., Miura, R.M., 1967. Phys. Rev. Lett. 19, 1095.
Geike, J., 1994. Phys. Rev. E 49, 3539.
Giachetti, R., Sodano, P., Sorace, E., Tognetti, V., 1984. Phys. Rev. B 30, 4014.
Gillan, M.J., 1985. J. Phys. C 18, 4885.
Gillan, M.J., Holloway, R.W., 1985. J. Phys. C 18, 4903.
González, J.A., Martń-Landrove, M., 1994. Phys. Lett. A 191, 409.
Gordon, M.B., Villain, J., 1979. J. Phys. C 12, L151.
Grauer, R., Birnir, B., 1992. Physica D 56, 165.
Gredeskul, S.A., Kivshar, Yu.S., Maslov, L.M., Sánchez, A., Vázquez, L., 1992. Phys. Rev. A 45, 8867.
Gredeskul, S.A., Kivshar, Yu.S., 1992. Phys. Rep. 216, 1.
Griffits, R.B., Chou, W., 1986. Phys. Rev. Lett. 56, 1929.
Griffits, R.B., 1990. In: van Beijeren, H. (Ed.), Fundamental Problems in Statistical Mechanics – VII. Elsevier, Amsterdam.
Grønbech-Jensen, N., Kivshar, Yu.S., Samuelsen, M.R., 1991. Phys. Rev. B 43, 5698.
Gupta, B.C., Kundu, K., 1997. Phys. Lett. A 235, 176.
Haas, C., 1978. Solid State Commun. 26, 709.
Haldane, F.D.M., Villain, J., 1981. J. Physique (Paris) 42, 1673.

Haken, H., 1980. Synergetics. Springer, Berlin.
Harten, U., Lahee, A.M., Toennies, J.P., Wöll, Ch., 1985. Phys. Rev. Lett. 54, 2619.
Hasegawa, A., 1970. Phys. Rev. Lett. 24, 1165.
Haus, J.W., Kehr, K.W., 1987. Phys. Rep. 150, 263.
Hennig, D., Tsironis, G.P., 1999. Phys. Rep., in press.
Hobart, R., Celli, V., 1962. J. Appl. Phys. 33, 60.
Hobart, R., 1965a. J. Appl. Phys. 36, 1944.
Hobart, R., 1965b. J. Appl. Phys. 36, 1948.
Hobart, R., 1966. J. Appl. Phys. 37, 3573.
Hochstrasser, D., Bütner, H., Desfontaines, H., Peyrard, M., 1988. Phys. Rev. A 36, 5332.
Hohenwarter, G.K.G., Martens, J.S., McGinnis, D.P., Beyer, J.B., Nordman, J.E., Ginley, D.S., 1989. IEEE Trans. Magn. 25, 954.
Homma, S., Takeno, S., 1984. Progr. Theor. Phys. 72, 679.
Hontsu, S., Ishii, J., 1988. J. Appl. Phys. 63, 2021.
Hori, K., Takeno, S., 1992. J. Phys. Soc. Japan 61, 4263.
Hsu, Y., 1980. Phys. Rev. D 22, 1394.
Huang, G., Shen, J., Quan, H., 1993. Phys. Rev. B 48, 16795.
Igarashi, A., Munakata, T., 1989. J. Phys. Soc. Japan 58, 4025.
Indenbom, V.L., 1958. Sov. Phys.-Cryst. 3, 197.
Indenbom, V.L., Orlov, A.N., 1962. Sov. Phys.-Usp. 5, 272.
Ishibashi, Y., Suzuki, I., 1984. J. Phys. Soc. Japan 53, 4250.
Ishioka, S., 1973. J. Phys. Soc. Japan 34, 462.
Ishioka, S., 1974. J. Phys. Soc. Japan 36, 187.
Ishimori, Y., Munakata, T., 1982. J. Phys. Soc. Japan 51, 3367.
Ivanov, B.A., Kolezhuk, A.K., 1989. Pisma Zh. Eksp. Teor. Fiz. 49, 489 [JETP Lett. 49, 489 (1989)].
Ivanov, B.A., Kolezhuk, A.K., 1990. Phys. Lett. A 146, 190.
Jaworski, M., 1987. Phys. Lett. A 125, 115.
Joergensen, E., Koshelets, V.P., Monaco, R., Mygind, J., Samuelsen, M.R., 1982. Phys. Rev. Lett. 49, 1093.
Joos, B., 1982. Solid State Commun. 42, 709.
Josephson, B.D., 1965. Adv. Phys. 14, 419.
Kac, A.M., Helfand, E., 1973. J. Math. Phys. 4, 1078.
Kalosakas, G., Zolotaryuk, A.V., Tsironis, G.P., Economou, E.N., 1997. Phys. Rev. E 56, 1088.
Karpman, V.I., 1967. Pis'ma Zh. Eksp. Teor. Fiz. 6, 829 [JETP Lett. 6, 277 (1967)].
Kazantsev, P.A., Pokrovsky, V.L., 1968. Zh. Eksp. Teor. Fiz. 58, 677 [Sov. Phys. JETP 31, 362 (1970)].
Kehr, K.W., Richter, D., Swendsen, R.H., 1978. J. Phys. F 8, 433.
Kenfack, A., Kofané, T.C., 1994. Sol. State Commun. 89, 513.
Kiselev, S.A., Bickham, S.R., Sievers, A.J., 1993. Phys. Rev. B 48, 13508.
Kiselev, S.A., Bickham, S.R., Sievers, A.J., 1995. Comments Condens. Matter Phys. 17, 135.
Kivshar, Yu.S., 1991a. Phys. Rev. A 43, 3117.
Kivshar, Yu.S., 1991b. Phys. Lett. A 161, 80.
Kivshar, Yu.S., 1992. Phys. Rev. B 46, 8652.
Kivshar, Yu.S., 1993a. Phys. Lett. A 173, 172.
Kivshar, Yu.S., 1993b. Phys. Rev. E 48, 4132.
Kivshar, Yu.S., Malomed, B.A., 1987. Europhys. Lett. 4, 1215.
Kivshar, Yu.S., Malomed, B.A., 1988. J. Phys. A 21, 1553.
Kivshar, Yu.S., Malomed, B.A., 1989. Rev. Mod. Phys. 61, 763.
Kivshar, Yu.S., Zhang, F., Vázquez, L., 1991. Phys. Rev. Lett. 67, 1177.
Kivshar, Yu.S., Peyrard, M., 1992. Phys. Rev. A 46, 3198.
Kivshar, Yu.S., Sánchez, A., Chubykalo, O.A., Kosevich, A.M., Vázquez, L., 1992. J. Phys. A 25, 5711.
Kivshar, Yu.S., Campbell, D.K., 1993. Phys. Rev. E 48, 3077.
Kivshar, Yu.S., Salerno, M., 1994. Phys. Rev. E 49, 3543.

Kivshar, Yu.S., Krolikowski, W., Chubykalo, O.A., 1994. Phys. Rev. E 50, 5020.
Kivshar, Yu.S., Zhang, F., Kovalev, A.S., 1997. Phys. Rev. B 55, 14265.
Kochendörfer, A., Seeger, A., 1950. Z. Physik 127, 533 (in German).
Konno, K., Kameyama, W., Sanuki, H., 1974. J. Phys. Soc. Japan 37, 171.
Kontorova, T.A., Frenkel, Ya.I., 1938a. Zh. Eksp. Teor. Fiz. 8, 89 (in Russian).
Kontorova, T.A., Frenkel, Ya.I., 1938b. Zh. Eksp. Teor. Fiz. 8, 1340 (in Russian).
Kosevich, A.M., 1972. Fundamentals of the Crystal Lattice Mechanics. Nauka, Moscow (in Russian).
Kosevich, A.M., Kovalev, A.S., 1973. Solid State Commun. 12, 763.
Kosevich A.M., Kovalev, A.S., 1974a. Zh. Eksp. Teor. Fiz. 67, 1793 [Sov. Phys. JETP 40, 891 (1974)].
Kosevich, A.M., Kovalev, A.S., 1974b. Radiation and Other Defects in Solids. Institute of Physics Publ., Tbilisi (in Russian).
Kosevich, A.M., Kovalev, A.S.,1975. Fiz. Nizk. Temp. 1, 1544 [Sov. J. Low Temp. Phys. 1, 742 (1975)].
Kovalev, A.S., 1994. Fiz. Nizk. Temp. 20, 1034.
Kovalev, A.S., Kondratyuk, A.D., Kosevich, A.M., Landau, A.I., 1993. Phys. Stat. Sol. (b) 177, 117.
Kovalev, A.S., Fei Zhang, Kivshar, Yu.S., 1995. Phys. Rev. B 51, 3218.
Kramers, H.A., 1940. Physica 7, 284.
Kratochvil, J., Indenbom, V.L., 1963. Czech. J. Phys. B 13, 814.
Krivoglaz, M.A., 1961. Zh. Eksp. Teor. Fiz. 40, 567 [Sov. Phys.-JETP 13, 397 (1961)].
Krolikowski, W., Kivshar, Yu.S., 1996. J. Opt. Soc. Am. B 13, 876.
Kubo, R., 1966. Rep. Progr. Phys. 29, 255.
Kunz, C., 1986a. Phys. Rev. A 34, 510.
Kunz, C., 1986b. Phys. Rev. B 34, 8144.
Kunz, C., Combs, J.A., 1985. Phys. Rev. B 31, 527.
Kurosawa, T., 1962. J. Appl. Phys. Suppl. 33, 320.
Landau, A.I., Kovalev, A.S., Kondratyuk, A.D., 1993. Phys. Stat. Sol. (b) 179, 373.
Lazutkin, V.F., Schachmannski, I.G., Tabanov, M.B., 1989. Physica D 40, 235.
Lifshitz, I.M., 1943. Phys. (USSR), 7, 215, 249.
Lifshitz, I.M., 1944. Phys. (USSR) 8, 89.
Lomdahl, P.S., Samuelsen, M.R., 1986. Phys. Rev. A 34, 664.
Lomdahl, P.S., Samuelsen, M.R., 1988. Phys. Lett. A 128, 427.
Lomdahl, P.S., Srolovitz, D.J., 1986. Phys. Rev. Lett. 57, 2702.
Lothe, J., Hirth, J.P., 1959. Phys. Rev. 115, 543.
Lou, S.-Y., Huang, G., 1995. Mod. Phys. Lett. B 9, 1231.
Lyuksyutov, I.F., 1982. Zh. Eksp. Teor. Fiz. 82, 1267 [Sov. Phys. JETP 55, 737 (1982)].
Lyuksyutov, I.F., Naumovets, A.G., Pokrovsky, V.L., 1988. Two-Dimensional Crystals. Naukova Dumka, Kiev (English Translation: Academic Press, Boston, 1992).
MacKay, R., Aubry, S., 1994. Nonlinearity 7, 1623.
Maki, K., Kumar, P., 1976. Phys. Rev. B 14, 118, 3920.
Malomed, B.A., 1990. Phys. Rev. B 41, 2616.
Malomed, B.A., 1992. J. Phys. A 25, 755.
Malomed, B.A., Milchev, A., 1990. Phys. Rev. B 41, 4240.
Malomed, B.A., Nepomnyashchy, A.A., 1992. Phys. Rev. B 45, 12435.
Malomed, B.A., Campbell, D.K., Knowles, N., Flesh, R.J., 1993. Phys. Lett. A 178, 271.
Malomed, B.A., Weinstein, M.I., 1996. Phys. Lett. A 220, 91.
Mansfield, M., Needs, R.J., 1990. J. Phys.: Condens. Matter 2, 2361.
Maradudin, A.A., 1966. Theoretical and Experimental Aspects of the Effects of Point Defects and Disorder on the Vibrations of Crystals. Academic Press, New York.
Marchand, M., Hood, K., Caillé, A., 1987. Phys. Rev. Lett. 58, 1660.
Marchesoni, F., 1986. Phys. Lett. A 115, 29.
Marchesoni, F., Willis, C.R., 1987. Phys. Rev. A 36, 4559.
Marchesoni, F., Willis, C.R., 1990. Europhys. Lett. 12, 491.

Marianer, S., Floria, L.M., 1988. Phys. Rev. B 38, 12054.
Marianer S., Bishop, A.R., Pouget, J., 1988. In: Lesar, R., Bishop, A.R., Heffner, R. (Eds.), Competing Interactions and Microstructures: Statics and Dynamics, Springer Proceedings in Physics, vol. 27. Springer, Berlin.
Marianer, S., Bishop, A.R., 1988. Phys. Rev. B 37, 9893.
Markov, I., Milchev, A., 1985. Thin Solid Films 126, 83.
Markov, I., Trayanov, A., 1987. J. Phys. C 21, 2475.
Martinez Alonso, L., 1986. Phys. Lett. A 114, 285.
Maugin, G.A., Miled, A., 1986. Phys. Rev. B 33, 4830.
Mazor, A., Bishop, A.R., McLaughlin, D.W., 1986. Phys. Lett. A 119, 273.
Mazor, A., Bishop, A.R., 1987. Physica D 27, 269.
McLaughlin, D.W., Scott, A.C., 1978. Phys. Rev. A 18, 1652.
Mikeska, H., 1978. J. Phys. C 11 L29.
Milchev, A., 1986. Phys. Rev. B 33, 2062.
Milchev, A., 1990. Physica D 41, 262.
Milchev, A., Markov, I., 1984. Surf. Sci. 136, 503.
Milchev, A., Mazzucehelli, G.M., 1988. Phys. Rev. B 38, 2808.
Milchev, A., Fraggis, Th., Pnevmatikos, St., 1992. Phys. Rev. B 45, 10348.
Mori, H., 1965. Progr. Theor. Phys. 33, 423.
Nabarro, F.R.N., 1947. Proc. Roy. Soc. (London) 59, 256.
Oboznov, V.A., Ustinov, A.V., 1989. Phys. Lett. A 139, 481.
Ogata, M., Wada, Y., 1985. J. Phys. Soc. Japan 54, 3425.
Ogata, M., Wada, Y., 1986. J. Phys. Soc. Japan 55, 1252.
Ostrovskii, L.A, 1966. Zh. Eksp. Teor. Fiz. 51, 1189 [Sov. Phys. JETP 24, 797 (1967)].
Pagano, S., Monaco, R., Costabile, G., 1989. IEEE Trans. Magn. 25, 1080.
Page, J.B., 1990. Phys. Rev. B 41, 7835.
Paneth, H.R., 1950. Phys. Rev. 80, 708.
Pascual, P., Vázquez, L., 1985. Phys. Rev. B 32, 8305.
Patel, J.R., Chandhuri, A.R., 1966. Phys. Rev. 143, 601.
Pedersen, N.F., 1986. In: Barone, A. (Ed.), Josephson Effect – Achievements and Trends. World Scientific, Singapore.
Peierls, R., 1940. Proc. Roy. Soc. (London) 52, 34.
Perring, J.K., Skyrme, T.H.R., 1962. Nucl. Phys. 31, 550.
Petukhov, B.V., 1971. Fiz. Tverd. Tela 13, 1445 [Sov. Phys.-Solid State 13, 1207 (1971)].
Petukhov, B.V., 1983. Fiz. Tverd. Tela 25, 1822 [Sov. Phys.-Solid State 25, 1048 (1983)].
Peyrard, M., Bishop, A.R., 1989. Phys. Rev. Lett. 62, 2755.
Peyrard, M., Remoissenet, M., 1982. Phys. Rev. B 26, 2886.
Peyrard, M., Campbell, D.K., 1983. Physica D 9, 33.
Peyrard, M., Kruskal, M.D., 1984. Physica D 14, 88.
Pnevmatikos, St., 1988. Phys. Rev. Lett. 60, 1534.
Pnevmatikos, St., Kivshar, Yu.S., Savin, A.V., Zolotaryuk, A.V., Velgakis, M.J., 1991. Phys. Rev. A 43, 5518.
Pietronero, L., Strässler, S., 1978. Sol. State Commun. 27, 1041.
Pouget, J., Maugin, G.A., 1984. Phys. Rev. B 30, 5306.
Pouget, J., Maugin, G.A., 1985. Phys. Rev. B 31, 4633.
Pouget, J., Aubry, S., Bishop, A.R., Lomdahl, P.S., 1989. Phys. Rev. B 39, 9500.
Pouget, J, Remoissenet, M, Tamga, J.M., 1993. Phys. Rev. E 47, 14 866.
Pokrovsky, V.L., 1981. J. Phys. (Paris) 42, 761.
Pokrovsky, V.L., Virosztek, A., 1983. J. Phys. C 16, 4513.
Putterman, S.J., Roberts, P.H., 1993. Proc. R. Soc. (London) 440, 135.
Reisinger, H., Schwabl, F., 1983. Z. Phys. B 52, 151.
Remoissenet, M., 1978. Sol. State Commun. 27, 681.
Remoissenet, M., 1981. J. Phys. C 14, L335.
Remoissenet, M., 1986. Phys. Rev. B 33, 2386.

Remoissenet, M., Flytzanis, N., 1985. J. Phys. C 18, 1573.
Remoissenet, M., Peyrard, M., 1984. Phys. Rev. B 29, 3153.
Ricchetty, M., Metzger, W., Heuman, H., 1988. Proc. Nat. Acad. Sci. 84, 4610.
Rice, M.J., 1984. Phys. Rev. B 28, 3587.
Rosenau, Ph., 1986. Phys. Lett. A 118, 222.
Rubinstein, J., 1970. J. Math. Phys. 11, 258.
Sagdeev, I.R., Vinokur, V.M., 1987. J. Physique 48, 1395.
Salerno, M., 1991. Phys. Rev. A 44, 5292.
Salerno, M., 1992a. Phys. Rev. A 46, 6856.
Salerno, M., 1992b. Phys. Lett. A 167, 43.
Salerno, M., Kivshar, Yu.S., 1994. Phys. Lett. A 193, 263.
Sanders, W.T., 1962. Phys. Rev. 128, 1540.
Sandusky, K.W., Page, J.B., Schmidt, K.E., 1992. Phys. Rev. B 46, 6161.
Sánchez, A., Vázquez, L., 1992. Int. J. Mod. Phys. B 5, 2825.
Sarker, S.K., Krumhansl, J.A., 1981. Phys. Rev. B 23, 2374.
Sasaki, K., Maki, K., 1987a. Phys. Rev. B 35, 257.
Sasaki, K., Maki, K., 1987b. Phys. Rev. B 35, 263.
Savin, A.V., 1995. Zh. Eksp. Teor. Fiz. 108, 1105 [JETP 81, 608 (1995)].
Savin, A.V., Zolotaryuk, A.V., 1991. Phys. Rev. A 44, 8167.
Sayadi, M.K., Pouget, J., 1991. J. Phys. A: Math. Gen. 24, 2151.
Scharf, R., Bishop, A.R., 1991. Phys. Rev. A 43, 6535.
Schiefman, J., Kumar, P., 1979. Phys. Scripta 20, 435.
Schneider, T., 1986. In: Trullinger, S.E. (Ed.), Solitons. Springer, Berlin, Ch. 7.
Scott, A.C., 1969. Amer. J. Phys. 37, 52.
Scott, A., 1985. Philos. Trans. R. Soc. (London) A 315, 423.
Scott, A.C., Christiansen, P.L., 1990. Phys. Scripta 42, 257.
Seeger, A. 1948. Diplomarbeit, T.H. Stuttgart.
Seeger, A. 1980a. Proc. Roy. Soc. London A 371, 173.
Seeger, A., 1980b. In: Kröner, E., Anthony, K.H. (Eds.), Continuum Models of Discrete Systems. University of Waterloo, Waterloo, Ont., p. 253.
Seeger, A., Kochendörfer, A., 1951. Z. Physik 130, 321.
Seeger, A., Donth, H., Kochendörfer, A., 1953. Z. Physik 134, 173.
Segur, H., 1983. J. Math. Phys. 24, 1439.
Sievers, A.J., Takeno, S., 1988. Phys. Rev. Lett. 61, 970.
Sievers, A.J., Page, J.B., 1995. In: Horton, G.K., Maradudin, A.A. (Eds.), Dynamical Properties of Solids VII. Phonon Physics: The Cutting Edge. Elsevier, Amsterdam, p. 137.
Slot, J.J.M., Janssen, T., 1988a. Physica D 32, 27.
Slot, J.J.M., Janssen, T., 1988b. J. Phys. A 21, 3559.
Snyman, J.A., van der Merwe J.H., 1974. Surface Sci. 45, 619.
Snyman, J.A., Snyman, H.C., 1981. Surface Sci. 105, 357.
Sodano, P., El-Batanouny, M., Willis, C.R., 1986. Phys. Rev. B 34, 4936.
Speight, J.M., Ward, R.S., 1994. Nonlinearity 7, 475.
Stancioff, P., Willis, C.R., El-Batanouny, M., Burdick, S., 1986. Phys. Rev. B 33, 1912.
Suezawa, M., Sumino, K., 1976. Phys. Stat. Sol. (a) 36, 263.
Sugiyama, A., 1979. J. Phys. Soc. Japan 47, 1238.
Takeno, S., Homma, S., 1986. J. Phys. Soc. Japan 55, 65.
Takeno, S., Kisoda, K., Sievers, A.J., 1988. Progr. Theor. Phys. 94 (Suppl.) 242.
Takeno, S., Hori, K., 1990. J. Phys. Soc. Japan 59, 3037.
Takeno, S., Peyrard, M., 1996. Physica D 92, 140.
Taki, M., Spatschek, K.H., Fernandez, J.C., Grauer, R., Reinisch, G., 1989. Physica D 40, 65.
Talapov, A.L., 1982. Zh. Eksp. Teor. Phys. 83, 442.

Theodorakopoulos, N., 1979. Z. Physik 33, 385.
Theodorakopoulos, N., Klein, R., 1980. Phys. Stat. Sol. (a) 61, 107.
Theodorakopoulos, N., Klein, R., 1981. In: Bernasconi, J., Schneider, T. (Eds.), Physics in One Dimension, Springer, Berlin.
Theodorakopoulos, N., Wünderlich, W., Klein, R., 1980. Solid State Commun. 33, 213.
Theodorakopoulos, N., Weller, W., 1988. Phys. Rev. B 38, 2749.
Toda, M., 1967. J. Phys. Soc. Japan 22, 431; ibid, 23, 501.
Toda, M., 1981. Theory of Nonlinear Lattices. Springer, Berlin.
Tsurui, A., 1973. J. Phys. Soc. Japan 34, 1462.
Tsuzuki, T., Sasaki, K., 1988. Progr. Theor. Phys. 94 (Suppl.), 73.
Ustinov, A.V., 1989. Phys. Lett. A 136, 155.
Ustinov, A.V., Cirillo, M., Malomed, B.A., 1993. Phys. Rev. B 47, 8357.
Ustinov, A.V., Cirillo, M., Malomed, B.A., Kivshar, Yu.S., 1994. Physica B 194/195, 1765.
Vakhitov, N.G., Kolokolov, A.A., 1973. Izv. VUZov Radiofiz. 16, 1020 [Radiophys. Quant. Electron. 16, 783 (1973)].
Vakhnenko, A.A., Gaididei, Yu.B., 1986. Theor. Mat. Fiz. 68, 350 [Theor. Math. Phys. 68, 873 (1987)].
van der Merwe, J.H., 1970. J. Appl. Phys. 41, 4725.
van der Zant, H.S.J., Orlando, T.P., Watanabe, S., Strogats, S.H., 1995. Phys. Rev. Lett. 74, 174.
Vernik, I.V., Oboznov, V.A., Ustinov, A.V., 1992. Phys. Lett. A 168, 319.
Vinokur, V.M., 1986. J. Physique (Paris) 47, 1425.
Vorotyntsev, M.A., Kornyshev, A.A., Rubinshtein, A.I., 1979. Dokl. Akad. Nauk SSSR 248, 1321 [Sov. Phys. Dokl. 24, 848 (1979)].
Wada, Y., Schrieffer, J.R., 1978. Phys. Rev. B 18, 3897.
Wada, Y., Ishiuchi, H., 1982. J. Phys. Soc. Japan 51, 1372.
Wang, J.C., Pickett, D.F., Jr., 1976. J. Chem. Phys. 65, 5378.
Watanabe, S., Strogats, S.H., van der Zant, H.S.J., Orlando, T.P., 1996. Physica D 97, 429.
Weiss, M., Elmer, F.-J., 1996. Phys. Rev. B 53, 7539.
Weiss, M., Elmer, F.-J., 1997. Z. Phys. B 104, 55.
Willaime, H., Cardoso, O., Tabeling, P., 1991. Phys. Rev. Lett. 67, 970.
Willis, C.R., El-Batanouny, M., Stancioff, P., 1986. Phys. Rev. B 33, 1904.
Willis, C.R., El-Batanouny, M., Burdick, S., Boesch, R., 1987. Phys. Rev. B 35, 3496.
Woafo, P., Kenne, J.P., Kofané, T.C., 1993. J. Phys.: Condens. Matter 5, L123.
Woafo, P., Kofané, T.C., 1994. Sol. State Commun. 89, 261.
Yakushevich, L.V., 1989. Phys. Lett. A 136, 413.
Yang, Y.N., Trafas, B.M., Siefert, R.L., Weaver, J.H., 1991. Phys. Rev. B 44, 3218.
Yokoi, C.S.O., Tang, L.H., Chou, W., 1988. Phys. Rev. B 37, 2173.
Yomosa, S., 1983. Phys. Rev. A 27, 2120.
Yomosa, S., 1984. Phys. Rev. A 30, 474.
Zabusky, N.J., Kruskal, M.D., 1965. Phys. Rev. Lett. 15, 240.
Zadrodziński, J., Jaworski, M., 1982. Z. Phys. B 49, 75.
Zakharov, V.E., Manakov, S.V., Novikov, S.P., Pitaevsky, L.P., 1980. Theory of Solitons. Nauka, Moscow [English Translation by Consultants Bureau, New York, 1984].
Zhang, C.T., 1987. Phys. Rev. A 35, 886.
Zhang, F., 1996. Phys. Rev. E 54, 4325.
Zhang, F., 1998. Phys. Rev. E, submitted.
Zhang, F., Kivshar, Yu.S., Malomed, B.A., Vázquez, L., 1991. Phys. Lett. A 159, 318.
Zhang, F., Kivshar, Yu.S., Vázquez, L., 1992a. Phys. Rev. A 45, 6019.
Zhang, F., Kivshar, Yu.S., Vázquez, L., 1992b. Phys. Rev. A 46, 5214.
Zhang, F., Kivshar, Yu.S., Vázquez, L., 1994. J. Phys. Soc. Japan 63, 466.
Zhou, G.Z., Zhang, C.T., 1991. Phys. Scripta 43, 347.
Zolotaryuk, A.V., Spatschek, K.H., Ladke, E.W., 1984. Phys. Lett. A 101, 517.
Zolotaryuk, A.V., 1986. Teor. Mat. Fiz. 68, 415 [Theor. Math. Phys. 68, 916 (1986)].
Zolotaryuk, A.V., Pnevmatikos, St., 1990. Phys. Lett. A 143, 233.